The Dissertation Committee for Kevin Wood Bieri Certifies that this is the approved version of the following dissertation:

Slow and fast gamma rhythms represent distinct memory processing states in the hippocampus

Committee:

Laura Colgin, Supervisor

Michael Drew

Nace Golding

Hitoshi Morikawa

Alison Preston

Slow and fast gamma rhythms represent distinct memory processing states in the hippocampus

by

Kevin Wood Bieri, B.S. Bioch.

Dissertation

Presented to the Faculty of the Graduate School of

The University of Texas at Austin

in Partial Fulfillment

of the Requirements

for the Degree of

Doctor of Philosophy

The University of Texas at Austin

May 2015

Acknowledgements

I would foremost like to thank Dr. Laura Colgin for being a great mentor the past four years. None of this would have been possible without her support and guidance. I would also like to thank the members of the Colgin Lab for making the workplace an easy-going and enjoyable place to be. Special thanks to Katelyn Bobbitt for building all the drives for this research, her expert skills in histology, and for keeping the lab running smoothly, Sean Trettel and Brian Gereke for lending programs at critical times, and Dr. Chenguang Zheng for working with me on the final experiment in this dissertation. I also want to acknowledge the faculty of CLM for providing a great environment, and the staff of CLM, particularly Krystal Phu, Chris Weatherly, Cindy Thompson, and Wilbert King, for making life as a graduate student as stress free as possible. Lastly, I want to say thanks to my family and friends for all the encouragement and support over the years.

Slow and fast gamma rhythms represent distinct memory processing states in the hippocampus

Kevin Wood Bieri, Ph.D.

The University of Texas at Austin, 2015

Supervisor: Laura Colgin

The hippocampus is central to learning and memory and participates in both the encoding of new memories and their retrieval. It is not known, however, how these dual functions are processed within the same structure without causing interference between what is actively experienced and what is remembered. Different frequencies of gamma oscillations selectively route inputs to area CA1 of the hippocampus, suggesting that gamma subtypes play a role in differentiating between streams of incoming information. Slow gamma oscillations (~25–55 Hz) couple CA1 to area CA3, a region that is thought to store neuronal representations of past events and is thus important for memory retrieval. Fast gamma oscillations (~60–100 Hz) couple CA1 to MEC, a region that supplies the hippocampus with information about ongoing experiences. In this dissertation, I use hippocampal recordings in freely behaving rats to provide evidence that such slow and fast gamma coupling supports distinct memory retrieval and encoding modes in the hippocampus. This is first examined in the principal neurons of the hippocampus, called 'place cells', which are thought to provide the 'where' component of episodic memory. It was found that place cells alternated between distinct spatial coding modes, representing upcoming locations during slow gamma and recent locations during fast gamma. This concept was explored further in 'place cell sequences', which represent

trajectories through space, and are thought to store sequential events of an experience. Sequences coded paths sweeping ahead of the animal during slow gamma, and coded ongoing, real-time locations during fast gamma. Also, it was found that different phases of the slow gamma cycle coded specific locations, suggesting a mechanism for how slow gamma promotes retrieval of multi-item memories. Lastly, slow and fast gamma were examined during novel and familiar experiences. Fast gamma was enhanced during encoding of novel object-place associations, while slow gamma coupling between CA3 and CA1 was associated with retrieval of familiar object-place associations. Taken together, these results support the hypothesis that distinct gamma subtypes provide a novel mechanism for separating the dual "reading" and "writing" functions of the hippocampus.

Table of Contents

List of Figures

Chapter 1: Introduction

In day-to-day life our experiences are continually recorded and retrieved, providing continuity with the past and the ability to modify the future. For the most part, this process is seamless and happens with little conscious effort – new memories are encoded as we go about our day, and old memories are triggered when needed. The ability of the brain to integrate new and stored information at rapid time scales into a cohesive and meaningful experience is something we take for granted. Attempts have been made to localize these two mnemonic processes - the 'reading' and 'writing' of memory - and have shown that a single structure in the brain, called the hippocampus, is involved with both. A perplexing question is how a single network of neurons might convey stored memories to the rest of the brain, while taking in and recording new information, without creating interference between what is current and what is being remembered. The disassociation between these two types of information likely involves the complex coordination of neurons in the hippocampus and its specialized subregions, granting the ability to rapidly encode new information on one hand, and seamlessly retrieve relevant stored information on the other. The purpose of this dissertation is to explore experimental evidence that different frequencies of gamma oscillations play a key role in this coordination. I begin in this chapter with a brief discussion of the relevant hippocampal and oscillation physiology, as well as the methods used in their study.

1.1 THE HIPPOCAMPUS

Background

The hippocampus is a small structure buried deep in the medial portion of the human temporal lobe with a distinct curved shape that early anatomists compared to a sea

horse, the Latin word of which gives the structure its name (Figure 1.1A). In rodents, the hippocampus is proportionately larger, and its long axis curves rostrodorsally in a C shape, with the dorsal portion resting close beneath the neocortex (Figure 1.1B). Classically considered part of the limbic system, early physiologists assigned a variety of functions to the hippocampus including smell, emotion, attention, and others (Andersen et al., 2007, for a review). Early studies of its role in memory were made by observing deficits in patients with damage to the temporal lobe, or in patients who had portions of the medial temporal lobe removed to treat various neurological conditions. Most famous was a patient named H.M., who underwent bilateral resection of the anterior hippocampus and its associated regions to treat pharmacologic-resistant epilepsy (Milner et al., 1968; Scoville and Milner, 1957). H.M. was relieved of seizures, but unfortunately developed profound anterograde amnesia and some degree of retrograde amnesia. Interestingly, H.M. did not suffer deficits in all types of memory, but completely lacked the ability to remember events, facts, or things that involve conscious recollection. He existed as if he was perpetually "waking from a dream". The type of memory he lacked, recall of events and facts, is called 'declarative', or 'explicit' memory, and is considered a core function of the hippocampus.

Studies in the rat hippocampus have suggested that the hippocampus is also critical for spatial navigation (O'Keefe and Nadel, 1978; Moser et al., 2008). The principal neurons of the hippocampus, 'place cells', code location (O'Keefe and Dostrovsky, 1971; O'Keefe, 1976), and are thought to provide the 'where' component of memory. Much work on hippocampal memory function has been performed by studying these cells.

Anatomy

The hippocampus is intimately involved with a number of surrounding structures which are collectively called the 'hippocampal formation' (Figure 1.1C). This includes the hippocampus proper, dentate gyrus (DG), entorhinal cortex (EC), subiculum, presubiculum, and parasubiculum. The hippocampus proper is further divided into areas CA1, CA2, and CA3. Early anatomists described the connections between these regions as a unidirectional, tri-synaptic circuit, in the following order: EC → DG → CA3 → CA1. While this 'trisynaptic loop' is an important feature of hippocampal anatomy, recent work has provided a more complete and complex picture of the hippocampal formation, described below.

The EC is often considered the gateway to the hippocampus. Part of the neocortex, it is situated caudally and ventrally relative to the hippocampus proper. It receives projections from a large number of cortical areas, which it relays to the rest of the hippocampal formation via a collection of fibers called the perforant path. Contributing to this pathway are layer II EC neurons, which project to the DG and CA3, and layer III neurons which project to area CA1 and the subiculum. The DG and area CA3 do not send feedback projections to the EC; however, CA1 and the subiculum send feedback projections to the deep layers of EC, layers V and VI. Within the EC, layer V sends projections to layers II and III (Gloveli et al., 2001; Van Haeften et al., 2003), thereby completing a loop between the cortex and the hippocampus. The EC provides the strongest output from the hippocampal formation, sending projections to many of the same neocortical regions from which it receives input.

The DG has three layers (the granule cell layer, the molecular layer, and the polymorphic cell layer) and sits between the EC and area CA3 in a distinct V shape. Of the hippocampal formation, the DG might be the most exclusive in terms of connectivity.

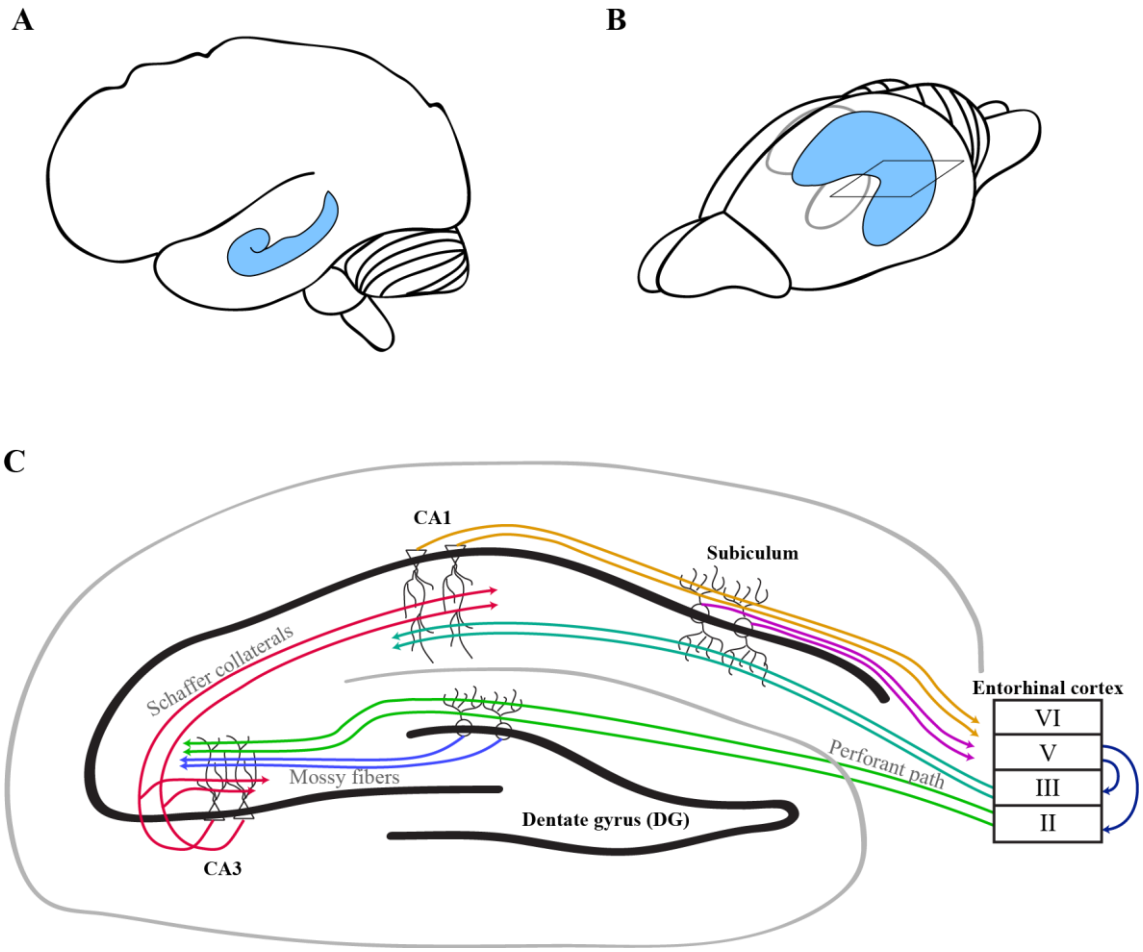

Figure 1.1: Hippocampal anatomy.
The hippocampus (shown in blue) in the brain of a human (**A**), and rat (**B**). **C.** The projections of the rat hippocampus.

The granule cells, the principal cells of DG, project to area CA3 via "mossy fibers" and receive disynaptic feedback from mossy cells, a second type of DG cell that receives input from DG granule cells. As described above, the primary input to the DG is from layer II of EC. It receives no direct input from other cortical regions but does receive input from multiple sub-cortical structures.

The hippocampus proper is a continuous infolding of the medial edge of the neocortex, but is structurally more primitive, often referred to as 'archicortex'. It has a

characteristic laminar organization, with cell bodies residing in stratum pyramidale. CA3 resides closest to the DG and receives input from mossy fibers of the granule cells, which terminate in stratum lucidum. This layer is unique to area CA3 and demarcates the boundary between CA3 and CA2, which does not receive input from DG. CA3 also receives input from EC layer II, which synapses in stratum lacunosum-moleculare. The most striking feature of CA3 is that its largest source of input is from its own axons. The functional significance of these connections is discussed in the following section. Area CA2 is a small region between CA3 and CA1, which primarily receives inputs from EC layer II and CA3. Both CA3 and CA2 have no known direct projections to the neocortex.

Adjacent to CA2 is area CA1, which is recognizable as an increase in the density of cells in stratum pyramidale. CA1 receives input from layer III EC, terminating in stratum lacunosum moleculare, as is the case for the EC inputs terminating in CA3. CA1 receives its strongest input however from CA3, whose fibers, called 'Schaffer collaterals', terminate in stratum radiatum. The axons of CA1 cells travel basally through stratum oriens, and unlike CA2 and CA3, project to EC, to roughly the same regions from which the CA1 cells received inputs. CA1 also sends projections to other regions of the neocortex and to the subiculum.

The final region of the hippocampal formation, the subiculum, is continuous with CA1 and is recognizable as a decrease in density of cells in the cell body layer, and the discontinuation of stratum radiatum and its associated CA3 input. The subiculum is a major output region, which sends projections to layer V of EC and to multiple subcortical and cortical regions.

Place cells

The principal neurons of the hippocampus are called 'place cells'. Place cells activate when an animal is in a specific region of an environment, called a 'place field'

(Figure 1.2). Place fields represent an approximately normally distributed firing rate as a function of location and are thought to represent memory for locations. Place cells were first characterized in rats (O'Keefe and Dostrovsky, 1971) but were later shown to exist in a variety of mammals, including humans interacting with a virtual reality environment (Ekstrom et al., 2003). The spatial selectivity of place cells is thought to play a central role in spatial navigation by providing a cognitive map of the environment.

In addition to navigation, a growing number of studies suggest that place cells are directly involved with memory. The location of each place cell's place field develops with time (O'Keefe and Nadel, 1978; Wilson and McNaughton, 1993; Leutgeb et al., 2004), as opposed to purely sensory receptive fields, and place fields change in an experience-dependent manner (Mehta et al., 1997; Lee et al., 2004). Place cells also activate in spatially ordered sequences. The ability of the hippocampus to coordinate multi-item spatial sequences might represent a broader substrate for handling episodic memories, which are sequences of events. In line with this, sequences of place cells representing spatial paths activate at choice points on mazes, suggesting memory recall (Johnson and Redish, 2007), and track trajectories to remembered goal locations (Pfeiffer and Foster, 2013). Also, place cell activity appears to predict the future trajectory of animals (Wikenheiser and Redish, 2015). Moreover, during periods of rest, place cell sequences that were active during experience are reactivated in the same order, a phenomenon called 'replay'. This is thought to play a role in long term memory consolidation by strengthening the synaptic connections between the active neurons (Skaggs and McNaughton, 1996). The role of place cells in broader memory function, as opposed to purely spatial, is also supported by their ability to represent stimuli such as odors (Wood et al., 1999), and time (MacDonald et al., 2011). The latter might be particularly important for maintaining the temporal structure of events within an episodic

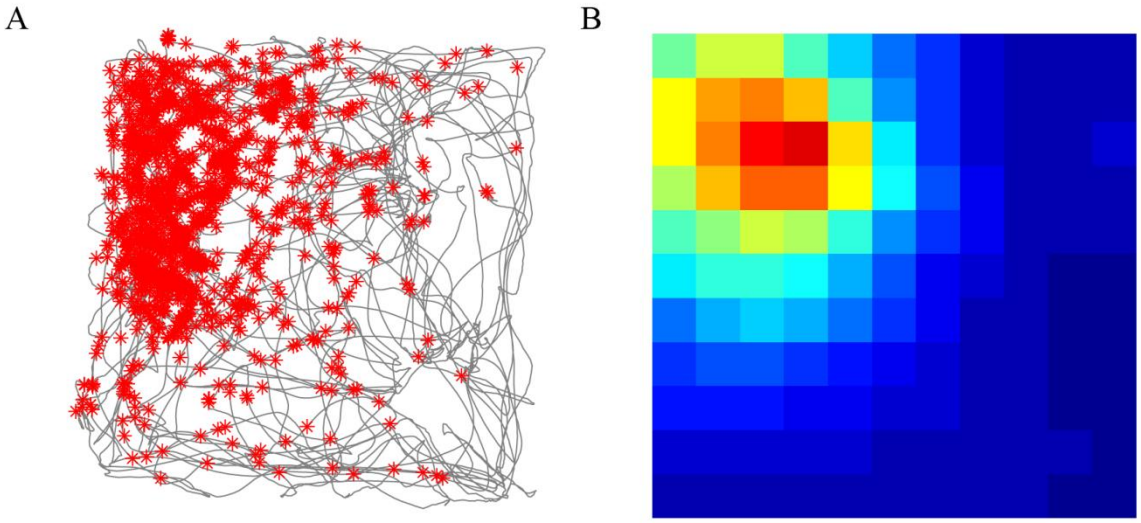

Figure 1.2: Example place cell.
A. Spiking locations of a CA1 place cell (red stars) in a rat exploring a 60 x 60 cm box (trajectory in grey line). **B.** Locations with high spiking probability (red) and low spiking probability (blue) are depicted for the same place cell shown in A.

memory. Although the specific role of place cells in memory operations remains an active area of study, there is clear evidence that they are involved with spatial aspects of memory. Their spatial coding properties thus offer a valuable window into how the hippocampus stores and retrieves information about the external world during memory encoding and retrieval.

Hippocampal function

Attempting to understand how memory encoding and retrieval takes place in the hippocampus is a difficult task considering the complexity of the connectivity. Based on the feedforward projections in the network and the extensive recurrent collateral system in CA3, David Marr established a basic outline of hippocampal function that remains at the center of many current models (Marr, 1971). In this framework, the role of the hippocampus is to store simplified versions of neocortical representations, serving as an 'index' of remembered experiences. Retrieval of these experiences is thought to occur by

activating the index through partial or incomplete cues, which then restores the full representation of the initial experience in the output to the neocortex. The hippocampus is thought to strengthen these neocortical representations through memory consolidation, which happens over a highly variable amount of time, from hours to years. Retrieval may then occur entirely independently of the hippocampus. A complete description of these processes is outside the scope of this dissertation; however, encoding and retrieval within the hippocampal structure is described below.

The encoding of the hippocampal representation is thought to rely on input from EC. The EC receives multimodal, highly processed representations from the neocortex, which it then transfers to DG and CA3. DG is thought to act as pattern separator, generating distinct patterns of activity from the inputs it receives from EC, even when they are very similar (McNaughton and Morris, 1987; Amaral et al., 1990; Treves and Rolls, 1994; O'Reilly and McClelland, 1994; Hasselmo and Wyble, 1997). This is thought to keep experiences distinct from each other during memory encoding. The signal from DG activates unique patterns of activity in the dense auto-associative connections within area CA3 (Willshaw et al., 1969; Gardner-Medwin, 1976; Hopfield, 1982; Kohonen et al., 1984). The powerful mossy fiber synapse from DG is thought to strongly excite CA3 cells and thereby stimulate plasticity within the CA3 network, allowing storage of the representation, and association with the initial input from EC.

Evidence that the EC codes ongoing sensory experience important for memory encoding is demonstrated by the spatial firing properties of 'grid cells' (Brun et al., 2002; Fyhn et al., 2004; Hafting et al., 2005), which track an animal's current location. These cells make direct connections to hippocampal place cells (Zhang et al., 2013) and affect the spatial information they code (Brun et al., 2008).

The retrieval of stored activity patterns is thought to occur when the CA3 network is cued by inputs from EC. The CA3 network is thought to be an optimal structure for retrieving stored information, since its auto-associative properties allow incomplete or corrupted cues to trigger the full activity pattern. This process is called pattern completion (McNaughton and Morris, 1987). The role of CA3 in memory retrieval has been demonstrated in rats with removal of the input from CA3 to CA1. Without this connection, memory acquisition of a spatial recognition task appears intact, but spatial recall is impaired (Brun et al., 2002). Moreover, rats lose the ability to remember the spatial location of a hidden platform in a pool of water (Morris water maze task) (Sutherland et al., 1983; Steffenach et al., 2002). Also, fMRI studies in humans show increases in CA3 activity during successful retrieval of associative memories (Chen et al., 2011).

CA1 is thought to receive input from CA3 during memory retrieval, as well as EC input during memory encoding. This has led to the idea that CA1 acts as comparator between stored information from CA3 and novel information from EC (Gray, 1982; Hasselmo and Schnell, 1994; Hasselmo and Wyble, 1997). Evidence of mismatch detection by CA1 has been observed in high resolution human fMRI studies, in which CA1 activity increases when subjects view mismatched associations or expectations (Chen et al., 2011; Duncan et al., 2012). Mismatch recognition between two streams of information might signal novelty and encourage memory encoding (Hasselmo and Wyble, 1997; Lisman and Grace, 2005).

As can be seen, a great deal of information is passed between the different subregions of the hippocampus. Novel information originates from EC and is stored in CA3, while activity in CA3 may represent a response to EC input, or the retrieval of stored information within its own network. Both of these streams of information are sent

to CA1, which may result in memory retrieval, encoding, or consolidation. A key question is how the flow of all this information is balanced and coordinated. As will be described in the next section, oscillatory dynamics might shed some light on this question.

1.2 OSCILLATIONS

Background

Neural oscillations are periodic fluctuations in the voltage of the extracellular local field potential (LFP) in brain tissue, and generally speaking, resemble a sinusoidal wave. Different types of oscillations are classified by their frequency, and have well-defined correlations with different behavioral and cognitive states, such as sleep (~2–4 Hz; delta), active exploration (~4-9 Hz; theta), awake relaxation (~10 Hz; alpha), and high order cognitive functions such as attention (~30–100 Hz; gamma). This suggested to early physiologists that they may play distinct functional roles.

What do oscillations represent?

As mentioned above, oscillations are recorded as changes in the voltage of the extracellular space of brain tissue, which is referred to as the local field potential (LFP). Broadly speaking, the LFP represents the collective activity of a large group of neurons, whose electrical activity is summed in space. For this reason, oscillations are generally most prominent in brain regions where neurons are physically aligned in an organized fashion, allowing summation of current sinks and sources that might otherwise cancel out. Hippocampal neurons are tightly packed with vertically aligned dendrites and exhibit some of the most prominent oscillations in the brain. In addition to physical orientation,

neuronal activity must also be temporally aligned. That is, neurons' electrical activity must co-occur in time, such that its summation results in a cohesive, collective pattern.

The type of electrical activity that each neuron contributes to the LFP has been a long area of study. Each neuron receives excitatory and inhibitory synapses, which generate excitatory and inhibitory post-synaptic potentials (PSPs) in its dendrites. If the membrane potential threshold is exceeded, the neuron sends output in the form of an action potential (AP). Most research suggests that temporally aligned PSPs make up the majority of the electrical activity recorded in the LFP, with less contribution from APs (Einevoll et al., 2013). This idea dates back to early studies of the LFP (Bremer, 1938; Bremer, 1949; Eccles, 1951) and can be explained by the different temporal dynamics of PSPs and APs. APs only last ~1–2 ms and their amplitude falls off rapidly as a function of distance due to the low pass filtering properties of brain tissue. PSPs, on the other hand, last much longer and may propagate further distances before being substantially attenuated. This makes it much more likely that any at given location a greater number of PSPs are present in the LFP from neighboring and perhaps more distant neurons than APs, which are only detectable at locations immediately adjacent to the neuron.

It should be noted however, that electrical events other than PSPs contribute some degree of activity to the LFP, including afterhyperpolarizations, calcium spikes, and activity originating from glial cells (Einevoll et al., 2013). Also, APs might directly influence measurement of oscillatory components with frequencies >~100 Hz (Petterson and Einevoll, 2008; Schomburg et al., 2012). However, the influence of these factors is likely small relative to the contribution of PSPs, and primarily limited to frequency ranges outside of those examined in this work.

Functions of oscillations

The contribution of PSPs to the LFP suggests that oscillations predominantly represent fluctuations in the input received by a network, rather than direct changes to its output. Thus, oscillations reflect alternating periods of inhibition and excitation in the network, during which neurons are less likely, or more likely, to be active. The periodic nature of this process provides a temporal metric that might be important in systems that involve precise timing, such as fine motor coordination and perception, or functions that rely on pace-making activity such as walking, running, breathing, and control of heart rate. Generally, it is thought that oscillations provide temporal coordination to the activity of neurons, the specifics of which depend on a variety of factors, such as the frequency, region, and mechanism of generation.

1.3 HIPPOCAMPAL OSCILLATIONS

During waking behavior, the hippocampus exhibits 4 types of rhythmic LFP patterns – theta (~6–12 Hz), beta (~12–30 Hz), gamma (~25–100 Hz), and sharp wave-ripples (~100–200 Hz). The fastest of these, ripples, occurs when the animal is at rest (as well as during slow-wave sleep) and is thought to play a role in memory consolidation. Beta appears to be involved with olfactory processing (Vanderwolf and Zibrowski, 2001), but may also play a role in memory (Igarashi et al., 2014). The most prominent LFP patterns during active waking behaviors, and those most often linked to memory function, are theta and gamma.

Theta

The hippocampal theta rhythm is striking in its regularity and large amplitude, resembling a nearly uniform sinusoidal wave (Figure 1.3). Theta was first observed in the rabbit in 1938 by Jung and Kornmuller, and later in other species, including rats, cats,

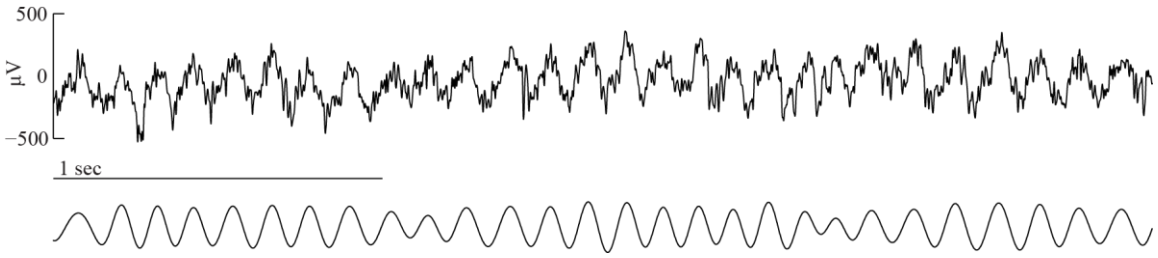

Figure 1.3: Hippocampal theta.
Theta from area CA1 in the hippocampus of a freely behaving rat. Shown is the raw unfiltered trace (top) and the same trace after bandpass filtering (6–12 Hz) (bottom).

monkeys and humans (Green and Arduini, 1954; Grastyan et al., 1959; Vanderwolf, 1969; Ekstrom et al., 2005). A number of studies have shown that the inhibitory projections from the medial septum (MS) are responsible for generating theta (Stewart and Fox, 1990; Toth et al., 1997; Hangya et al., 2009); however, other studies suggest that theta pace-making might involve other sources, including the EC (Buzsaki et al., 1983; Kamondi et al., 1998) and interneurons within the hippocampus itself (Goutagny et al., 2009). Early attempts to link theta with memory showed that simple learning tasks, such as reward conditioning and discrimination learning, correlated with changes in theta activity (Grastyan et al., 1959; Adey et al., 1960). However, the role of theta in memory remained controversial as these learning tasks overlapped with behaviors that were also shown to be strongly tied to theta. Much of the early work on theta attempted to elucidate these behavioral correlates and showed that theta was tightly linked to physical mobility, as well as states of arousal and attention (regardless of physical movement) (Vanderwolf, 1969; Kramis et al., 1975). However, an accumulating body of studies, decades old and recent, have returned to the initial idea that theta is involved with learning and memory (Landfield et al., 1972; Berry and Thompson, 1978; Winson, 1978; Macrides et al., 1982; Mitchell et al., 1982; Mizumori et al., 1990; M'Harzi and Jarrard, 1992; Klimesch et al., 1996; Osipova et al., 2006; Robbe and Buzsaki, 2009; Rutishauser et al., 2010; Liebe et

al., 2012), as well as synaptic plasticity (Larson et al., 1986; Staubli and Lynch, 1987; Greenstein et al., 1988; Pavlides et al., 1988; Orr et al., 2001; Hyman et al., 2003).

The mechanisms by which theta promotes memory function remain an active area of study. One idea is that theta oscillations coordinate sequences of information that might be important for the encoding or retrieval of episodic memories. The existence of sequences during theta oscillations (i.e. "theta sequences") was first theorized as a logical corollary to a phenomenon called "theta phase precession", in which spikes fire on progressively earlier phases of theta as an animal passes through a place cell's place field (O'Keefe and Recce, 1993; Skaggs et al., 1996). When place cells are viewed as an ensemble, this appears as a compressed representation of space within each individual cycle of theta in the form of a spatial path (Skaggs et al., 1996; Foster and Wilson, 2007). In a study by Gupta et al. (2012), it was shown that the spatial characteristics of these paths correlate with multiple factors, including landmark location, the duration of the theta cycle, running speed, and the number of gamma cycles. It was proposed that spatial paths sweeping in front of the animal represent a retrieval dependent 'look ahead' of the upcoming environment. The importance of place cell theta sequences in memory encoding and retrieval, and their unique relationship to gamma, are explored in Chapter 3.

The findings from Gupta et al. (2012) also illustrate the concept of information packaging by individual theta cycles. Because theta represents large fluctuations in the excitability of the hippocampal network, information might be naturally segregated by each inhibitory phase of the cycle. This was demonstrated in a study by Jezek et al. (2011), which familiarized rats to two environments that could be instantaneously interchanged, thereby 'teleporting' the rat from one environment to the other. When one environment changed to the other, separate representations of the environments flickered

between separate theta cycles before settling on the representation matching the current environment. This supports the idea that information belonging to one set of stimuli is selectively activated on each theta cycle, and kept separate from other stimuli. This likely represents a broader mechanism in cognitive processing, but might be important for memory function where collections of related stimuli must remain distinct from others.

Gamma

Unlike theta, gamma oscillations are highly variable. Gamma occurs over a wide range of frequencies, ~25–100Hz, and its amplitude fluctuates greatly, making it non-stationary. Gamma also appears during virtually all behavioral states (Buzsaki et al., 1983), making formulation of theories about its function difficult. Anatomically, gamma is ubiquitous across the hippocampal network, but it appears in small, local patches (Sirota et al., 2008). This is in contrast to theta oscillations, which sweep across the hippocampus as a traveling wave (Lubenov and Siapas, 2009; Patel et al., 2012). Interestingly, gamma has a close relationship to theta, appearing as short bursts of activity nested within the comparatively larger theta cycle, with gamma amplitude fluctuating as a function of theta phase (Bragin et al., 1995).

Although theta and gamma co-occur, they are generated by separate mechanisms. A substantial amount of evidence points to rhythmic IPSPs on pyramidal cells from fast spiking interneurons as the primary source of gamma activity. Spike times of interneurons are highly correlated with specific phases of gamma oscillations, as opposed to pyramidal cells which do not fire repetitively in phase with gamma (Buzsaki et al., 1983; Penttonen et al., 1998). Also, reversing the polarity of IPSPs by injecting chloride into pyramidal neurons results in an intracellular gamma oscillation that is coherent with the gamma measured in the LFP (Soltensz and Duschenes, 1993), and intracellular gamma oscillations reverse near the equilibrium potential for chloride (Penttonen et al.,

1998). Moreover, when gamma is induced pharmacologically, it can be blocked by GABA receptor antagonists (Whittington et al., 1995). The exact mechanism by which the rhythmic firing of interneurons is generated is an active area of research, but it may rely on feedback connections within interneuron networks (I-I networks), feedback from pyramidal cells (E-I network), or some combination of both (Buzsaki and Wang, 2012).

The role of inhibition in gamma oscillations has interesting functional implications. Because the majority of the network might be suppressed at any given time, rhythmic and synchronous release from inhibition might serve to group the activity of a small subset of neurons coding related information. Such selective grouping of neurons forms the foundation of the temporal correlation hypothesis, initially proposed by von der Malsburg (1981) as a solution to the well-known 'binding problem' (Rosenblatt, 1962). This concept is perhaps best understood in the hierarchal structure of the visual system. When viewing the world, different features (i.e. color, shape, movement) are processed in parallel by separate regions in the brain, yet we perceive a single cohesive image. Somehow neurons that code the color of an object as red must associate with neurons that code its shape as a square (for example), in order to get the perception of a 'red square'. Representing color and shape by separate regions is thought be more efficient than having a dedicated set of neurons for each color-shape combination, but leaves open the question of how these two sensory features are ultimately linked. The temporal correlation hypothesis posits that synchrony across different neurons serves to bind the associated features. Seminal work from Wolf Singer and colleagues provided evidence that synchrony in the gamma range might underlie this process. In the primary visual cortex, it was shown that two neurons synchronized their firing to gamma when coding a single bar of light passing through their receptive fields, but not when two smaller, separate bars passed through the same path (Gray et al., 1989). The synchrony of the two

neurons was thought to represent binding of the two sides of the bar into a single perceptual item. This process has been described as a dynamical grouping process, in which constellations of neurons that code different features of a stimulus are selectively activated, forming functional *assemblies*. In the hippocampus, this process might occur as a 'winner take all' mechanism, in which the most excited cells selectively activate during the release from inhibition on each gamma cycle (de Almeida et al., 2009). Selective gamma activation in this way might associate the most salient components of a memory, or mediate the activation of specific groups of place cells during spatial processing.

The grouping of place cell assemblies by gamma might also explain how place cell sequences are organized within individual theta cycles (Lisman and Idiart, 1995; Lisman and Jensen, 2013). In this model, individual items of a sequence are coded by distinct place cell assemblies, which are activated on successive gamma cycles nested within the slower theta cycle. In this way, pieces of information are kept separate from one another, and their order is maintained. Interestingly the number of items held in short term memory by an average person corresponds roughly to the number of gamma cycles in each theta cycle (~7) (Lisman and Idiart, 1995), suggesting that theta-nested gamma might play a role in maintaining representations of recent events. This neural code might also be important for retrieving stored sequences from long-term memory, or timing spikes in a way that is optimal for plasticity during memory encoding (Lisman and Jensen, 2013). The idea of a theta/gamma neural code agrees with results from Gupta et al. (2012) that showed that the length of spatial paths represented by theta sequences correlates with the number of gamma cycles in the theta cycle (Gupta et al., 2012). This model is explored further in Chapter 3 with regard to different frequencies of gamma oscillations.

Gamma has also been proposed to facilitate interregional communication through cross-regional coherence. In this idea, the sender and receiver regions of the brain are placed in mutual states of alternating excitation and inhibition through synchronous oscillations, increasing the impact of their communication. This was proposed by Pascal Fries in 2005, as the "communication through coherence" hypothesis. Experimental support for this hypothesis was provided in studies of the cat and monkey visual cortex that showed that gamma power correlations across regions were higher during periods when the gamma phase relationship was optimal and consistent (Womelsdorf et al., 2007). Thus, gamma coherence might provide an important mechanism for selectively routing information between different brain regions, including different subregions of the hippocampal network.

In general, the rapid timescale of gamma has made it an interesting candidate for a variety of functions that require precise temporal coordination and occur beyond the time scale of conscious perception, such as sensory binding, attentional selection of salient stimuli, and episodic memory encoding. A number of human studies have shown an association between gamma activity and episodic memory processing (reviewed in Nyhus and Curran, 2010). However, the exact mechanisms, and the specific roles in different stages of memory function, remain controversial. Recently, a growing body of research has shown that different *frequencies* of gamma oscillations might be selectively involved with different hippocampal subregions, suggesting they might play distinct functional roles. The following section reviews these findings.

1.4 SLOW AND FAST GAMMA

For decades of research, the frequency ranges used to define gamma have varied from lab to lab, including narrow ranges centered around 40 Hz, and larger ranges

spanning ~25–140 Hz. Some evidence has supported the idea that gamma frequency varies as a continuous process depending on behavior (Ahmed and Mehta, 2012). A growing body of research, however, has supported the hypothesis that gamma occurs as two distinct variants – a slow form and a fast form (Figure 1.4).

The first suggestion that the hippocampal network may exhibit different frequencies of gamma oscillations was provided in a study by Bragin et al. (1995), which used current source density (CSD) analysis. This method uses the second spatial derivative of the LFP to estimate spatiotemporal patterns of current flow. CSD analyses suggested that gamma activity was strongest in the terminal zone of perforant path fibers, implying that input from EC is responsible for gamma generation. Accordingly, when EC lesions were performed, gamma activity disappeared in these areas. However, a second source of gamma activity appeared in the terminal zone of the Schaffer collaterals. Interestingly, the average frequency of this gamma activity was significantly lower than the gamma in the terminal zone of EC in control animals. This suggested that a distinct form of gamma may be generated by CA3.

A later study by Colgin et al. (2009) performed paired recordings in areas CA1 and CA3, and in CA1 and the medial entorhinal cortex (MEC). In CA1, the instantaneous frequencies of gamma formed a bimodal distribution, with peaks around ~25–50 Hz and ~60–100 Hz. Moreover, episodes of ~25–50 Hz 'slow' gamma and ~60-100 Hz 'fast' gamma were unlikely to co-occur within the same theta cycle and preferentially occurred at significantly different phases of theta. Also, during periods of slow gamma activity in CA1, there were prominent slow gamma oscillations in CA3 but not in MEC. Instead, when fast gamma oscillations were prominent in CA1, MEC exhibited synchronous fast gamma activity, but much less co-occurring fast gamma activity was observed in CA3. CA3 neurons preferentially spiked at a particular phase (i.e., exhibited 'phase-locking')

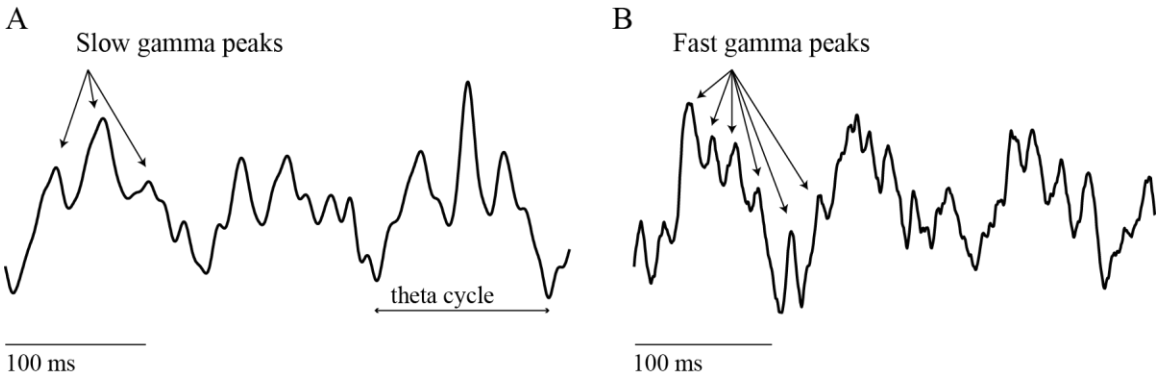

Figure 1.4: Slow and fast gamma rhythms.
Slow gamma (**A**) and fast gamma (**B**) from area CA1 in the hippocampus of a freely behaving rat.

of slow gamma oscillations in CA1, but exhibited significantly less phase-locking to fast gamma in CA1. Conversely, the neurons of layer III MEC were phase-locked to CA1 fast gamma, but not to CA1 slow gamma. Taken together, these results suggested that slow gamma in CA1 was entrained by inputs from CA3, while fast gamma in CA1 was entrained by inputs from layer III MEC.

Subsequent studies have supported this conclusion. Using 2-dimensional electrode arrays, Schomburg and colleagues (2014) showed that fast gamma activity (~60–110 Hz) was strongest in stratum lacunosum-moleculare, the terminal zone of EC input, while slow gamma activity (~30–60 Hz) was strongest in stratum radiatum, the terminal zone of CA3 input (Schomburg et al, 2014). The inputs were found to be segregated by theta phase, and the timing of neuronal activity depended on the strength of each input. Layer specificity of different subtypes of gamma activity was also reported in Belluscio et al. (2012), which showed strong slow gamma (30–50 Hz) activity in stratum radiatum and strong fast gamma (50–90 Hz) activity in stratum lacunosum-moleculare. In a study by Yamamoto and colleagues (2014), fast gamma (~65–120 Hz) activity in CA1 was significantly lower when layer III EC projections were silenced optogenetically and

in transgenic mice in which layer III EC inputs were selectively inhibited. Taken together, the evidence points to the conclusion that gamma occurs as two distinct subvariants – CA3-driven slow gamma (~25–55 Hz) and EC-driven fast gamma (~60–100 Hz).

Separate functions

The distinct anatomical pathways and physiological properties associated with slow and fast gamma suggest that they perform different functions in the hippocampal network. The coordination of activity between CA1 and CA3 by slow gamma might be important for retrieving representations of stored memories from the auto-associative network in CA3. Several lines of evidence support this hypothesis. Tort and colleagues showed that coupling between CA3 slow gamma amplitude and theta phase strongly increased as rats learned to associate an item to a spatial context (Tort et al., 2009). The coupling was positively correlated to memory performance and was strongest during the pre-stimulus period when retrieval of the context-item association was most likely to occur. Similarly, Shirvalkar et al. (2010) reported that stronger coupling between slow gamma and theta predicted successful memory retrieval on a trial-by-trial basis using a match-to-place task in rats. Moreover, pharmacological disruption of theta-slow gamma coupling correlated with impaired memory performance, while stimulation of theta-slow gamma coupling enhanced memory performance. Another recent study found that slow gamma activity increased during the sampling of an odor cue in a delayed spatial alternation task, a time when odor-cued memory retrieval was likely to occur (Takahashi et al., 2014).

In contrast to the above, other studies have reported increases in slow gamma activity during periods of memory encoding. In a novel object recognition task, Trimper et al. (2014) found an increase in CA1–CA3 slow gamma coupling during exploration of

novel objects. Coupling was particularly strong during exploration of objects that were subsequently remembered, implying that memory encoding had taken place. An alternative explanation to encoding, is that memory retrieval of a more general object-place association was taking place, since the animal was previously exposed to multiple trials of novel objects placed in the same location. In another study, slow gamma power increased during exploration of a novel W-maze (Kemere et al., 2013). However, this coincided with a comparable increase in fast gamma power. Also, the animal had previous experience with a different W-maze, making it unclear if memory retrieval was taking place for the previous W-maze environment. In humans, it was found that rhinal-hippocampal coupling in the slow gamma (~40 Hz) range was maximal during encoding of words from a single-trial word list protocol (Fell et al., 2001). In a similar study, gamma activity was highest near the slow gamma range (~54 Hz) during successful encoding of words displayed on a screen (Gruber et al, 2004). However, successful retrieval was also associated with increased gamma activity in the slow gamma range (~49 Hz). Taken together, these results do not indicate a clear relationship between slow gamma and memory encoding or retrieval. It is possible that ambiguities in the behavioral tasks are partly responsible for its association with memory encoding; however, more work is needed to determine if this is the case.

Fast gamma couples CA1 to MEC, which transmits ongoing sensory and spatial experience to the hippocampus (see above). This information might be critical during the encoding of novel experiences and associations. In line with this, Jutras et al. (2009) found an increase in the rhythmic firing of hippocampal cells to fast gamma during successful encoding of novel images in monkeys. In humans, fast gamma activity, but not slow gamma activity, increased during successful encoding of words in a free-recall task (Sederberg et al., 2007). In rats, administration of scopolamine decreased memory

encoding and fast gamma activity, while slow gamma and memory retrieval remained unchanged (Newman et al., 2013). In rats using a place-based navigation strategy, which is thought to rely on current cues from the environment as opposed to stored sequences of locations, fast gamma power was increased relative to slow gamma power in CA1 (Cabral et al., 2014). Also, as previously mentioned, fast gamma activity (along with slow gamma activity) increased during exploration of a novel W-maze in rats (Kemere et al, 2013). Fast gamma might encourage the encoding of novel memory representations by influencing plasticity. The coupling of fast gamma and theta resembles "theta burst stimulation" protocols that exhibit optimal synaptic changes in the hippocampus thought to underlie memory formation (Larson et al., 1986; Larson and Lynch, 1986). Moreover, spike trains firing at gamma frequencies would be spaced ~10 ms apart, a timing which is optimal for spike-timing dependent plasticity (Bi and Poo, 1988).

In contrast to the studies described above, Yamamoto et al. found an association between fast gamma and memory retrieval (Yamamoto et al., 2014). They observed an increase in fast gamma power on the choice point of a delayed spatial alternation task, a location where memory retrieval is thought to take place (Montgomery and Buzsaki, 2007). An alternate explanation proposed by the authors is that fast gamma is important for maintaining previously retrieved memories in working memory, which would be important for decision-making. In agreement with this idea, Schomburg et al. reported an increase in both gamma types during the choice arm of a delayed spatial alternation task, which might represent memory retrieval by slow gamma, rapidly followed by working memory support from fast gamma (Schomburg et al., 2014).

As can be seen, the exact functional roles of slow and fast gamma during memory processing remain controversial. Both gamma types have been observed during memory encoding as well as retrieval, and in a variety of animal models and experimental

paradigms. In addition to the confusion surrounding the association between gamma type and mnemonic function, it also remains unclear how these specific processes are coordinated, and mechanistically, why slow and fast gamma might be optimal for specific mnemonic processes. The research in this dissertation attempts to shed light on some of these questions.

1.5 Overview of dissertation

In this dissertation, I pursue the hypothesis that the hippocampus engages in distinct memory processing modes that are supported by different gamma types. Specifically, it is proposed that memory retrieval is supported by slow gamma, promoting communication of stored information from CA3 to CA1, and that memory encoding is supported by fast gamma, which couples the hippocampus to EC inputs that transmit information about novel experiences.

In Chapter 2, this idea is demonstrated in the coding properties of individual place cells. It is shown that place cells rapidly alternate between distinct spatial coding modes, retrieving upcoming locations during slow gamma and encoding recently visited locations during fast gamma. Using a Bayesian decoding approach, this idea is extended to simultaneously recorded ensembles of place cells, suggesting that these processing states are coordinated across the whole network.

In Chapter 3, spatial paths coded by sequences of place cells are examined during slow and fast gamma. It is shown that sequences represent spatial paths in a temporally compressed fashion during slow gamma, reflecting retrieval of the upcoming trajectory, and that sequences code locations in real-time during fast gamma. Also, place cells code specific locations on different gamma phases within individual slow gamma cycles, offering a potential mechanism for the time-compressed nature of memory retrieval.

In Chapter 4, a novel object recognition task is used to examine whether slow and fast gamma are associated with memory encoding and retrieval at the behavioral level. It is shown that fast gamma is required for encoding of novel object-place associations, while slow gamma CA3-CA1 coupling might be involved with retrieval of familiar object-place associations.

In Chapter 5, the results are summarized and discussed, and key questions are proposed for future study.

Experimental methods

To record electrical activity from the hippocampus, rats were surgically implanted with 'hyperdrives' consisting of 14 independently moveable tetrodes (Gothard et al., 1996), 2 of which were used as references, and 12 of which were used for data collection. After recovery from surgery, tetrodes were slowly lowered into the hippocampus over a period of several days, using anatomical coordinates and characteristic electrical activity as a guide.

Tetrodes are advantageous because they allow the collection of single unit activity in addition to the raw LFP recordings, and their small size minimizes tissue damage. Tetrodes are made of 4 electrically isolated electrodes bundled together, providing 4 simultaneously recorded signals from each tetrode. Because the amplitude of action potentials falls off rapidly with distance, individual cells can be triangulated by comparing the waveform properties of the signals collected from each electrode. In addition to single unit activity and the LFP, the position of the animal is tracked using LED lights on the headstage/pre-amplifier of the hyperdrive. The headstage/pre-amplifier is connected to a lightweight cable that feeds into a data acquisition system, allowing the animal to move freely during behavioral tasks while neural activity is monitored in real

time. The complete methods are described in Appendix A, and the Methods section in each chapter.

Analyses

A periodic signal can be described by three parameters - amplitude, phase, and frequency. When analyzing a neural oscillation, the first parameter usually examined is amplitude, which is typically measured in terms of oscillatory power (Figure 1.5). Power is proportional to the square of the amplitude and roughly indicates how many neurons in the network are participating in the signal. Most LFP signals consist of multiple, superimposed oscillatory components of different frequencies. Commonly, the contribution of each frequency component to the signal is determined by computing the power spectral density (PSD), which provides the power as a function of frequency. In this work, power was computed using a convolving Morlet wavelet (Tallon-Baudry et al., 1997), which provides the power as function of time in addition to frequency. This is important for analyzing gamma oscillations, which are non-stationary, and would likely be averaged out if the time dimension were not considered. Moreover, it facilitates

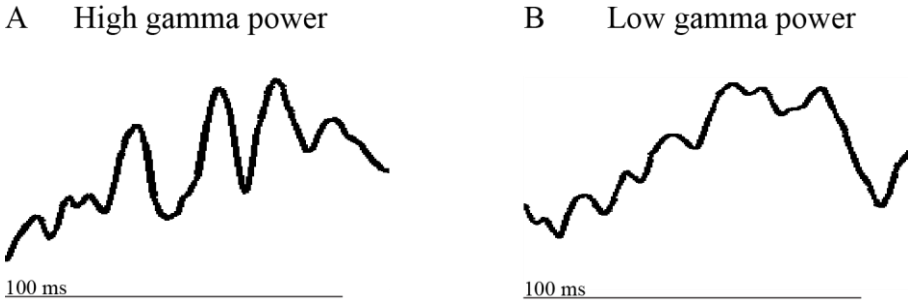

Figure 1.5: Power.
Example CA1 traces with high gamma power (**A**), and low gamma power (**B**).

comparison of power across different time points.

The phase represents the proportion of each cycle that has elapsed and is measured in degrees or radians. The instantaneous phase can be used to determine coupling between two oscillations, measured in terms of phase synchrony (Lachaux et al., 1999) (Figure 1.6). This method computes the difference between the phases of each signal of a particular frequency at each time point, which is called the relative phase. If the relative phases over a given span of time are consistent, then the phase synchrony measure is high, indicating a strong degree of oscillatory coupling. Coupling between different regions might indicate that communication between those regions is enhanced (see discussion of "communication through coherence" hypothesis, above), or selection of specific neuronal assemblies in distributed neurons (see "temporal correlation hypothesis", above).

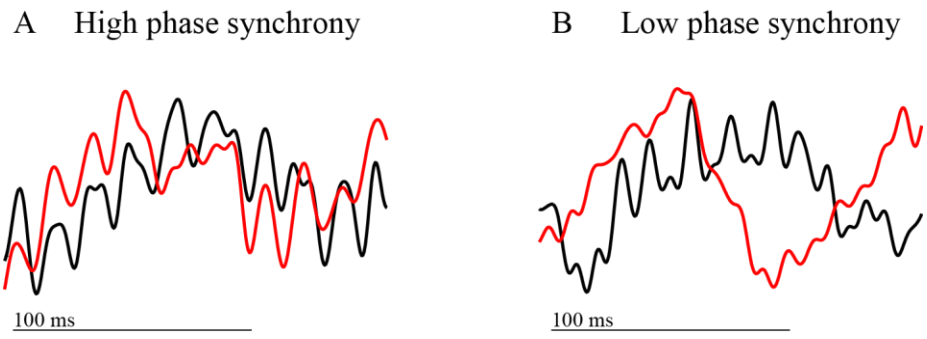

Figure 1.6: Phase synchrony.
High phase synchrony (**A**) and low phase synchrony (**B**) between simultaneous CA1 (black) and CA3 (red) traces. Note the coupling for theta and gamma in (A), which is largely absent in (B).

The phase is also used to determine the degree of phase-locking of single unit activity to a given frequency component (Figure 1.7). This is done by determining the phase of the signal of a particular frequency at each spike time. The consistency of the resulting collection of phases can be measured in terms of mean vector length (MVL) of the phase distribution. A high MVL indicates that the cell was phase-locked to the oscillation, suggesting that the activity of the cell is entrained by the oscillation, and that the cell might be participating in a specific assembly that is coordinated by the oscillation.

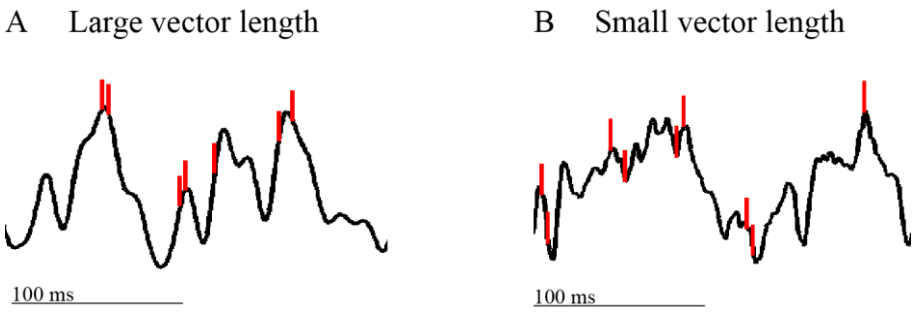

Figure 1.7: Phase locking.
High phase-locking (**A**) and low phase-locking (**B**) for spikes (red lines) to CA1 trace (black lines). Note the spikes in (A) all occur close to gamma peaks, and occur on peaks and troughs in (B).

The spatial firing properties of each cell are characterized by determining the location of the animal at each spike time. The distribution of spiking activity as a function of location can be used to define the place field (Figure 1.2). The peak or center of mass (COM) of this distribution can be used to signify the preferred spiking location of a cell as a single value, which is useful when relating the spatial properties of place cells to other parameters.

Chapter 2: Slow and fast gamma coordinate different spatial coding modes in hippocampal place cells

The following chapter is adapted with permission from: Bieri, K.W., Bobbitt, K.N., and Colgin, L.L. Slow and fast gamma rhythms coordinate different spatial coding modes in hippocampal place cells. Neuron. 82:670-681 (2014). PMCID: PMC4109650. Colgin, L.L. supervised this work. Bobbitt, K.N. helped identify single unit activity in a portion of the data.

2.1 SUMMARY

Previous work has hinted that prospective and retrospective coding modes exist in hippocampus. Prospective coding is believed to reflect memory retrieval processes, whereas retrospective coding is thought to be important for memory encoding. Here, we show in rats that separate prospective and retrospective modes exist in hippocampal subfield CA1 and that slow and fast gamma rhythms differentially coordinate place cells during the two modes. Slow gamma power and phase-locking of spikes increased during prospective coding; fast gamma power and phase-locking increased during retrospective coding. Additionally, slow gamma spikes occurred earlier in place fields than fast gamma spikes, and cell ensembles retrieved upcoming positions during slow gamma and encoded past positions during fast gamma. These results imply that alternating slow and fast gamma states allow the hippocampus to switch between prospective and retrospective modes, possibly to prevent interference between memory retrieval and encoding.

2.2 INTRODUCTION

Place cells are neurons in the hippocampus that fire selectively in specific locations in space that are called 'place fields' (O'Keefe and Dostrovsky, 1971; O'Keefe,

1976). Place cells do not code spatial location uniformly on all traversals through their place fields. Spikes from individual place cells are often 'misaligned' with respect to their average place field (Muller and Kubie, 1989; Battaglia et al., 2004). Place field shifts in the direction opposite to the animal's direction of motion have been termed 'prospective' firing events, and forward shifts in the same direction as the rat's motion have been termed 'retrospective' firing events (Battaglia et al., 2004). Analogous prospective and retrospective firing properties have been observed in grid cells in the medial entorhinal cortex (MEC) (De Almeida et al., 2012). In grid cells, prospective and retrospective coding events have been shown to be coordinated across simultaneously active cells, suggesting that these events reflect different information processing modes in the entorhinal network. The prospective mode may reflect retrieval of stored information, whereas the retrospective mode may serve as a short-term memory buffer that facilitates memory encoding (De Almeida et al., 2012). Considering that prospective and retrospective firing occurs in individual place cells (Muller and Kubie, 1989; Battaglia et al., 2004), it is possible that prospective and retrospective network modes also exist in the hippocampus. In support of this idea, ensembles of place cells represent upcoming positions at some times (Gupta et al., 2012) and represent recent positions at other times (Barbieri et al., 2005; Gupta et al., 2012). If such modes exist in the hippocampal network, a mechanism must exist to ensure that simultaneously active cells carry out the same type of coding at the same time.

One possibility is that gamma rhythms provide a mechanism for coordinating simultaneously active cells during prospective and retrospective coding. Gamma rhythms are thought to coordinate neuronal ensembles by synchronizing the activity of cells that code related information (Bragin et al., 1995; Harris et al., 2003; Fries, 2009; Colgin and Moser, 2010). Additionally, gamma rhythms split into distinct fast and slow subtypes that

differentially route separate streams of information (Colgin et al., 2009). Fast gamma couples the hippocampus with inputs from medial entorhinal cortex (MEC), which convey information about current spatial location (Brun et al., 2002; Fyhn et al., 2004; Hafting et al., 2005) that is necessary for new memory encoding (Brun et al., 2008). Slow gamma rhythms link hippocampal subfield CA1 to inputs from CA3 that appear to play a role in memory retrieval (Brun et al., 2002; Sutherland et al., 1983; Steffenach et al., 2002). Additionally, slow and fast gamma emerge on different phases of the theta rhythms with which they co-occur (Colgin et al., 2009), and encoding and retrieval processes operate most effectively when separated on different phases of theta (Hasselmo et al., 2002).

If fast gamma rhythms regulate the hippocampal network during spatial memory encoding, then fast gamma would be expected to coordinate cell ensembles during retrospective coding. If slow gamma rhythms reflect a memory retrieval mode, then slow gamma would be expected to coordinate cell ensembles during prospective coding. We tested these hypotheses by recording the activity of ensembles of place cells in the hippocampus of rats running on a linear track. We found that CA1 place cells preferentially represent recent locations during fast gamma rhythms and upcoming locations during slow gamma rhythms. These findings provide the first evidence that fast and slow gamma rhythms reflect different spatial memory processing modes in the hippocampal network.

2.3 RESULTS

Spatial coding modes in single units

To investigate whether spatial coding differs during slow and fast gamma rhythms, we recorded neuronal ensembles from the dorsal hippocampus in a group of 5 rats that ran stereotyped paths on a linear track. We first characterized spatial coding in 692 CA1 place cells. We followed a theoretical framework that has been proposed previously (Battaglia et al., 2004; De Almeida et al., 2012). In this framework, prospective coding is defined to occur when a place cell's firing peak is in the first half of the place field, and retrospective coding is defined to occur when the cell mainly fires in the second half of the field (Figure 2.1A). We observed prospective and retrospective coding modes significantly more often in the experimental data than in surrogate data in which spikes were randomly shuffled across runs ($\chi 2(1) = 56.826$, $p < 0.0001$; Figure 2.1B), indicating that coding modes were not merely a random process. Classification of prospective and retrospective coding modes was not affected by inhomogeneous spatial sampling across place fields that overlap with the ends of the track because such fields were excluded from analyses (see Methods). Retrospective and prospective coding events did not reflect position tracking errors because no differences in tracked areas from raw video recordings were observed between prospective, retrospective, and ambiguous events (data not shown, see Bieri et al., 2014). Previous findings have shown that place cells code locations ahead of an animal's actual location when the animal is leaving a reward site and represent locations behind the actual location when the animal is approaching a reward site (Gupta et al., 2012). Consistent with these previous results, we found that prospective coding events tended to occur when rats were leaving a reward location (i.e., the ends of the track), whereas retrospective coding events tended to occur

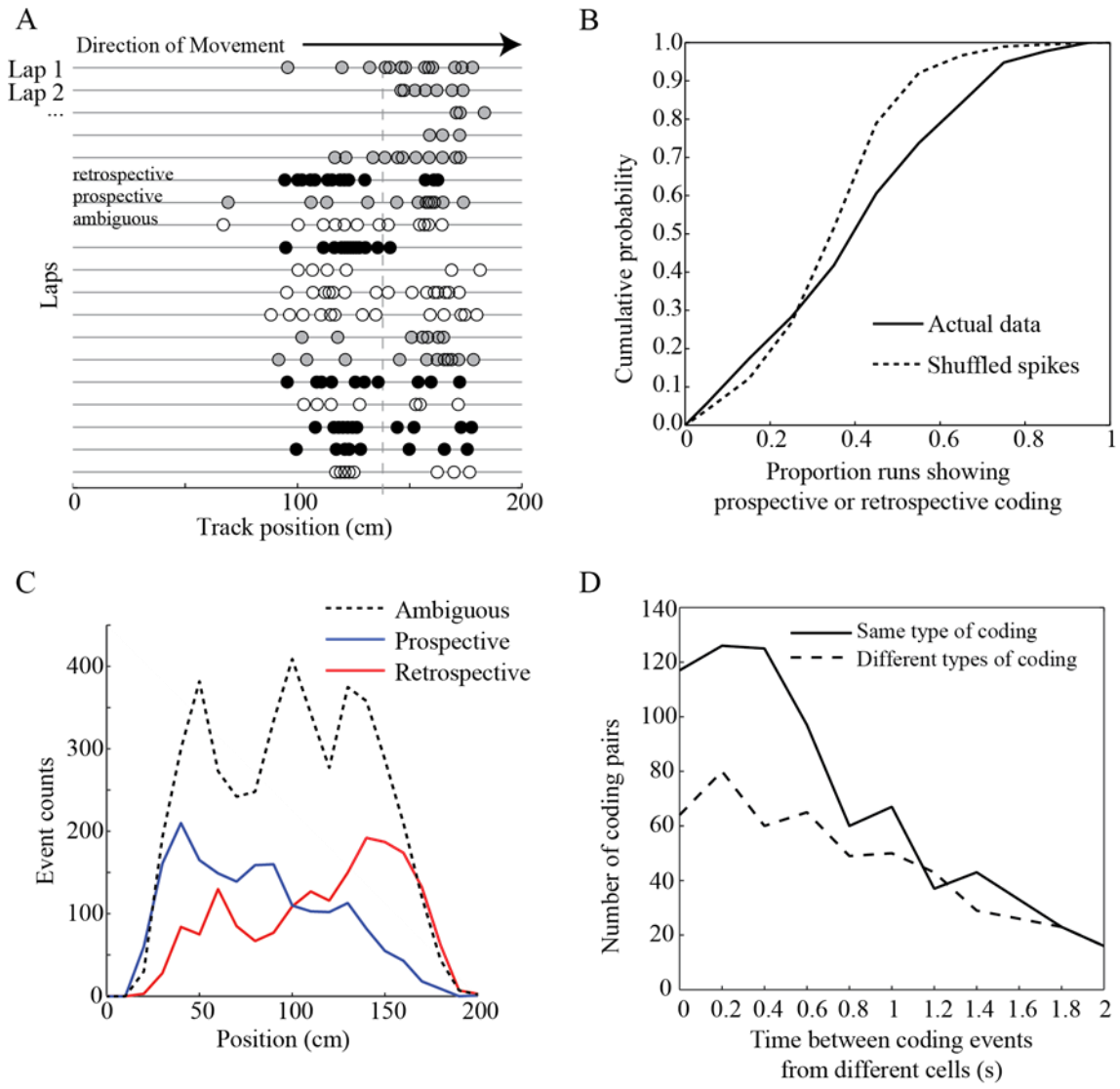
A
Direction of Movement
Lap 1
Lap 2
...
retrospective
prospective
ambiguous
Laps
0
100
200
Track position (cm)
B
Cumulative probability
1.0
0.9
0.8
0.7
0.6
0.5
0.4
0.3
0.2
0.1
0.0
0
0.2
0.4
0.6
0.8
1
Actual data
Shuffled spikes
Proportion runs showing
prospective or retrospective coding
C
Ambiguous
Prospective
Retrospective
Event counts
400
300
200
100
0
0
50
100
150
200
Position (cm)
D
Number of coding pairs
140
120
100
80
60
40
20
0
Same type of coding
Different types of coding
0
0.2
0.4
0.6
0.8
1
1.2
1.4
1.6
1.8
2
Time between coding events
from different cells (s)

Figure 2.1

Figure 2.1: Characterization of spatial coding modes.
A. Individual spike positions for an example CA1 place cell recorded in a rat running on a linear track. Successive laps in the rightward direction are shown for a 10 min session. The mean field position across all laps is indicated with a vertical dashed line. Passes through a place field were classified as ‘‘prospective’’ (black circles) if greater than or equal to two-thirds of spikes were in the first half of the field and ‘‘retrospective’’ (gray circles) if greater than or equal to two-thirds of spikes were in the second half of the field. Passes that did not fall under either of these definitions were classified as ambiguous (white circles). **B.** Prospective and retrospective coding occur more often than expected by chance. A greater proportion of runs exhibit some type of coding mode, either prospective or retrospective, in the actual data compared to shuffled data, in which a larger number of ambiguous runs occur. **C.** Prospective and retrospective coding events correlate with different locations on the linear track. Prospective coding events tended to occur as rats were leaving the end of the track. Retrospective coding events tended to occur as rats approached the end of the track. Ambiguous events were observed more often than prospective and retrospective events and occurred on both the ends and the middle of the track. **D.** Prospective and retrospective coding events were detected for all recorded CA1 place cells. Successive coding events from place cell pairs were likely to be of the same type if they occurred closely in time (i.e., <0.8 s).

as rats approached a reward location (Figure 2.1C).

We next investigated whether the occurrence of prospective and retrospective coding modes was correlated across different cells, as has been shown for grid cells in MEC (De Almeida et al., 2012). We found that pairs of cells were likely to exhibit the same type of coding when the time interval between traversals through the cells' place field centers was relatively short. When two cells fired within time windows of less than 800 ms, cell pairs exhibited the same type of coding significantly more often than they exhibited different types of coding (Figure 2.1D; $c2(1) = 15.5$, $p = 0.0001$ for t = 0–200 ms; $c2(1) = 10.3$, $p = 0.001$ for t = 200– 400 ms; $c2(1) = 22.8$, $p = 0.0001$ for t = 400–600 ms; $c2(1) = 6.3$, $p = 0.01$ for t = 600–800 ms). This indicates that the majority of cells that are active at the same time engage in the same type of coding, either prospective or retrospective, and that prospective and retrospective coding modes are coordinated across the CA1 network. The timescale of this coordination is similar to the timescale of switching between slow and fast gamma states in the hippocampus (Colgin et al., 2009). Moreover, local field potentials (LFPs) should reflect activity in the majority of neurons that show coordinated coding more than activity in the minority of neurons that do not show coordinated coding. Therefore, we set out to examine the hypothesis that slow and fast gamma rhythms coordinate place cells during prospective and retrospective coding at the level of single units and cell ensembles.

Spatial coding modes during slow and fast gamma

To investigate whether slow and fast gamma rhythms coordinate single-unit firing during prospective and retrospective coding, we first quantified the power of slow and fast gamma rhythms in CA1 stratum pyramidale during prospective and retrospective

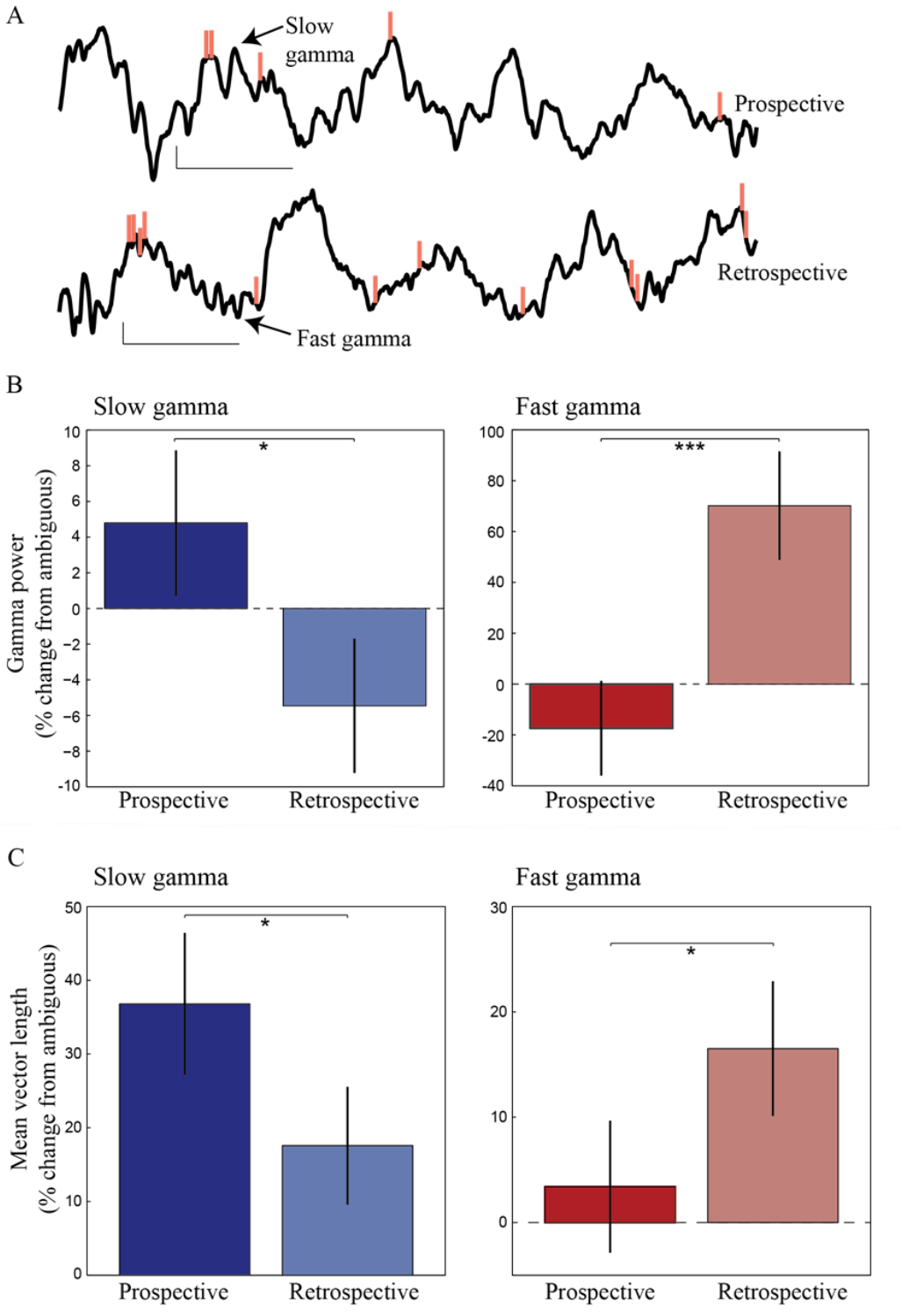
A
Slow
gamma
Prospective
Retrospective
Fast gamma
B
Slow gamma
Fast gamma
Gamma power
(% change from ambiguous)
*
***
Prospective
Retrospective
C
Mean vector length
(% change from ambiguous)
*
*

Figure 2.2

Figure 2.2: Slow and fast gamma during spatial coding modes.
A. Example LFP recordings from CA1 stratum pyramidale are shown with corresponding spikes from an example place cell (orange vertical lines, same place cell as shown in Figure 2.1A). Slow gamma during a prospective coding event is shown above, and fast gamma during a retrospective coding event is shown below (calibration: 100 ms, 0.2 mV). The top recording corresponds to one of the prospective coding events shown in Figure 2.1A (fifth row from the bottom), and the bottom recording corresponds to a retrospective coding event in Figure 2.1A (fifth row from the top). **B.** Slow (blue) and fast (red) gamma power in CA1 during prospective and retrospective coding events. Power is plotted as the percent change (mean ± SEM) relative to power during ambiguous runs. Slow gamma power was higher during prospective coding than during retrospective coding. Fast gamma power was greater for retrospective coding compared to prospective coding. **C.** Phase locking of interneuron spike times (mean ± SEM) to slow and fast gamma during prospective and retrospective coding events. Slow gamma phase locking was greater during prospective coding than during retrospective coding. Fast gamma phase locking was greater during retrospective coding than during prospective coding.

events in individual cells (Figures 2.2A and 2.2B). We found that slow and fast gamma power were differentially enhanced depending on the type of coding that was occurring (interaction between gamma type and coding type: two-way repeated-measures ANOVA, $F(1, 3{,}642) = 20.0$, $p = 0.0001$). Slow gamma power was significantly higher during prospective coding modes than retrospective coding modes ($t(3{,}642) = 2.1$, $p = 0.04$). In contrast, fast gamma power was significantly higher during retrospective coding events (prospective versus retrospective: $t(3{,}642) = 3.5$, $p = 0.0004$). These differential effects of prospective and retrospective coding on slow and fast gamma power are consistent with the hypothesis that slow and fast gamma coordinate cells during prospective and retrospective coding, respectively. Interestingly, a significant main effect of gamma type was also found ($F(1, 3{,}642) = 1{,}477.1$, $p = 0.0001$), indicating that fast gamma power increases during retrospective coding were significantly greater than slow gamma power increases during prospective coding. This may suggest that many place cells become synchronized by fast gamma during retrospective coding, while perhaps a more limited number of place cells get recruited by slow gamma during prospective coding.

‘‘Ambiguous’’ runs are runs in which approximately equal numbers of spikes occurred in the first and second halves of the place field. Such runs could reflect a switch from prospective to retrospective coding as the rat passed through the field. We thus analyzed whether slow and fast gamma power changed between the first and second halves of place fields during ambiguous runs. We found that slow gamma power was significantly greater in the first half of place fields than in the second half (two-tailed paired t test: $t(4{,}417) = 2.65$, $p = 0.01$; Figure 2.3A). However, no difference in fast gamma power was observed between the first and second halves of place fields ($t(4{,}417) = 0.34$, $p = 0.7$). These findings imply that slow gamma in ambiguous runs may be slightly stronger during the early component of a cell’s place field compared to the later

component. However, fast gamma occurs evenly in both the initial and late parts of a place field when spikes occur across the entire field.

CA1 gamma rhythms reflect rhythmic inhibitory potentials in pyramidal neurons produced by rhythmic firing of GABAergic interneurons (Soltesz and Deschenes, 1993; Penttonen et al., 1998). We investigated whether putative interneurons exhibited slow gamma rhythmic firing during prospective coding and fast gamma rhythmic firing during retrospective coding. We analyzed slow and fast gamma phase locking in 201 putative interneurons in CA1 that were recorded simultaneously with CA1 place cells. We found that the degree of gamma phase locking seen in interneurons during prospective and retrospective coding events was different for slow and fast gamma rhythms (Figure 2.2C; interaction between gamma type and coding type: two-way repeated-measures ANOVA, $F(1, 502) = 12.2$, $p = 0.001$). Interneurons were significantly more phase locked to slow gamma rhythms during prospective coding (prospective versus retrospective: $t(502) = 2.0$, $p = 0.05$) and fast gamma rhythms during retrospective coding (prospective versus retrospective: $t(502) = 1.9$, $p = 0.05$; Figure 2.3B). Analogous results were not obtained for individual place cells. Because of the low firing rate of place cells compared to interneurons, the low number of spikes remaining after selection of spikes during periods of prospective or retrospective coding probably prevented effective detection of phase locking. Moreover, previous work indicated that spikes occurring during slow and fast gamma periods must first be selected in order to reliably detect slow and fast gamma phase locking in place cells (Colgin et al., 2009). This is because slow and fast gamma rhythms are not stationary across time (i.e., not continuously present), and thus many phase estimates are meaningless if slow and fast gamma are not preselected (Colgin et al., 2009). Preselection of slow and fast gamma spikes was not possible in this analysis because spikes were selected for each place field traversal (i.e., for prospective and

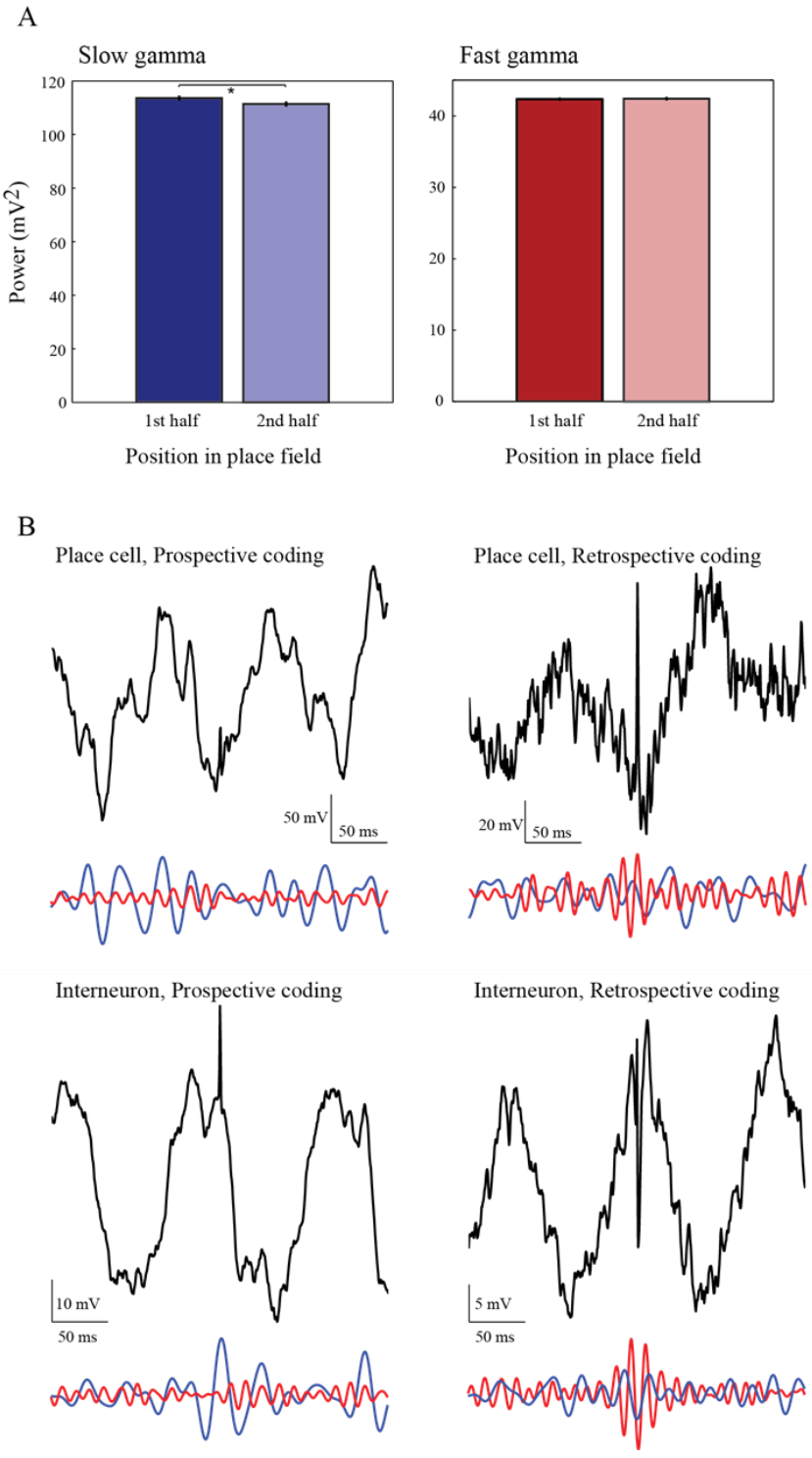
A
Slow gamma
Fast gamma
Power (mV2)
120
100
80
60
40
20
0
40
30
20
10
0
*
1st half
2nd half
Position in place field
B
Place cell, Prospective coding
Place cell, Retrospective coding
50 mV
50 ms
20 mV
50 ms
Interneuron, Prospective coding
Interneuron, Retrospective coding
10 mV
50 ms
5 mV
50 ms

Figure 2.3

Figure 2.3: Slow and fast gamma during place cell and interneuron activity.
A. Slow and fast gamma power during the first and second halves of place fields during ambiguous runs. Slow and fast gamma power were measured during the first and second halves of place fields during runs that were classified as ambiguous. Slow gamma power was larger during the first half of place fields compared to the second half. No difference in fast gamma power was observed between the early and late portions of place fields. **B.** Spike-triggered averages (STAs) of LFP recordings for example place cells and interneurons during periods of prospective and retrospective coding. For each example, raw traces are shown above, and bandpass filtered versions are shown below (blue: 25-55 Hz, red: 60-100 Hz). Note how robust slow gamma rhythms can be seen in the STAs during prospective coding, and fast gamma rhythms can be seen in the STAs during retrospective coding.

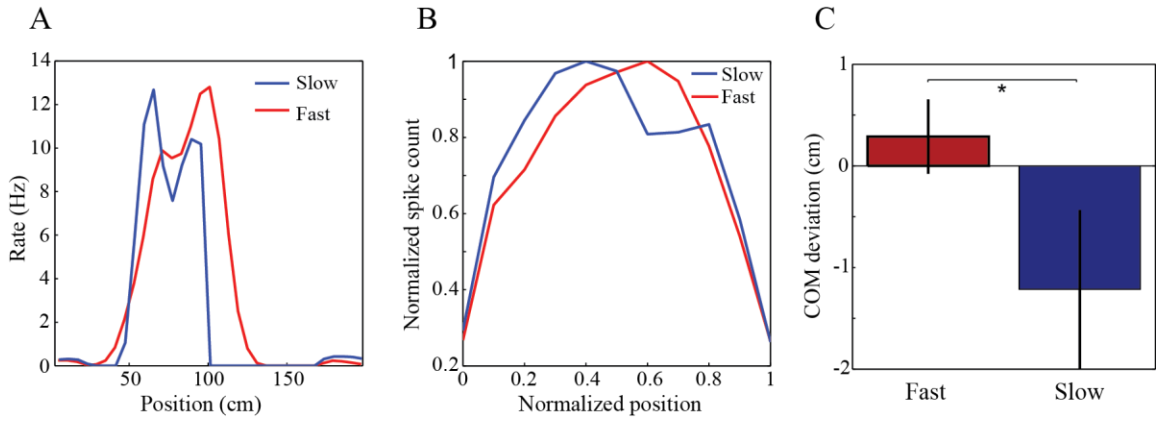

Figure 2.4: Place fields during slow and fast gamma.
A. Rate maps constructed for spikes occurring during slow and fast gamma for an example CA1 place cell from a rat running in the rightward direction. **B.** Spike counts across position combined for all spikes from all cells, subsampled for non-overlapping slow and fast gamma periods. Spike counts were normalized according to each cell's maximum, and the x axis shows normalized position within each cell's place field (ranging from 0 to 1). Leftward runs were reversed so that place fields from runs in both directions could be combined, such that animals were running from position = 0 to position = 1 in all cases. **C.** Center of mass (COM) deviations (mean ± SEM) for place fields subsampled for non-overlapping slow and fast gamma periods. Zero represents the place field COM for all spikes. Place field COMs were shifted significantly forward during fast gamma compared to place field COMs during slow gamma.

retrospective coding events), not according to the presence of slow or fast gamma.

The above results raise the possibility that spatial representations in place cells differ during slow and fast gamma states. We investigated this possibility by comparing place fields during slow and fast gamma. We found that the center of mass for place fields during slow gamma was shifted 1.2 ± 9.4 cm before the overall place field center (i.e., the center of mass of the place field constructed from all spikes). The center of mass for fast gamma-associated place fields was shifted 0.3 ± 5.5 cm after the overall place field center (fast gamma center of mass after slow gamma center of mass: $t(368) = 1.9$, $p = 0.05$; Figure 2.4). The backward shift observed during slow gamma is reminiscent of the backward shift that CA1 place fields develop within the first few track laps each day

(Mehta et al., 1997, 2000; Lee et al., 2004). Consistent with this earlier research, few prospective coding events were observed during the first minute on the track each day (Figure 2.5A). However, the probability of observing slow gamma was high during this same time period (Figure 2.5B), which was surprising considering that increases in slow gamma power were associated with prospective coding when all laps across all recording sessions were analyzed (Figure 2.2B; see Discussion).

Theta phase precession during slow and fast gamma

The above results indicate that place cells tend to code upcoming places during slow gamma and recent places during fast gamma. Place cell spikes occur on earlier and earlier phases of theta as a rat progresses through a cell's place field in a phenomenon termed ''theta phase precession'' (O'Keefe and Recce, 1993; Skaggs et al., 1996). Theta phase precession has been proposed to represent a prospective network mode involving the cued retrieval of upcoming places (Tsodyks et al., 1996; Jensen and Lisman, 1996, 2005; Lisman and Redish, 2009), as well as a mechanism for compressing spatial

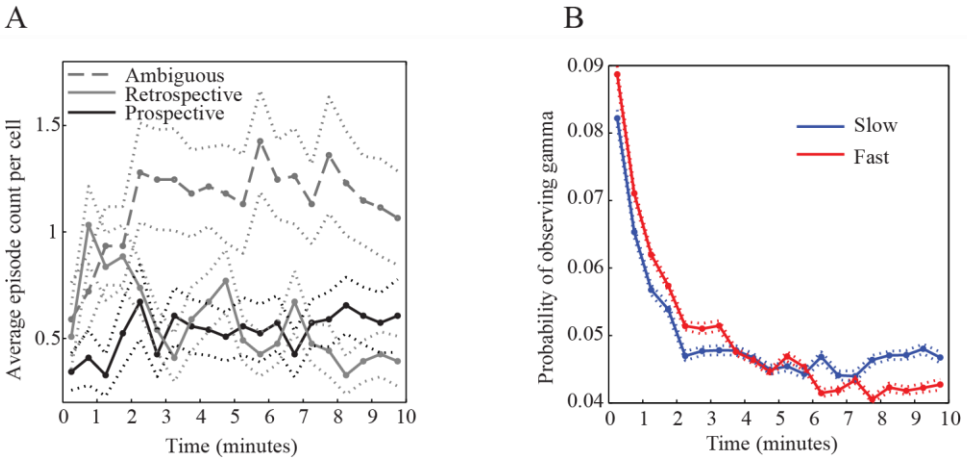

Figure 2.5: Time course of coding events and gamma.
A. The mean (±SEM) distribution of ambiguous, retrospective, and prospective coding events during the first 10 min session of each day is shown. **B.** The mean (±SEM) probability of detecting slow and fast gamma episodes across the first 10 min recording session for each day is shown.

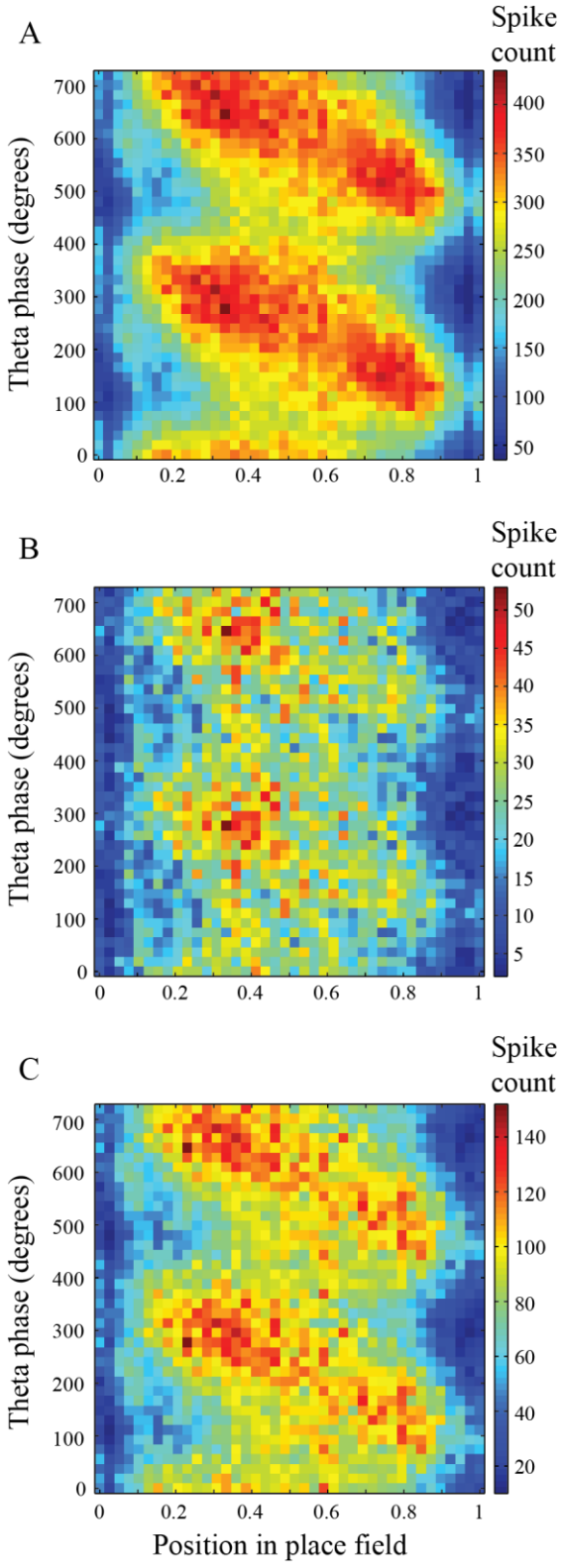

Figure 2.6: Theta phase precession during slow and fast gamma.
For each panel, normalized position within the place field is plotted on the x axis, and the theta phase at which each spike occurred is plotted on the y axis. **A.** Theta phase precession is depicted for all spikes. **B.** The relationship between theta phase and position is shown during periods of slow gamma. Note how spikes primarily occur in the first half of the place field. **C.** The relationship between theta phase and position is shown during periods of fast gamma. Spikes occur across the full range of positions and theta phases. Note that spike counts in (B) and (C) do not sum to spike counts in (A) because (A) also includes periods when neither fast nor slow gamma was detected.

sequences into a temporal structure that is ideal for memory encoding (Skaggs et al., 1996). We examined the relationship between theta phase and position for spikes emitted during periods of slow and fast gamma and combined the data across all place cells and all animals (Figure 2.6). As expected, normal theta phase precession was observed when all spikes were included (Figure 2.6A). Remarkably, we found that slow gamma spikes did not tend to occur across the full range of theta phases and positions within the place field but instead tended to be restricted to late theta phases and early portions of the place field (Figure 2.6B). On the other hand, spikes emitted during fast gamma periods occurred across all positions and displayed theta phase precession (Figure 2.6C). Theta phase distributions during slow gamma periods and fast gamma periods were significantly different when all phases were considered (Watson-Williams test, $F(1, 80{,}725) = 123.7$, $p = 0.0001$) and when data were randomly downsampled such that each cell had an equal number of phase estimates during slow and fast gamma periods (Watson-Williams test, $F(1, 35{,}563) = 59.9$, $p = 0.0001$). Moreover, the correlation between phase and position differed depending on whether slow or fast gamma was present ($F(2,2{,}004) = 15.6$, $p = 0.0001$) and was significantly higher for periods of fast gamma compared to periods of slow gamma ($t(1{,}192) = 3.2$, $p = 0.002$). These differences again remained significant when data were randomly downsampled such that each cell had an equal number of theta phase estimates for slow and fast gamma ($F(2, 948) = 13.0$, $p = 0.0001$; correlation between phase and position greater for fast gamma compared to slow gamma: $t(474) = 3.4$, $p = 0.001$). These effects did not appear to be due to discrepancies in theta phase estimation resulting from theta power and frequency differences between track positions associated with slow and fast gamma (data not shown, see Bieri et al., 2014).

Controlling for other factors

Were differences in spatial coding during slow and fast gamma simply a side effect of the relationship between running speed and gamma frequency (Ahmed and Mehta, 2012)? This is unlikely for several reasons. Running speeds on the linear track follow a stereotypical pattern in well-trained rats: rats begin each lap slowly, reach maximal speed in the middle of the track, and then slow down again before reaching the other end (Figure 2.7). If slow and fast gamma effects merely reflected changes in running speed, we would expect to observe slow gamma at the ends of the track and fast gamma in the center of the track. In contrast, we found that both slow and fast gamma tended to occur near the ends and in the middle of the track (Figure 2.7). Additionally, we accounted for running speed using a general linear model with gamma power as a repeated factor and running speed as a covariate. Accounting for the interaction between gamma type and running speed, and accounting for running speed, we found that the

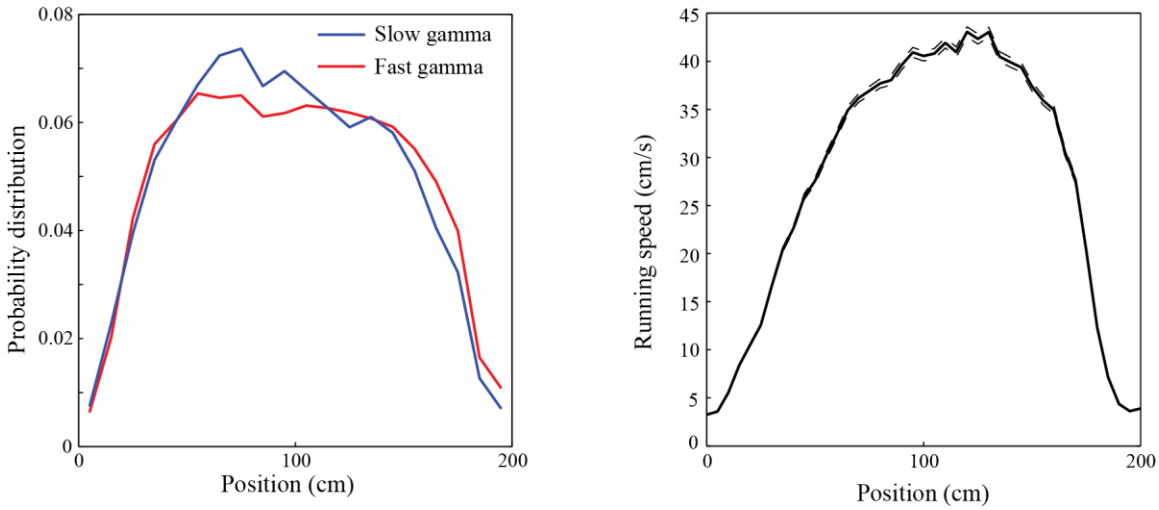

Figure 2.7: Gamma and running speed at different track locations.
(Left) The probability of slow and fast gamma occurrence is plotted against position on the linear track. Probabilities were dwell time normalized. Leftward runs were reversed, so that the direction of rat movement is from 0 cm to 200 cm. (Right) Mean running speed (± 95% confidence intervals) is plotted against position on the linear track. Note how locations where slow and fast gamma tended to occur on the linear track cannot be explained by correlations between gamma frequency and running speed (Ahmed and Mehta, 2012).

interaction between gamma type and coding type remained significant ($F(1, 3{,}641) = 24.891$, $p < 0.0001$). Lastly, we matched prospective and retrospective coding events according to running speed and found that the slow and fast gamma effects persisted. Specifically, a significant interaction between coding type and gamma type was again observed ($F(1, 3{,}446) = 25.508$, $p < 0.0001$). Post hoc testing showed that slow gamma during prospective coding exhibited greater power than during retrospective coding ($t(1{,}723) = 2.00$, $p = 0.05$), and fast gamma exhibited higher power for retrospective coding compared to prospective coding ($t(1{,}723) = 4.34$, $p < 0.0001$). Our results were also not explained by differences due to track location because effects remained significant when the location of each coding event was included as a covariate (gamma type by coding type interaction: $F(1, 3{,}641) = 22.88$, $p < 0.0001$) and when data were randomly downsampled such that each location exhibited equivalent amounts of each coding type ($F(1, 2{,}536) = 11.88$, $p < 0.001$).

Spatial coding at the ensemble level during slow and fast gamma

The above results imply that slow and fast gamma rhythms coordinate prospective and retrospective coding, respectively, in place cells. Yet, the above results were obtained

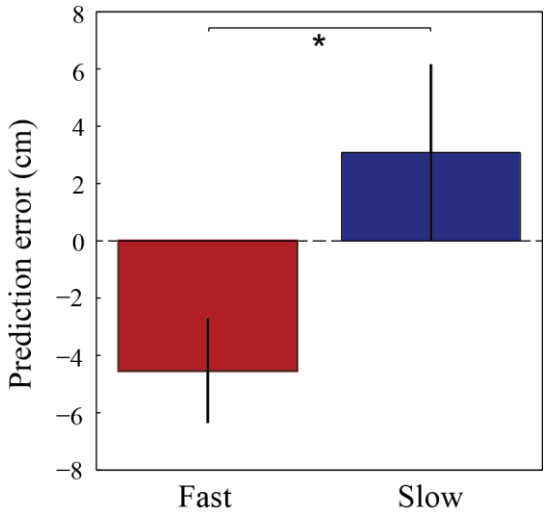

Figure 2.8: Reconstruction errors during slow and fast gamma. Reconstruction, or prediction, errors are defined as the difference between the position estimated by Bayesian decoding and the animal's actual position. Prediction errors (mean ± SEM) were negative on average during fast gamma and positive on average during slow gamma. Negative prediction errors indicate that the decoded position is behind the actual position, whereas positive prediction errors indicate that the decoded position is ahead of the actual position.

from isolated single units and did not directly address the question of whether slow and fast gamma rhythms coordinate spatial coding at the network level. To address this question, we detected theta cycles containing sequences of active place cells (‘‘theta sequences’’) and employed Bayesian decoding (Brown et al., 1998; Zhang et al., 1998; Jensen and Lisman, 2000) to estimate the spatial trajectory represented by the spikes in each theta sequence (as in Gupta et al., 2012). We then measured the prediction error (i.e., predicted position – actual position) for theta sequences associated with slow and fast gamma. We found that prediction errors during slow and fast gamma were significantly different ($t(511) = 2.1$, $p = 0.04$; Figure 2.8), with slow gamma associated with positive prediction errors (3.1 ± 50.2 cm) and fast gamma associated with negative prediction errors (4.5 ± 28.8 cm). We then compared slow and fast gamma during theta sequences having cumulative prediction errors less than or greater than zero and found significantly greater fast gamma power for negative prediction errors ($t(51,648) = 10.6$, $p < 0.0001$). We found a trend toward higher slow gamma power for positive prediction errors compared to negative prediction errors ($t(51,648) = 1.7$, $p = 0.09$). However, when we omitted theta cycles with prediction errors close to 0 cm and examined those theta cycles with prediction errors greater than 1 cm or less than 1 cm, slow gamma power was significantly higher for positive errors compared to negative errors ($t(49,216) = 2.1$, $p = 0.04$) and, again, fast gamma power was significantly greater for negative errors than for positive errors ($t(49,216) = 10.5$, $p < 0.0001$). The slow gamma effect became more pronounced when only those theta cycles with prediction errors greater than or less than 2 cm were considered (slow gamma power significantly higher for positive errors than negative errors: $t(46,127) = 2.5$, $p = 0.01$; fast gamma power significantly higher for negative errors than positive errors: $t(46,127) = 10.1$, $p < 0.0001$). Examples of theta sequences showing positive and negative prediction errors associated with slow and fast

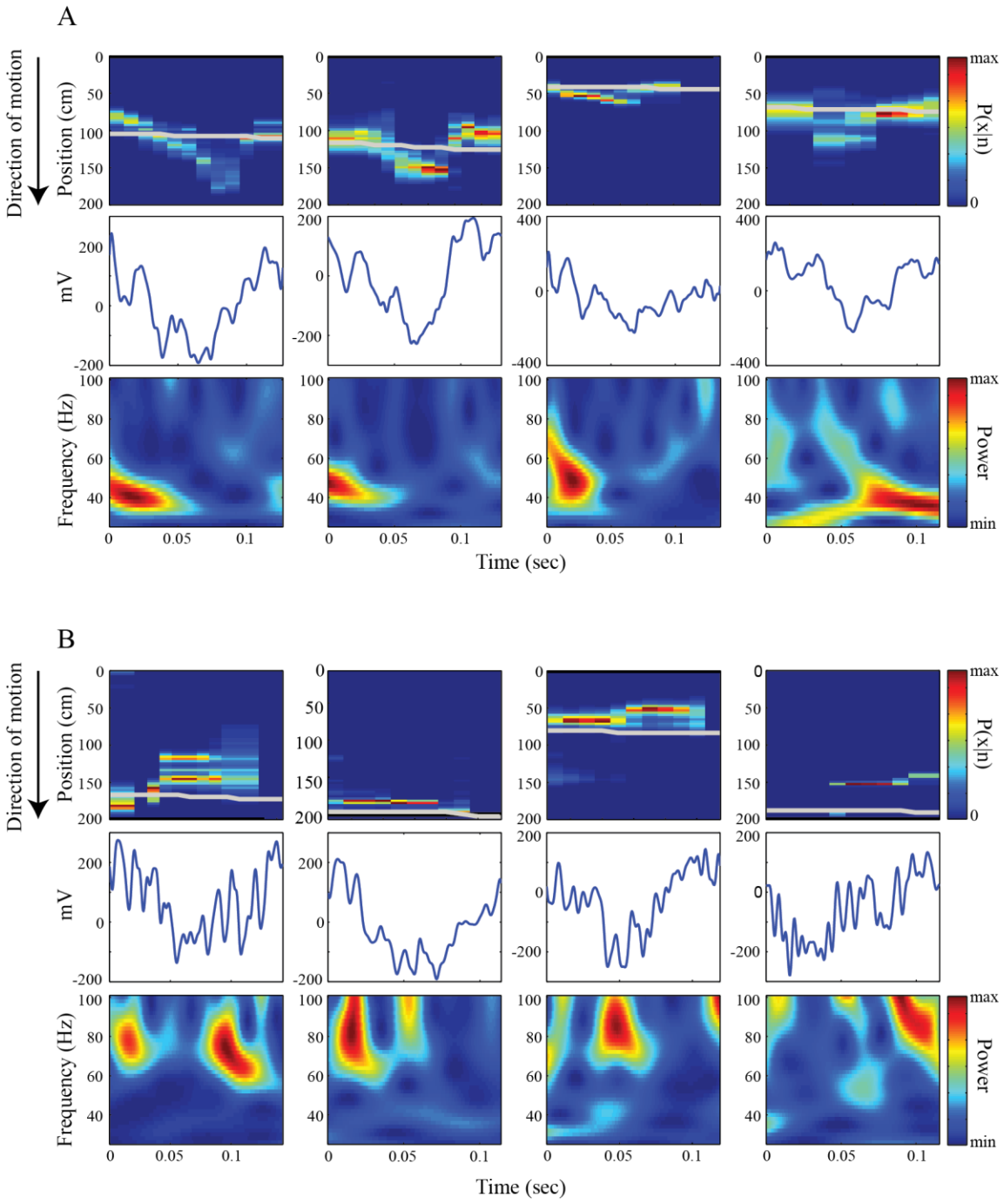
A
Direction of motion
Position (cm)
mV
Frequency (Hz)
Time (sec)
P(x|n)
max
0
Power
max
min
B
Direction of motion
Position (cm)
mV
Frequency (Hz)
Time (sec)
P(x|n)
max
0
Power
max
min

Figure 2.9

Figure 2.9: Examples of reconstructed positions from theta cycles.
Top: Bayesian decoded spatial probability distributions for example theta cycles (raw traces shown in middle panels); the gray line indicates the rat's actual position. Rats were running from 0 to 200 cm. Bottom: color-coded power across time (x axis) for the range of gamma frequencies (y axis). **A.** Examples showing positive prediction errors associated with slow gamma. **B.** Examples showing negative prediction errors associated with fast gamma.

gamma, respectively, are shown in Figure 2.9. Note how theta sequences associated with positive prediction errors (i.e., predicted position ahead of the actual position; Figure 2.9A) resemble ‘‘ahead sequences’’ that have been reported previously by Gupta and colleagues (2012) to occur predominantly as animals leave reward sites. Such sequences may be related to sequences that reactivate during sharp waves (Carr et al., 2012). On the other hand, theta sequences that are associated with negative prediction errors (i.e., predicted position behind the actual position, Figure 2.9B) match ‘‘behind sequences,’’ which have been reported to occur as animals approach reward sites (Gupta et al., 2012). In the current study, reward sites were located at the ends of the track. The present data are consistent with the findings of Gupta and colleagues because positive prediction errors tended to occur (Figure 2.10A), and slow gamma occurred more often than fast gamma (Figure 2.10B), as rats left the end of the track. On the other hand, as rats approached the end of the track, negative prediction errors were more prevalent, and fast gamma occurred more often than slow gamma.

Theta modulation of slow and fast gamma

Earlier findings indicated that both slow and fast gamma are modulated by theta phase but tend to occur on different theta phases and cycles (Colgin et al., 2009). Consistent with these earlier findings, plotting gamma power within individual theta cycles revealed theta phase locked slow gamma as rats began a track run and theta phase locked fast gamma as rats ended a track run (Figure 2.11). Moreover, slow gamma was most strongly phase locked to theta during prospective coding events (mean vector length [MVL] = 0.035) compared to retrospective coding events (MVL = 0.002) and ambiguous events (MVL = 0.022). On the other hand, fast gamma exhibited strongest phase locking to theta during retrospective events (MVL = 0.025) compared to prospective (MVL = 0.011) and ambiguous (MVL = 0.012) events. These results suggest that the phenomena

reported above involve theta-modulated slow and fast gamma rather than slow and fast gamma in isolation.

2.4 Discussion

The present results suggest that distributed place cells participate in distinct network processing modes that alternate according to whether slow and fast gamma rhythms are present. The results indicate that the slow and fast gamma modes coordinate place cell assemblies during prediction of upcoming locations and encoding of recent locations, respectively. Similarly, alternating prospective and retrospective modes have been reported in entorhinal cortex grid cells (De Almeida et al., 2012), but they were not

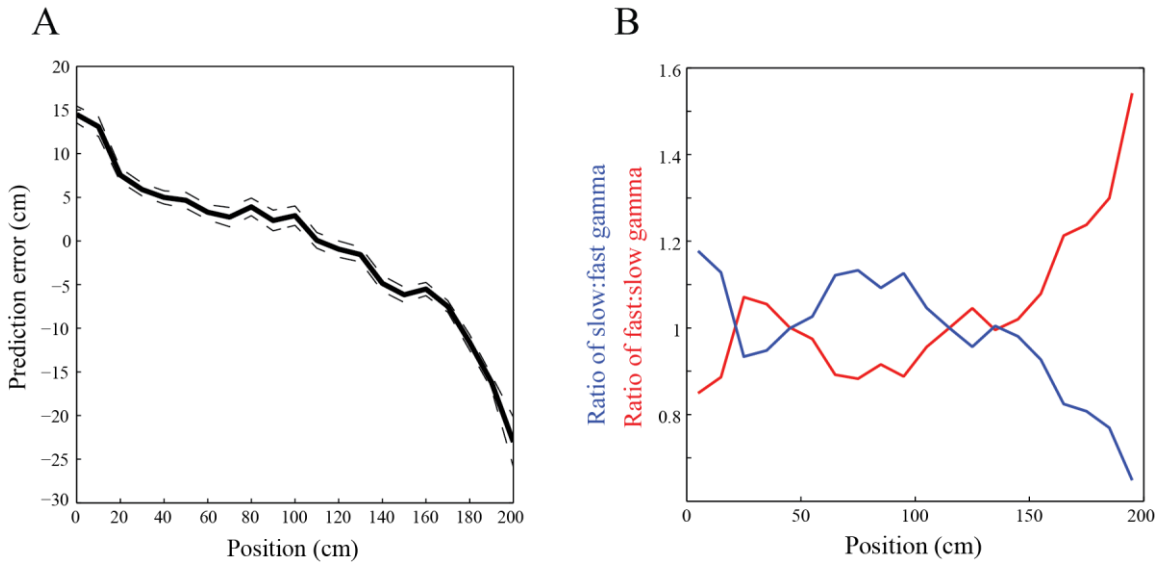

Figure 2.10: Prediction errors and gamma at different track locations.
Leftward runs were reversed. **A.** Mean prediction errors ± 95% confidence intervals are plotted against position on the track. Note that positive prediction errors were associated with positions where rats were leaving the end of the track, and negative prediction errors were associated with positions where rats were approaching the end of the track. **B.** The ratio of the probability of slow gamma occurrence to the probability of fast gamma occurrence (blue) and the ratio of the probability of fast gamma occurrence to the probability of slow gamma occurrence (red) are plotted against position on the track. Note that these results are a transformed version of what is shown in the left panel of Figure 2.7.

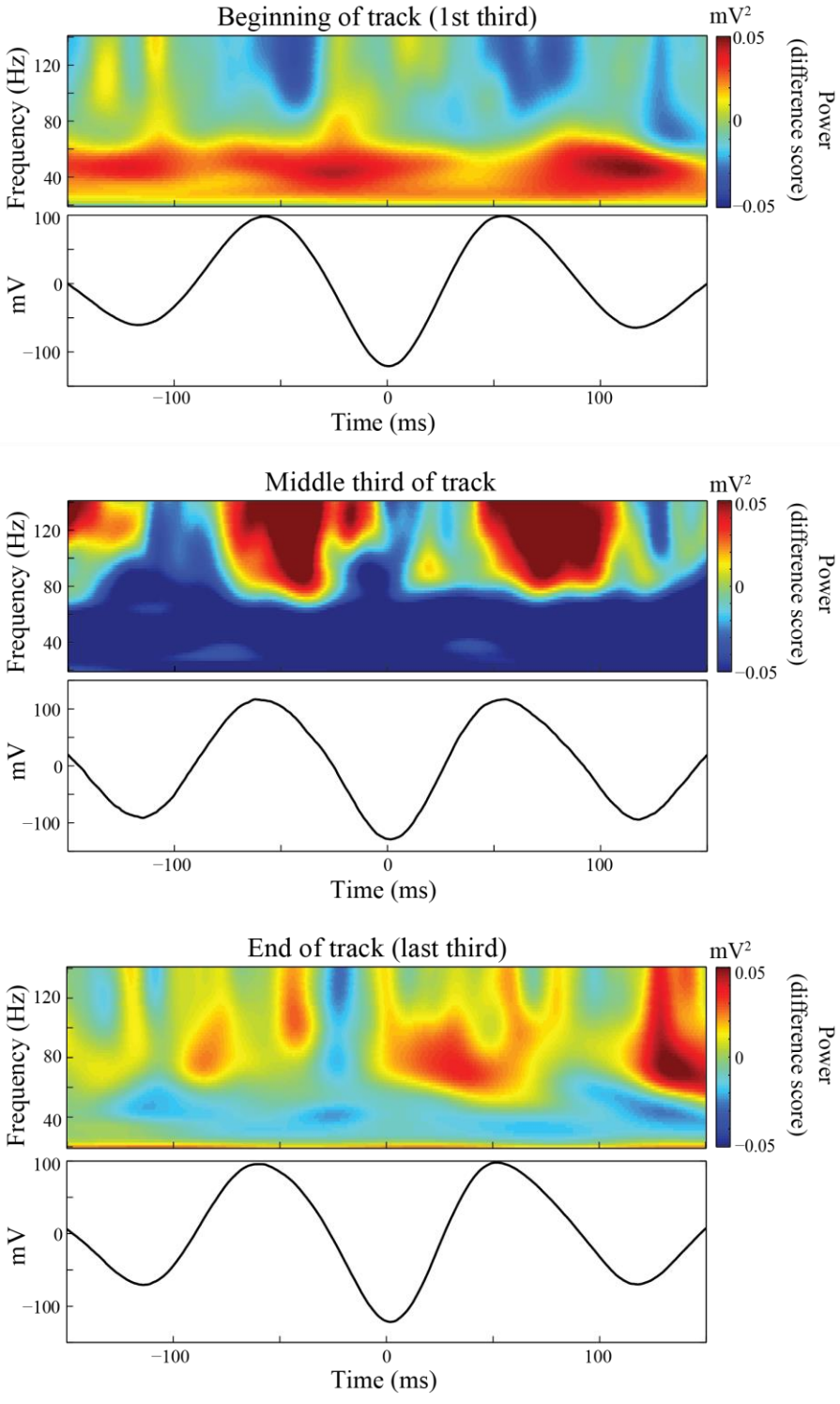
Beginning of track (1st third)
Middle third of track
End of track (last third)
Frequency (Hz)
120
80
40
mV²
0.05
0
−0.05
Power
(difference score)
100
0
−100
mV
−100
0
100
Time (ms)

Figure 2.11

Figure 2.11: Theta-locked spectral averages at different track locations.
For the beginning (top panels), middle (middle panels), and end (bottom panels) of the linear track, color-coded power across time (x-axis) and frequencies (y-axis) is shown above corresponding averaged theta cycles (averaged across all recordings in all animals). Power is shown as a difference score (i.e., average power across the whole track was subtracted from power for each third of the track). Slow and fast gamma both phase-lock to theta but tend to occur at different theta phases, as reported previously (Colgin et al., 2009). Note how slow and fast gamma are stronger at the start and end of the track, respectively, consistent with results shown in Figure 2.10B. Power observed in the middle third of the track peaks at frequencies >100 Hz, extends above 140 Hz, and likely reflects neuronal spiking (Belluscio et al., 2012).

linked to any type of oscillation. These prospective and retrospective coding modes are believed to reflect distinct memory processing states in the entorhinal-hippocampal network. Prospective coding is reminiscent of the backward expansion of CA1 place fields that develops with experience (Mehta et al., 1997, 2000; Lee et al., 2004). Development of such expansion is blocked by NMDA receptor antagonists (Ekstrom et al., 2001), which also block spatial learning (Morris et al., 1986). For these reasons, this expansion is believed to reflect the retrieval of spatial representations that formed during earlier experiences. Retrospective coding may be driven by persistent firing in entorhinal cortex neurons (Klink and Alonso, 1997; Yoshida et al., 2008; Hahn et al., 2012), which may be involved in short-term memory encoding (Suzuki et al., 1997).

It should be noted that the present work uses the terms ‘‘prospective coding’’ and ‘‘retrospective coding’’ to describe representations of locations at the spatial scale of individual place fields, following the terminology used in earlier studies of similar phenomena (Muller and Kubie, 1989; Battaglia et al., 2004; De Almeida et al., 2012). However, the same ‘‘prospective’’ and ‘‘retrospective’’ terminology has been used to refer to place cell coding at a larger spatial scale (Ferbinteanu and Shapiro, 2003). The Ferbinteanu and Shapiro study defined prospective coding as place cell firing rate changes that signal which way a rat is headed and retrospective coding as firing rate changes that indicate from which direction the rat has come. The present findings do not address the question of whether gamma rhythms are involved in these phenomena.

In the present study, prospective and retrospective coding events tended to occur at the beginning and end, respectively, of the linear track, consistent with findings reported by Gupta and colleagues (2012). However, the present findings additionally show that prospective and retrospective coding events were associated with the occurrence of slow and fast gamma, respectively. Prospective firing in CA1 has been

proposed to be triggered in part by temporal context information from CA3 (Hasselmo and Eichenbaum, 2005). Prospective ‘‘sweep ahead’’ events have been observed in CA3 place cells at choice points on a T-maze, locations where 40 Hz gamma (i.e., slow gamma) also prominently occurred (Johnson and Redish, 2007). These findings suggest that slow gamma coordination of place cells during prospective coding facilitates retrieval of representations of future locations in the hippocampal network. A previous study linked gamma coherence between CA3 and CA1 to memory retrieval but did not discriminate between slow and fast variants of gamma (Montgomery and Buzsaki, 2007). The CA3-CA1 coupling they observed, however, most likely involved slow gamma considering that CA3-CA1 coherence has been reported to be maximal in the slow gamma range (Colgin et al., 2009). Moreover, slow gamma has been proposed to mediate memory retrieval during sharp wave-associated replay in quiescent behavioral states (Carr et al., 2012).

If slow gamma-mediated prospective coding is related to retrieval of learned locations, as we propose, then it should be related to the backward shifts of place fields that develop with experience (Mehta et al., 1997, 2000; Lee et al., 2004). Consistent with this, we observed few prospective events in CA1 during the first 30 s on the linear track each day (Figure 2.5A). However, we also observed that the probability of slow gamma occurrence was high during this time (Figure 2.5B), which seems to contradict our results linking slow gamma with prospective coding. Differences between CA3 and CA1 may provide a possible explanation for this paradox. In a well-learned environment, CA1 place fields shift backward over the course of the first few laps of each day, but stable spatial representations emerge immediately in CA3 (Lee et al., 2004; Roth et al., 2012). This suggests that CA3 maintains long-term memories of spatial locations and that these memories are transmitted to CA1 during the first few laps of each day. Slow gamma may

occur during the first few laps of each day as stored spatial memories are reactivated in CA3, but emergence of these memories in CA1 may follow a slower time course. CA1 cells may not respond to slow gamma-mediated inputs from CA3 until after CA3-CA1 synapses have undergone NMDA receptor-dependent synaptic strengthening that occurs during this time (Ekstrom et al., 2001). This could explain why few prospective coding events were seen in CA1 during the first few laps of each day.

Here, we posit that prospective coding relies on slow gamma coupling of CA1 and CA3 during retrieval of stored memory representations. Yet, this does not explain prospective coding in grid cells (De Almeida et al., 2012). It is possible that grid cell representations of upcoming locations are inherited from CA1, considering that CA1 projects to MEC layer V (Swanson and Cowan, 1977), which projects to layers II and III (van Haeften et al., 2003). However, this remains an interesting question for later study.

Our findings also provide insights regarding the functional significance of theta phase precession (O'Keefe and Recce, 1993; Skaggs et al., 1996). It is unlikely that theta phase precession simply reflects retrieval of upcoming locations because prospective coding was associated with slow gamma, and phase precession was less pronounced during periods of slow gamma. Specifically, spikes were largely restricted to the late theta phase component of theta phase precession. In other words, upcoming locations were preferentially represented and spiking was suppressed at early theta phases when slow gamma rhythms were present (Figure 2.6B). Theta phase precession did occur, however, during fast gamma periods (Figure 2.6C) when cells preferentially represented locations in the recent past. These findings support the interpretation that spikes occurring on early theta phases code recently visited locations (Dragoi and Buzsaki, 2006), not current location as otherwise suggested (Lisman and Redish, 2009). Recent events are thought to be maintained in short term memory by persistent firing in

entorhinal cortex (Jensen and Lisman, 2005; Suzuki et al., 1997; Hasselmo and Stern, 2006), and fast gamma promotes inputs from entorhinal cortex (Colgin et al., 2009). Fast gamma inputs from MEC may also activate representations of current location slightly later in the theta cycle. Representations of upcoming locations could then be triggered as a result of associations that were formed across sequentially activated place cells during prior learning. We predict that cells coding current location would not trigger firing of cells coding upcoming locations in a novel environment, and thus spikes on late theta phases would be absent during fast gamma in a novel environment. The theta phases at which spikes occurred were only weakly correlated with position during the first lap on a linear track on a given day (Mehta et al., 2002). Thus, it is possible that the relationship between theta phase and position would be greatly diminished during periods of fast gamma in a novel environment. In any case, this remains an interesting question for later study. Another interesting question is how slow and fast gamma modes relate to different classes of gamma-modulated cells in CA1 reported by Senior and colleagues (Senior et al., 2008). In that study, ‘‘TroPyr’’ cells fired at the trough of gamma and fired across the full range of theta phases during theta phase precession, whereas ‘‘RisPyr’’ cells fired at the rising phase of gamma as the animal was leaving a cell’s place field. The study did not differentiate between different frequencies of gamma. However, TroPyr cells may correspond to fast gamma-modulated cells. Place cells fired across the full range of theta phase precession during fast gamma in the present study (Figure 2.6C), and earlier work showed that cells that were significantly phase locked to fast gamma tended to fire on the fast gamma trough (Colgin et al., 2009). The relationship between RisPyr cells and slow and fast gamma remains unclear, however. Place cells that were significantly phase-locked to slow gamma did tend to fire on the rising phase of slow gamma (Colgin et al., 2009). However, place cells fired in the initial part of their place fields during periods of

slow gamma (Figure 2.6B), whereas RisPyr cells tended to fire in the later portions of their place fields (Senior et al., 2008). Although it is possible that our results were influenced by factors unrelated to memory (e.g., consumption of reward), the relationship of slow and fast gamma rhythms to prospective and retrospective coding modes suggests that different frequencies of gamma coordinate different types of spatial memory processing. Fast gamma may correspond to an encoding mode, similar to that proposed previously for theta-modulated gamma during learning (Jensen and Lisman, 1996; Lisman and Otmakhova, 2001). In this mode, representations for recently visited locations may be held in a short-term memory buffer that provides the repetitive firing necessary to encode new memories. On the other hand, slow gamma may correspond to a retrieval mode, in which firing is facilitated before the center of the place field and suppressed in the later part of the place field. This may prevent ongoing encoding from interfering with retrieval of previously stored spatial memories, as can occur if these processes are engaged at the same time (Hasselmo et al., 2002). Considering that slow and fast gamma rhythms occur in other brain regions (Kay, 2003; van der Meer and Redish, 2009; Igarashi et al., 2013; Manabe and Mori, 2013), separate slow and fast gamma modes may mediate different types of information processing throughout the brain.

2.5 METHODS

Subjects. Five male Long Evans rats weighing approximately 350-500 grams were used in the study. During the data collection period, rats were placed on a food deprivation regimen that maintained them at ~90% of their free-feeding body weight.

Testing procedures. After recovering from surgery, rats were trained to run three 10-minute sessions per day on a linear track. The linear track was 2 m long, 10 cm wide, and placed 64 cm above the floor. Rats were trained to run back and forth on the track, receiving small pieces of sweetened cereal or vanilla cookies on the ends. Every rat was trained on the linear track for at least 3 days prior to the start of recording. Between recording sessions, rats rested for ~10 minutes in a towel-lined, elevated flower pot.

Place fields. Position was tracked using red and green LEDs on the rat's headstage. Spatial firing rate distributions ("place fields") for each well-isolated putative pyramidal cell were constructed in the standard manner by summing the total number of spikes that occurred in a given location bin (5 cm), dividing by the amount of time that the animal spent in that bin, and smoothing with a 25 cm (5 bins) SD Gaussian centered on each bin.

Place field acceptance criteria for single unit analyses. Individual place fields were required to have at least 3 contiguous bins with a firing rate above the lower of either 1 Hz or 10% of the peak firing rate of the cell. Additionally, the average firing rate across the rate map had to exceed 2.5 Hz. In order to exclude incomplete place fields, the start and stop bins were required to fall at least 15 cm away from the ends of the track for the field to be included in subsequent place field analyses. To account for trailing place field tails, the boundaries of the defined place fields were expanded in both directions until the minimum firing rate criterion (i.e., 1 Hz or 10% of the peak firing rate, whichever was lower) was exceeded or the position was less than 15 cm from an end of the track. Within these expanded boundaries, place fields were defined according to the collection of bins that contained spikes, unless the firing rate rose above the minimum again before the 15 cm limits from the track end were reached. In this case, the last bin before the rise in rate

occurred was counted as the place field boundary. Place fields for left and right running directions on the track were analyzed separately.

Classification of individual place cell coding modes. 692 CA1 cells from 5 rats were used for classification of coding modes. If multiple days of the same cell were recorded, only data from the first acceptable day was used for that cell. Animals' movements along the linear track were collapsed into one dimension for ease of analysis. Place field passes in which the animal's running speed dropped below 5 cm/s were discarded. The average place field center was then defined as the center of mass of the positions of the remaining spikes. Prospective passes were defined as those in which >= 2/3 of spikes occurred before the place field center. Retrospective passes were defined as those in which >= 2/3 of spikes occurred after the place field center. All remaining passes through the place field were categorized as ambiguous. To determine the time difference between cell pairs exhibiting the same or different type of coding, ambiguous passes were excluded. The time point for each coding event was defined as the time when the rat passed through the center of the spiking activity for that particular traversal through the field. To determine whether the place cell population exhibited coding modes more often than expected by chance, we determined the proportion of passes through the place field that would randomly exhibit coding modes for each cell. To do this, we preserved the number of spikes for each place cell, and preserved the number of spikes that occurred on each pass through a place field, but randomly shuffled the spikes' assignments to particular passes.

Gamma power during prospective and retrospective coding. Prospective, retrospective, and ambiguous passes through a place field were defined as described above for the population of CA1 cells. For each categorized place field traversal, the

period of time during which the place cell emitted spikes in the field defined the time windows that were used to estimate slow and fast gamma power. Time-varying slow and fast gamma power estimates were obtained for these time windows as described in Appendix A. A single estimate of slow gamma power and a single estimate of fast gamma power were then obtained for each categorized place field traversal by averaging power for each gamma type across the time window and across the frequency band of interest (i.e., 60-100 Hz for fast gamma and 25-55 Hz for slow gamma).

Phase-locking of interneuron spikes to slow and fast gamma. 201 interneurons recorded in or near the CA1 cell body layer were used for this analysis. For each interneuron, spikes that occurred during a traversal through a place field were selected and categorized as prospective if they occurred during a prospective traversal, retrospective if they occurred during a retrospective traversal, or ambiguous if they occurred during an ambiguous traversal. Slow and fast gamma phases in CA1 at the time of spike occurrence were estimated using the LFP recorded from the same tetrode as the corresponding interneuron. Slow and fast gamma phases were estimated by first bandpass filtering the LFP in the slow and fast gamma frequency ranges, respectively. Then, a Morlet wavelet transform was performed on each filtered signal in order to extract the slow and fast gamma phase components corresponding to each spike time. The mean circular vector lengths of the slow and fast gamma phase distributions for each interneuron were then determined.

Matching prospective and retrospective coding events according to running speed. Counts of retrospective and prospective events were binned by average running speed using intervals of 5 cm/s. The number of events was randomly downsampled so that the

numbers of retrospective and prospective events within each speed bin were equal. Measurements of slow and fast gamma were then obtained for the remaining events, as described above.

Detection of gamma episodes. To extract periods of slow and fast gamma activity in the LFP recordings, time-varying slow and fast gamma power were calculated, using the method described in Appendix A. Power at each time point was averaged across the slow and fast gamma frequency ranges to obtain an estimate of slow and fast gamma power for each time point. Time points were collected during which slow and fast gamma power exceeded 2 SD above the mean power of slow and fast gamma, respectively, across all time points. This method of slow and fast gamma detection has been used previously (Colgin et al., 2009). Time windows, 125 ms in length, were cut around the selected time points. In each 125 ms segment, the slow and fast gamma amplitude maxima were determined from the slow and fast gamma bandpass filtered versions of the recordings. Duplicated gamma windows, a consequence of detecting overlapping time windows, were avoided by discarding identical maxima values within a given gamma subtype and further requiring that maxima of a given gamma subtype be separated by at least 100 ms. The maxima were then used to define the centers of slow and fast gamma episodes. Slow and fast gamma episodes/periods were defined as 125 ms-long windows centered around the slow and fast gamma maxima.

Place fields during periods of slow and fast gamma. Spikes that occurred during slow and fast gamma episodes were selected and binned across position within their respective place fields. The center of mass for the overall place field, and the slow and fast gamma downsampled place fields, was calculated in the following manner. For each bin in the

place field, the product of the spike count and the position was calculated. These products were added together and divided by the sum of all of the spike counts to obtain the center of mass measure.

Theta phase precession. Theta phase was determined by band-pass filtering the LFP signal in the theta range (6–10Hz) and performing a Hilbert transform. Each spike was assigned a theta phase using the signal from the tetrode from which it was recorded. Spike locations were normalized using the boundaries of the place field (ranging from 0 to 1). Leftward runs were reversed such that movement always occurred from 0 to 1. Gamma episodes were detected as described above, and spikes occurring within slow and fast gamma episodes were used to construct the position phase plots.

Detecting individual theta cycles for Bayesian decoding. The LFP signal was chosen from the tetrode with the most recorded CA1 cells for that particular recording. The signal was separately band-pass filtered for theta (6–12 Hz) and delta (2–4 Hz), and the power for each was determined using a convolving Morlet wavelet (as described in Appendix A). The presence of theta activity was defined when theta power was greater than delta by 3 times or more. The maxima of the bandpass filtered signal were then identified as theta peaks for each recording. Individual theta cycles were cut from peak to peak, as in Gupta et al. (2012), and spikes occurring within those theta cycles were used to reconstruct position estimates for each theta cycle using a Bayesian decoding approach, described below.

Bayesian decoding analyses. The most likely position represented by spiking activity from a population of 456 CA1 cells and 87 CA3 cells was estimated using a Bayesian

decoding approach (Zhang et al., 1998; Brown et al., 1998; Jensen and Lisman, 2000). Recording sessions with fewer than 20 cells were not used, and cells were not excluded from Bayesian analyses on the basis of the place field acceptance criteria (see above). These factors explain why the number of CA1 cells listed here differs from the number used for the single unit analyses. Only theta cycles containing at least 2 active place cells were included in the analysis. Additionally, theta epochs were selected using the same theta/delta threshold method described above; spikes that occurred during non-theta epochs were not included. Place fields for each of the cells were constructed from each recording session on the linear track, as described in the "Place fields" section above. Decoding was performed for each theta cycle using a 40-ms sliding time window shifted by 10 ms at each step, as in Gupta et al. (2012). The probability of the animal to be at position x, given the number of spikes n from each cell collected in the time window t was estimated using Bayes rule:

$$P(x|n) = \frac{P(n|x)P(x)}{P(n)}$$

P(x) was calculated from the experimental tracking data. P(n|x) was estimated using the firing rates from the experimentally obtained place fields in the same 10-minute linear track session, assuming that the firing rates of different place cells are statistically independent and that the number of spikes from each cell has a Poisson distribution (Zhang et al., 1998; Jensen and Lisman, 2000). P(n), the normalizing constant, was set so that P(x|n) summed to 1. Reconstructed positions were identified for each time bin as the center of mass of the probability distribution, P(x|n). The reconstructed location at each time bin was then compared with the actual location identified from position tracking data. A prediction error was calculated for each time bin by subtracting the actual

position from the reconstructed position. Errors were then averaged across all time bins within a theta cycle to obtain a single prediction error estimate for each theta cycle. Slow and fast gamma power estimates were calculated for each theta cycle in the following manner. For every tetrode with cells that were used for Bayesian decoding, slow and fast gamma power were estimated within the theta cycle using the method described above. Slow and fast gamma power estimates were then averaged across tetrodes, and averaged across time within the theta cycle, to obtain a single slow gamma power estimate and a single fast gamma power estimate for each theta cycle. Theta cycles associated with slow or fast gamma were then detected by identifying theta cycles with slow and fast gamma power estimates that were 2 SD greater than the mean slow and fast gamma power, respectively, across all theta cycles.

Chapter 3: Sequences of place cells code spatial trajectories at different time scales during slow and fast gamma rhythms

3.1 SUMMARY

The hippocampus is central to episodic memory and spatial navigation (O'Keefe and Nadel, 1978), both of which rely on sequences of spatio-temporal information. 'Theta sequences' are temporally compressed representations of spatial paths by place cells (Dragoi and Buzsaki, 2006; Foster and Wilson, 2007; Gupta et al., 2012), hippocampal neurons that represent specific locations (O'Keefe and Dostrovsky, 1971). These sequences activate within individual cycles of the extracellular theta oscillation (~6–10 Hz) and may be important for the encoding or retrieval of spatial memories (Dragoi and Buzsaki, 2006; Johnson and Redish, 2007; Wikenheiser and Redish, 2015). A second type of oscillation in the hippocampus, gamma (~25–100 Hz), is thought to interact with theta to temporally organize theta sequences (Gupta et al., 2012; Lisman, 2005; Lisman and Jensen, 2013). However, it remains unclear how theta sequences are affected by different slow (~25–55 Hz) and fast (~60–100 Hz) subtypes of gamma (Colgin et al., 2009), which reflect different spatial coding modes in the hippocampus (Chapter 2; Bieri et al., 2014). In rats running on a linear track, we found that sequences during slow gamma showed a greater degree of temporal compression and extended further ahead of the animal compared to sequences during fast gamma, which were more likely to represent current locations in real time. Moreover, the slow gamma phases at which spikes occurred shifted as the sequence progressed, such that earlier locations were coded by spikes at early slow gamma phases and later locations were coded by spikes at late slow gamma phases. In contrast, place cells tended to fire at the same fast gamma phase, regardless of where their place field was located. These findings suggest that place

cell sequences that code future paths activate within a slow gamma cycle on a compressed time scale, whereas sequences that represent the ongoing trajectory activate across successive fast gamma cycles at the behavioral time scale.

3.2 RESULTS

The local field potential (LFP) and spiking activity from 650 place cells were recorded in hippocampal area CA1 of 5 rats traversing a linear track. The location of the rat was estimated from place cell ensemble activity during 21576 individual theta cycles using Bayesian decoding (Zhang et al., 1998; Brown et al., 1998; Gupta et al., 2012; Bieri et al., 2014). A regression line was fit to each decoded trajectory (Figure 3.1A) and was used to measure the slope (cm s-1), total distance ('x-span', cm) and total duration ('t-span', seconds) of each sequence. Each of these measures provided information about how spatial trajectories were represented by theta sequences. The slope measures the amount of distance represented by a sequence in a given amount of time and thus provides information about the degree of temporal compression of sequences. The x-span measure estimates the length of the represented trajectory, and the t-span measure quantifies the time period of sequence activation. Sequences of ordered locations that were unlikely to arise by chance were classified as "significant sequences". To consider a decoded sequence of place cell activity as a significant sequence, the R^2 value of the linear fit was required to be greater than 95% of the R^2 values obtained from time-bin shuffled versions of the sequence (see Methods). We found 58% of all sequences to be significant (Figure 3.1B).

We first examined the relationship between slow and fast gamma power and the temporal compression of sequences, assessed using the slope of the regression line. More temporally compressed sequences represented greater distances per unit time and thus

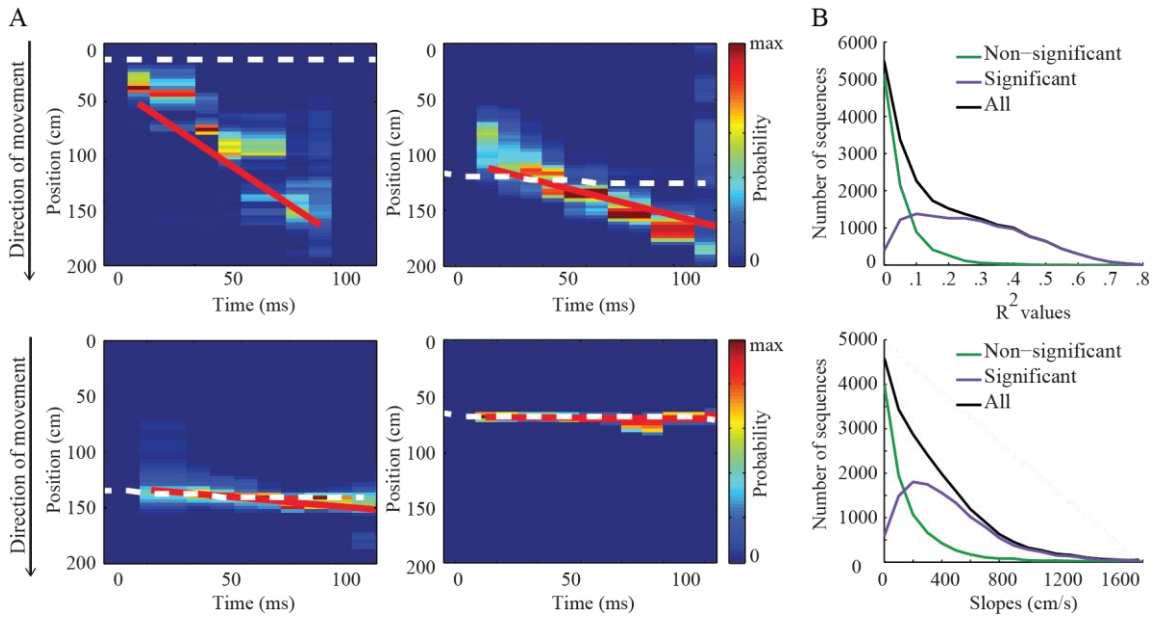

Figure 3.1: Characterization of theta sequences.
A. Example theta sequences showing the animal's true location (white dotted line), the predicted location based on Bayesian decoding of ensemble place cell activity (color-coded according to probability), and the associated best fit regression line (red line). **B.** The distribution of slopes and R^2 values of the regression lines for all decoded sequences.

were associated with larger slopes. Sequences with gamma power above the median for the gamma type not being considered were excluded from the analysis. In sequences that were significant, we found a significant interaction effect between gamma power and gamma type on slope (Figure 3.2A; multiple regression model interaction term; $t(3,12651) = 2.82$, $p = 0.005$). Slow gamma power and slope were positively correlated (Figure 3.2A; $t(1,6383) = 3.17$, $p = 0.002$), while fast gamma power was not significantly predicted by slope (Figure 3.2A; $t(1,6268) = 0.40$, $p = 0.7$). In sequences that were non-significant, there was no significant interaction effect between gamma type and gamma power on slope (Figure 3.2B; multiple regression interaction term; $t(3,8917) = 1.36$, $p = 0.2$), nor was there a significant main effect of gamma power ($t(2,8918) = 0.02$, $p = 1.0$) or gamma type ($t(2,8918) = 0.92$, $p = 0.4$).

The above results suggest that sequences represent more space per unit time during slow gamma compared to fast gamma. This may be due to an increase in the

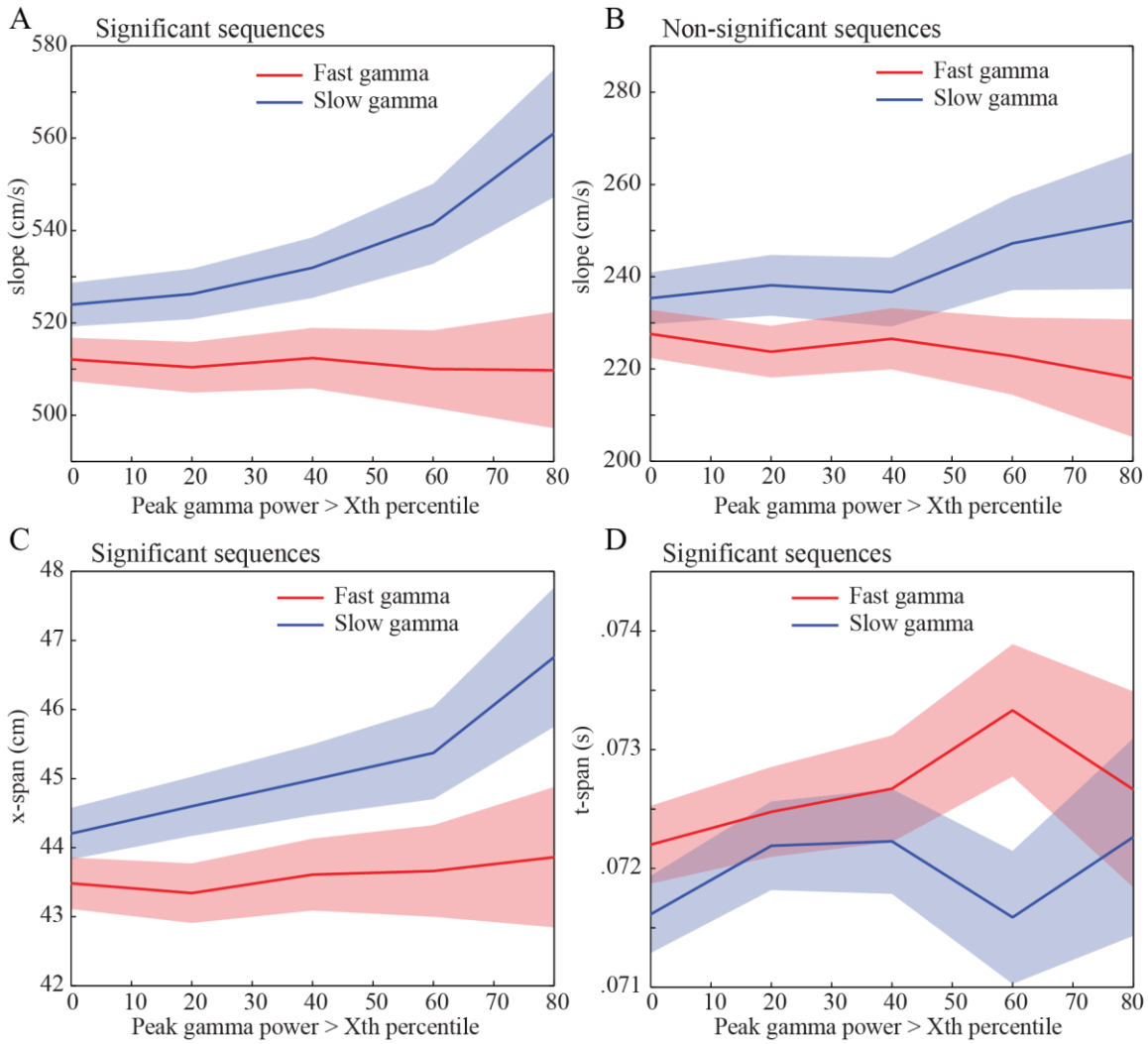

Figure 3.2: Properties of theta sequences during slow and fast gamma.
A. Sequence slope increased with slow gamma power but did not change significantly according to fast gamma power. **B.** There was no significant relationship between slow or fast gamma power and slope for non-significant sequences. **C.** Spatial length (x-span) increased with slow gamma power but did not depend on fast gamma power. **D.** Temporal duration (t-span) of sequences did not change differently depending on which type of gamma was present. Data represent mean ± SEM (shaded area). Sequences with gamma power above the median for the type (i.e. slow or fast) not being considered were excluded in all plots.

represented spatial path length, or representation of similar path lengths across shorter periods of time. To distinguish these possibilities, we separately analyzed the x-span and

t-span of each sequence. We found that x-span was differentially affected by slow and fast gamma power (Figure 3.2C; multiple regression model interaction term; $t(3,12651) = 2.18$, $p = 0.03$), similar to our slope findings. Slow gamma power and x-span were positively correlated (Figure 3.2C; $t(1,6383) = 2.90$, $p = 0.004$), while fast gamma power and x-span were not correlated (Figure 3.2C; $t(1,6268) = 0.31$, $p = 0.8$). No significant gamma power by gamma type interaction was found for t-span (Figure 3.2D; multiple regression model interaction term; $t(3,12651) = 0.24$, $p = 0.8$). There was a significant main effect of gamma power on t-span ($t(2,12652) = 2.70$, $p = 0.007$), but t-span did not differ significantly across gamma types ($t(2,12652) = 0.10$, $p = 0.9$). These findings suggest that slow gamma-associated sequences represent longer trajectories than fast gamma-associated sequences but that both kinds of sequences are active across similar time spans.

In addition to reflecting temporal compression properties of sequences, slope measures also provided spatial information. Specifically, sequences with flatter slopes more closely represented the rat's present location, whereas sequences with steeper slopes represented paths sweeping ahead of the animal. We sorted significant sequences into two groups, those with slopes below the median and those with slopes above the median, and assessed whether gamma power changed between these two groups. Slow and fast gamma power were differentially affected by slope magnitude (repeated measures ANOVA; gamma type x slope magnitude interaction; $F(1,12466) = 17.25$, $p < 0.001$). For fast gamma, sequences with flatter slopes exhibited significantly higher power than sequences with steeper slopes (Figure 3.3A; $t(12466) = 3.18$, $p = 0.001$). In contrast, slow gamma power was heightened during sequences with steeper slopes (Figure 3.3A; $t(12466) = 2.16$, $p = 0.03$). These findings suggest that place cell sequences

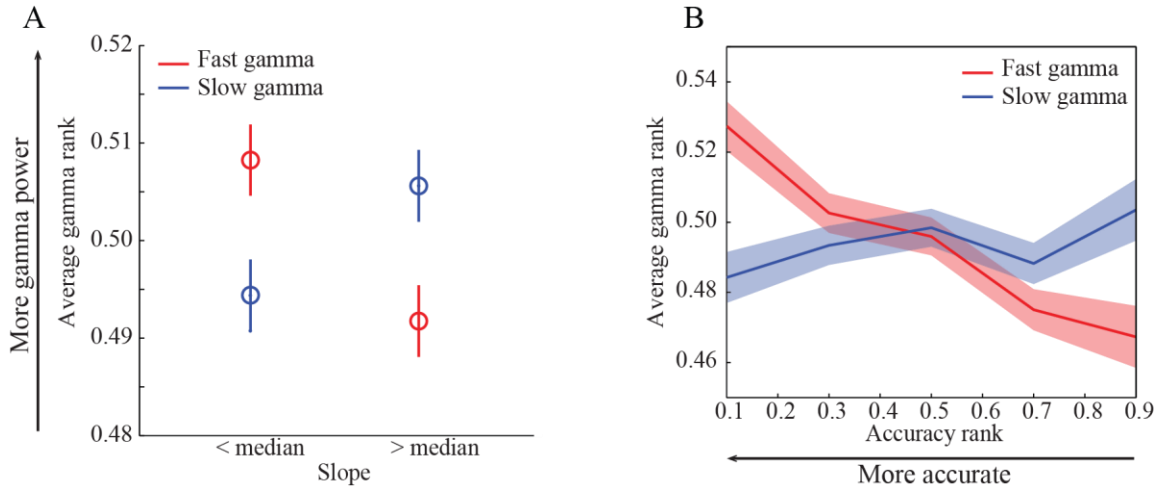

Figure 3.3: Accuracy of spatial sequences during slow and fast gamma.
A. Fast gamma power was significantly higher for sequences with relatively low slopes, and slow gamma power was significantly higher for sequences with relatively high slopes. **B.** Sequence accuracy relative to the animal's actual location was estimated based on slope and decoding error (see Methods). Only sequences with an average decoding error below the median were considered. Sequence accuracy increased with fast, but not slow, gamma power. Data represent mean ± SEM.

tend to accurately represent current location during fast gamma and tend to predict the animal's future trajectory during slow gamma.

To further test the hypothesis that fast gamma-associated sequences accurately represent current location, we assessed the relationship between gamma power and the accuracy of decoded sequences. A sequence was considered accurate if it had a low decoding error and a flat slope. All sequences (regardless of significance) were considered, except those with errors above the median error. This allowed inclusion of sequences that were non-significant due to a low slope while avoiding sequences that were inaccurate due to noise. We found a significant interaction effect between gamma type and accuracy on gamma power (Figure 3.3B; multiple regression model interaction term; $t(3,21572) = 5.48$, $p < 0.001$). Additionally, there was a significant positive correlation between fast gamma power and accuracy ($t(1,10786) = 6.47$, $p < 0.001$) but no correlation between slow gamma power and accuracy ($t(1,10786) = 1.28$, $p = 0.2$).

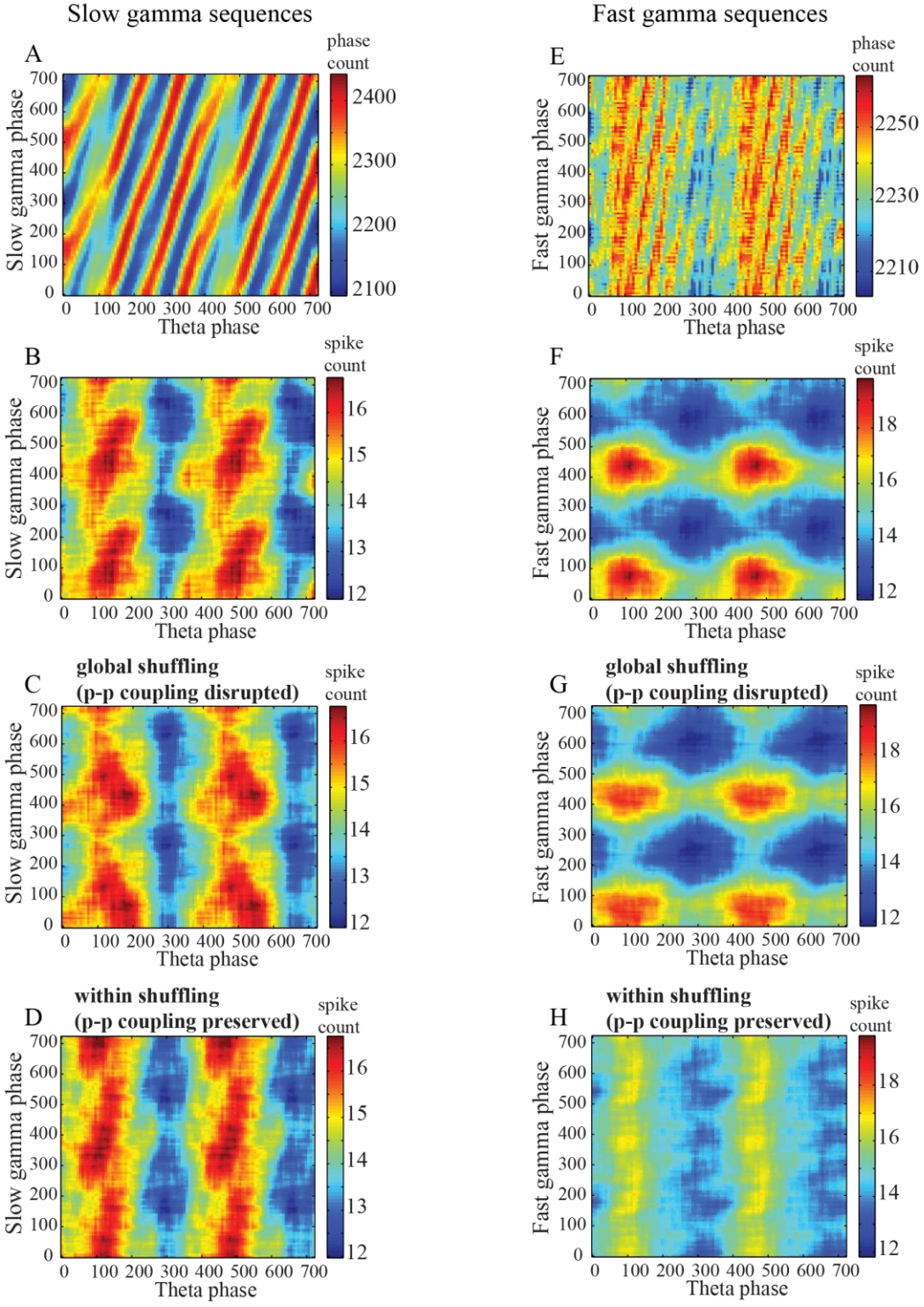
Slow gamma sequences
Fast gamma sequences
A
B
C
D
E
F
G
H
phase count
spike count
global shuffling (p-p coupling disrupted)
within shuffling (p-p coupling preserved)
Slow gamma phase
Fast gamma phase
Theta phase
0 100 200 300 400 500 600 700
2400
2300
2200
2100
2250
2230
2210
16
15
14
13
12
18

Figure 3.4

Figure 3.4: Phase-phase (p-p) coupling of theta and gamma.
A, E. p-p plots of continuous LFP recordings during slow gamma sequences (a), and fast gamma sequences (e). Theta-gamma p-p coupling was apparent, consistent with previously published reports (Belluscio et al., 2012). **B, F.** p-p plots for spike times. Slow gamma spike phases were coupled to theta phases (b), while fast gamma spike phases did not change according to theta phase (f). **C, G.** p-p plots of spikes after global shuffling (which disrupts theta-gamma p-p coupling; see Methods). Global shuffling disrupted slow gamma spike phase coupling to theta phase (c) but did not substantially change phase-phase plots for spikes from fast gamma sequences (g). **D, H.** p-p plots of spikes after within-sequence shuffling (which preserves theta-gamma p-p coupling; see Methods). Slow gamma spike phases remained coupled to theta phase (d), similar to the unshuffled data, while the relationship of fast gamma spikes to fast gamma phase was disrupted (h). Sequences with gamma power above the median for the gamma type (i.e. slow or fast) not being considered were excluded in all plots.

These findings support the hypothesis that place cell sequences more accurately represent the animal's actual location during fast gamma than during slow gamma.

Theta oscillations are phase-phase coupled ('p-p coupling') to slow and fast gamma oscillations (Belluscio et al., 2012) (Figure 3.4A and 3.4E), which may influence the temporal activity patterns of different neuronal ensembles. To test if spiking activity follows p-p coupling, we measured the theta and gamma firing phases during sequences with strong slow gamma ('slow gamma sequences') and strong fast gamma ('fast gamma sequences') (see Methods). We found that firing phases during slow gamma sequences reflected p-p coupling of theta and slow gamma (Figure 3.4B). In contrast, spikes during fast gamma remained phase-locked to fast gamma, regardless of theta phase (Figure 3.4F). When theta phase and gamma phase were randomly reassigned for each spike ('global shuffling'; Figure 3.4C and 3.4G), thereby disrupting p-p coupling between gamma and theta, slow gamma-theta p-p coupling was no longer apparent in the phase-phase plots for spikes during slow gamma sequences. In contrast, the distribution of fast gamma and theta phases for spikes during fast gamma sequences was not affected by the shuffling. When spike times were instead shuffled within each sequence ('within shuffling'; Figure 3.4D and 3.4H), which preserved theta-gamma p-p coupling, an opposite effect occurred; the relationship between spike times and fast gamma phase was disrupted, but theta-gamma phase-phase coupling was still apparent for slow gamma spikes. These results suggest that spiking activity during slow gamma sequences reflects theta-gamma oscillatory p-p coupling, whereas spikes phase-lock to fast gamma regardless of theta phase.

Place cell spikes occur at progressively earlier theta phases as an animal moves through a cell's place field, and thus spikes' theta phases provide spatial information (O'Keefe and Recce, 1993; Skaggs et al., 1996). To address the question of whether

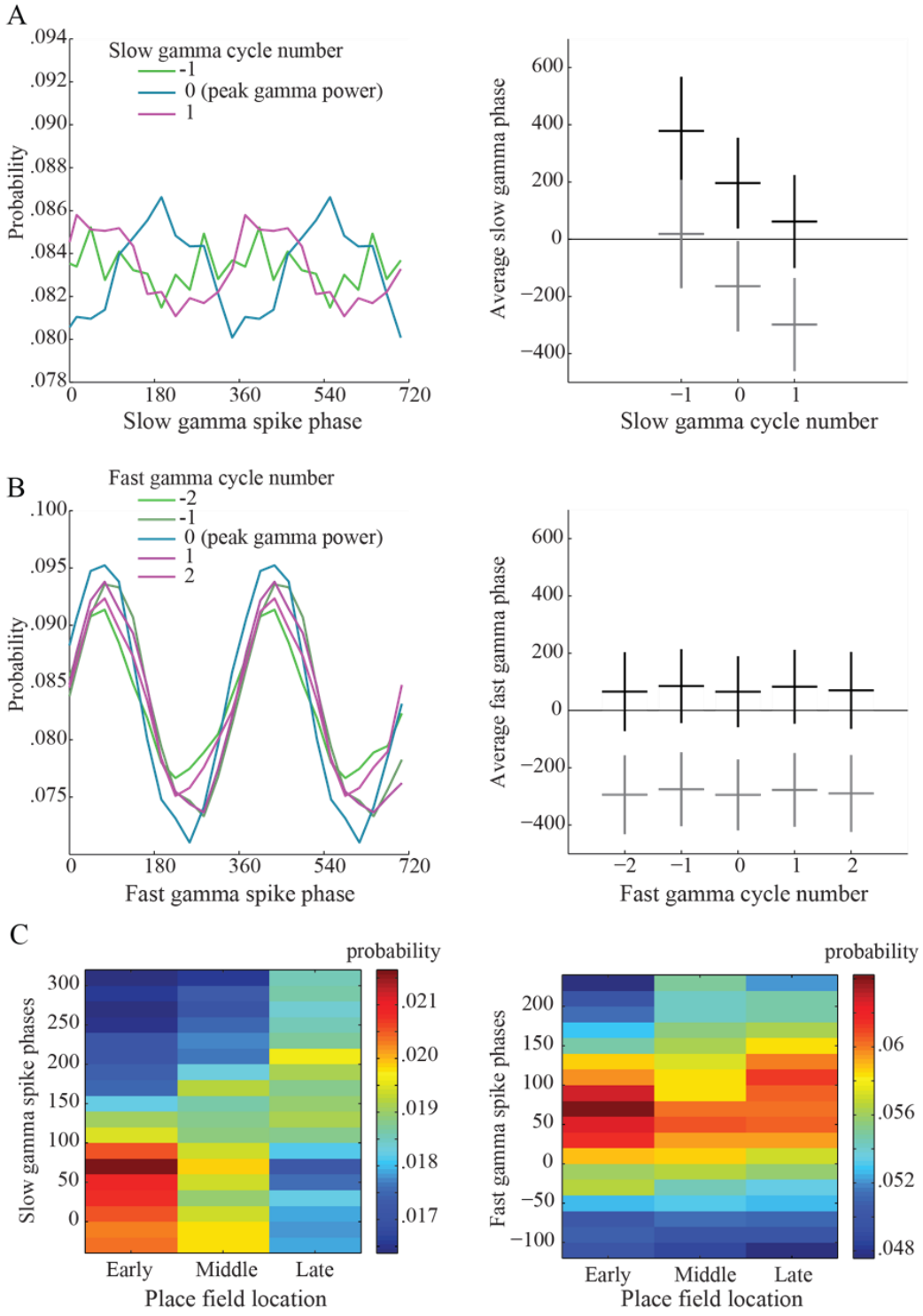
A
Slow gamma cycle number
-1
0 (peak gamma power)
1
Probability
Slow gamma spike phase
Average slow gamma phase
Slow gamma cycle number
B
Fast gamma cycle number
-2
-1
0 (peak gamma power)
1
2
Probability
Fast gamma spike phase
Average fast gamma phase
Fast gamma cycle number
C
probability
Slow gamma spike phases
Early
Middle
Late
Place field location
probability
Fast gamma spike phases
Early
Middle
Late
Place field location

Figure 3.5

Figure 3.5: Slow and fast gamma phases associated with place cell spike times.
A, B. Gamma cycles were temporally ordered for each sequence, centered at cycle 0 (corresponding to the gamma cycle with maximal amplitude). Black lines represent the mean phase angle, and grey lines represent the mean phase angle – 360° (to address the circular nature of phase estimates). Slow gamma spike phases shifted progressively across slow gamma cycles (A). Fast gamma spike phases remained consistent across different fast gamma cycles (B). **C.** Place cells were categorized by the location of their place field along the track ('Early', 'Middle', and 'Late' correspond to place fields near the beginning, middle, and end of the track, respectively). Place cells fired on different phases of slow gamma according to the location of their place field but fired consistently on the same phase of fast gamma regardless of their place field location. Data represent mean ± SD. Sequences with gamma power above the median for the type of gamma (i.e. slow or fast) not being considered were excluded in all plots.

slow and fast gamma phases code spatial information, we first assessed whether slow and fast gamma spike phases change systematically as theta sequences progress. We classified individual gamma cycles during slow gamma sequences and fast gamma sequences according to their temporal order, centered at the gamma cycle with highest amplitude (cycle '0'). Cycles occurring before cycle 0 were labeled with descending integer values, and cycles occurring after cycle 0 were labeled with increasing integer values. Average spike phases were then estimated for each cycle. Slow gamma spike phases had a significant dependence on slow gamma cycle number (Figure 3.5A; Multi-sample Mardia-Watson-Wheeler test; $W(2,19870) = 11.41$, $p = 0.02$), shifting backward as the sequence progressed. Fast gamma spike phases, however, did not differ across successive fast gamma cycles (Figure 3.5B; Multi-sample Mardia-Watson-Wheeler test; $W(4,18216) = 12.88$, $p = 0.1$). These findings raised the possibility that spatial information was conveyed by variations in slow gamma phases of spikes.

To explore this possibility, we next asked if place cells fired on different gamma phases depending on the location of their place fields. We grouped place cells during each sequence into three categories based on the location of their peak firing rate along the track. "Early" place cells fired near the beginning of the track, "middle" place cells fired in the middle of the track, and "late" place cells fired near the end of the track. We then estimated the mean gamma phase of spikes for each spatial category (i.e. early, middle, and late). Spike phases during slow gamma sequences were significantly different depending on spatial category (Figure 3.5C; Multi-sample Mardia-Watson-Wheeler test; $W(2,9250) = 22.92$, $p < 0.001$), with early and late slow gamma phases coding early and late place field locations, respectively. On the other hand, spike phases during fast gamma sequences did not change significantly across place field locations (Figure 3.5C; Multi-sample Mardia-Watson-Wheeler test; $W(2,9350) = 5.00$, $p = 0.3$).

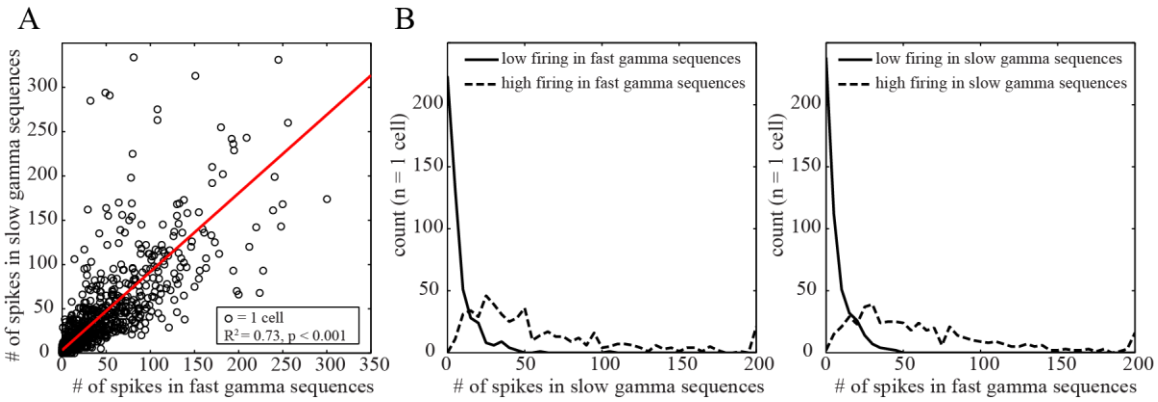

Figure 3.6: Individual place cells participate in both gamma types.
A. There was a strong positive correlation between the number of spikes each cell contributed to fast gamma sequences and to slow gamma sequences. **B.** Place cells were divided into low firing and high firing categories for each gamma type (see Methods). Place cells exhibited similar levels of activity during both gamma types.

These findings suggest that different slow gamma phases code different spatial locations, whereas fast gamma phases do not provide spatial information.

A previous study described two classes of place cells that fire at different phases of gamma (gamma trough-spiking pyramidal cells, termed "TroPyr", and gamma rising phase-spiking pyramidal cells, termed "RisPyr"; Senior et al., 2008). This study did not distinguish between slow and fast gamma, leaving open the possibility that each class is selectively driven by a gamma subtype. However, firing rates of individual cells were positively correlated during fast gamma sequences and slow gamma sequences (Figure 3.6), suggesting that place cells are equally active during either gamma type. This finding is inconsistent with the hypothesis that distinct classes of place cells, corresponding to 'TroPyr' and 'RisPyr' cells (Senior et al., 2008), fire selectively during slow and fast gamma. Moreover, both TroPyr and RisPyr cells exhibit some characteristics that are consistent with fast gamma and others that are consistent with slow gamma. TroPyr cells fire at the trough of gamma and exhibit theta phase precession, features associated with

fast gamma (Colgin et al., 2009; Bieri et al., 2014). Yet, RisPyr cells also exhibit properties that are associated with fast gamma, including retrospective coding (Bieri et al., 2012). Additionally, RisPyr cells fire at consistent gamma phases across the theta cycle, consistent with our present fast gamma results (Figure 3.5B). On the other hand, gamma phases of TroPyr spike times change progressively across the theta cycle, reminiscent of our present slow gamma results (Figure 3.5A). Yet, RisPyr cells also exhibit characteristics that are consistent with slow gamma. RisPyr cells fire on the rising phase of gamma and across a limited range of theta phases, consistent with spikes occurring during slow gamma (Colgin et al., 2009; Bieri et al., 2014). Together, these results support the conclusion that RisPyr and TroPyr cells are unlikely to correspond to subclasses of place cells that are selectively modulated by slow or fast gamma.

3.3 DISCUSSION

Here we show that place cell sequences that code trajectories extending ahead of the animal are compressed within slow gamma cycles, whereas fast gamma-associated sequences accurately represent current location on a slower time scale (Figure 3.7). Moreover, slow gamma phases of place cell spikes shifted across sequences, with earlier and later slow gamma phases representing earlier and later locations, respectively. In contrast, spikes occurred around the same fast gamma phase regardless of sequence progression or spatial information carried by the spike.

Our results agree with the hypothesis that slow and fast gamma reflect distinct spatial coding modes in the hippocampus, with 'prospective' coding of upcoming locations and 'retrospective' coding of recent locations occurring during slow and fast gamma, respectively (Chapter 2; Bieri et al., 2014). The predictive function of the slow gamma mode might rely on the temporal compression of stored spatial sequences,

providing a rapid "look ahead" toward upcoming locations. Such predictive firing has been observed at decision points and linked to subsequent goal destinations (Johnson and Redish, 2007; Wikenheiser and Redish, 2015). Also, slow gamma is enhanced when previously experienced sequences guide an animal's path (Cabral et al., 2014). Compressed sequences during awake sharp wave ripples (SWRs) also predict animals' future trajectories (Pfeiffer et al., 2013). Interestingly, sequence activation during awake SWRs coincides with transient increases in slow gamma (Carr et al., 2012). Together, these findings support the hypothesis that slow gamma promotes the retrieval of stored place cell sequences in a compressed, behaviorally useful form.

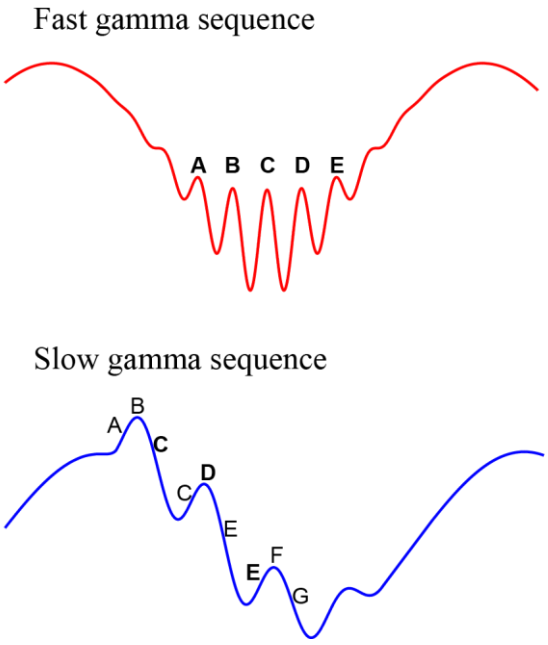

Figure 3.7: Schematic of sequence activation during slow and fast gamma. **A.** Individual locations are represented on separate fast gamma cycles. **B.** Multiple locations are represented in a time-compressed manner on each slow gamma cycle, triggering activation of place cells with fields located ahead of the animal's current position. Bold fonts indicate maximal firing.

On the other hand, theta sequences during fast gamma more accurately represented current position. These results are consistent with previous fast gamma findings. Fast gamma links CA1 to inputs from the medial entorhinal cortex (Colgin et al., 2009; Schomburg et al., 2014), which convey information about current location (Brun et al., 2002; Hafting et al., 2005; Zhang et al., 2013). Accordingly, place-based navigation is thought to rely on fast gamma (Cabral et al., 2014). Also, fast gamma

frequencies increase with increasing running speed, which likely enables faster transitions across ensembles within a sequence at higher running speeds (Zheng et al., 2015; Ahmed and Mehta, 2012). These findings support the conclusion that fast gamma promotes coding of ongoing spatial-temporal information.

In Chapter 2, we found that theta phase precession was disrupted during slow gamma, with spikes largely occurring at restricted theta phases corresponding to early locations within place fields. If single locations are represented on individual gamma cycles (Lisman, 2005), then relatively short distances would be coded during slow gamma, due to the low number of slow gamma cycles occurring within a theta cycle. However, we instead found an increase in spatial distance covered per unit time by theta sequences during slow gamma. This increase in represented distance occurred because multiple, not single, locations were represented within each slow gamma cycle. Moreover, place cells fired at different phases of slow gamma depending on the location they represented. This slow gamma phase coding is reminiscent of earlier findings in which different phases of ~30 Hz gamma in prefrontal cortex coded different items maintained in short-term memory (Siegel et al., 2009).

In contrast, spikes were locked to the same fast gamma phase across successive fast gamma cycles, in agreement with existing theories of hippocampal gamma (Lisman, 2005). Fast gamma-associated sequences represented relatively short distances that were closely tied to current location. Also, theta phase precession has been reported to persist during fast gamma (Bieri et al., 2014). Theta phase precession is thought to reflect coding of recently visited locations on earlier theta phases and upcoming locations on later theta phases (Dragoi and Buzsaki, 2006). A possible explanation for this collection of results is that spatial representations during fast gamma are limited to place fields that the animal is currently within (rather than non-local activity) and are centered on the

animal's current location. In this way, the total length of the behind and forward portions of the path may cover a shorter distance, and the decoded position may thus be more consistent with actual location. The relatively high frequency of fast gamma may also be optimal for representing single locations within a gamma cycle through a "winner take all" mechanism. In this framework, cells receiving the most excitatory input are selectively activated as the network is briefly released from inhibition during each gamma cycle (de Almeida et al., 2009). This brief window of opportunity may limit activity from spreading to cells that are not extrinsically driven.

The ability of the hippocampus to handle sequences of spatiotemporal information is a dynamic process, involving both sequence encoding and retrieval. The current study suggests a possible mechanism for achieving these dual functions through different gamma subtypes. During sequence retrieval, an initial cue may trigger the first ensemble in a linked sequence of place cell ensembles. The relatively long slow gamma period may then allow successive items within the sequence to be retrieved in a temporally compressed fashion. Fast gamma may instead provide a temporal coding scheme optimal for organizing ongoing sequences in real time. Fast gamma-mediated inputs from MEC (Colgin et al., 2009; Schomburg et al., 2014) may be compartmentalized within the relatively short fast gamma cycles, ensuring that place cells are selectively driven by inputs carrying information about the current environment.

3.3 METHODS

Subjects. Five male Long-Evans rats weighing approximately 350–500 g were used in the study. During the data collection period, rats were placed on a food deprivation regimen that maintained them at ~90% of their free-feeding body weight.

Testing procedures. Following the post-surgery recovery period, rats were trained to run three 10-minute sessions per day on a linear track. The linear track was 2 m long, 10 cm wide, and placed 64 cm above the floor. Rats were trained to run back and forth on the track, receiving small pieces of sweetened cereal or vanilla cookies at the ends. Every rat was trained on the linear track for at least 3 days prior to the start of recording to ensure familiarity with the environment. Between recording sessions, rats rested for ~10 minutes in a towel-lined, elevated ceramic container.

Place fields. Rats' trajectories were tracked using red and green LEDs on the headstage. Spatial firing rate distributions ("place fields") for each well-isolated putative pyramidal cell were constructed by summing the total number of spikes that occurred in a given location bin (3 cm), dividing by the amount of time that the animal spent in that bin, and smoothing with a 15 cm (5 bins) SD Gaussian centered on each bin. Place fields were spatially ordered by the location of their peak firing rate. A total of 650 CA1 place cells were used.

Detecting individual theta cycles for Bayesian decoding. LFP signals were band-pass filtered for theta (6–10 Hz) and delta (2–4 Hz), and the time-varying power for each was determined as described in Appendix A. For theta cycle selection, a single LFP signal was chosen for each session by identifying the channel with the highest time-averaged theta power and at least one recorded CA1 cell. Periods of theta activity were defined using the theta-delta power ratio (Csicsvari et al., 1999). Specifically, theta power was required to be at least three times greater than delta power. Data with insufficient theta activity were not included in analyses. Individual theta cycles were cut at the theta phase with the lowest number of spikes from all recorded CA1 cells during that session.

Bayesian decoding analyses. The most likely position represented by spiking activity from CA1 place cells was estimated using a Bayesian decoding approach (Zhang et al., 1998; Brown et al., 1998; Jensen and Lisman, 2000; Gutpa et al., 2012; Bieri et al., 2014). Recording sessions with fewer than 20 cells were not analyzed, and only theta cycles containing at least three active place cells and a running speed greater than 5 cm/s were decoded. Place fields were constructed for each recording session on the linear track, as described in the ‘‘Place fields’’ section above. Decoding was performed for each theta cycle using a 40 ms sliding time window shifted by 10 ms at each step. The probability of the animal to be at position x, given the number of spikes n from each cell collected in the time window t was estimated using Bayes rule:

$$P(x|n) = \frac{P(n|x)P(x)}{P(n)}$$

P(n | x) was estimated using the firing rates from the experimentally obtained place fields in the same 10 minute linear track session. It was assumed that the firing rates of different place cells were statistically independent and that the number of spikes from each cell followed a Poisson distribution (Zhang et al., 1998; Jensen and Lisman, 2000). P(n), the normalizing constant, was set so that P(x | n) summed to 1. P(x) was set to 1.

Theta sequence analysis. Theta sequences were characterized by first determining the longest contiguous set of time bins that contained spikes. Contiguity was broken when there were 2 or more adjacent time bins without spikes. For each time bin within the contiguous set of bins, 1000 data points were randomly drawn from the decoded probability distribution (P(x | t)) belonging to each time bin. The collected data points

within each theta sequence were fit with a regression line. To determine if the theta sequence was significant, a shuffling approach was used that was based on an approach previously described for sharp wave-related sequences (Karlsson and Frank, 2009). For each sequence, the order of the time bins was randomly shuffled 1000 times, and a new regression line was calculated. The R^2 value of the original regression line had to be larger than 95% of the shuffled R^2 values to be considered significant. The regression coefficient provided the slope of the theta sequence. Sequences with negative slopes were excluded from this study. The difference between the last and first time bin, and the difference between the positions associated with these time bins, provided the temporal duration of the sequence ("t-span") and spatial path length ("x-span"), respectively.

Gamma power during individual theta cycles. For every tetrode with cells used for Bayesian decoding, slow and fast gamma power were estimated using the method described in Appendix A. Slow and fast gamma power estimates were then z-scored across the entire recording session and averaged across tetrodes with cell recordings and across respective frequency ranges. The maximum value of the resulting time-varying power was used to obtain a single slow gamma value and a single fast gamma value for each theta cycle.

Gamma power rank. Sequences were ranked within each day according to slow gamma power and fast gamma power. A rank of 0 corresponded to lowest power, and a rank of 1 corresponded to highest power.

Sequence accuracy. The entire set of sequences was ranked separately by the average residual value of the regression fit and the slope. Lower rank values corresponded to

lower numerical values. The residual rank and the slope rank for each sequence were averaged and normalized between 0 (high accuracy) and 1 (low accuracy) such that high accuracy corresponded to lower slopes and smaller residual values. Sequences with residuals above the median were excluded from this analysis to avoid inclusion of non-accurate sequences due to noise.

Phase analyses. The time varying phases of slow gamma, fast gamma, and theta were determined by Hilbert transformation of respective bandpass filtered signals (25–55 Hz for slow gamma, 60–100 Hz for fast gamma, and 6–10 Hz for theta). Oscillatory peaks were defined as 0° for all bandwidths. The phase of each spike was determined by finding the LFP time stamp closest to each spike time. To determine the significance between different groups of phases (Figure 3.5), a multi-sample Mardia-Watson-Wheeler test was performed using Oriana 4.02 (Kovach Computing Services).

Categorization of slow gamma sequences and fast gamma sequences. Slow gamma sequences and fast gamma sequences were defined as sequences exhibiting peak power for the gamma type of interest that was higher than the median peak power for the gamma type of interest and peak power for the other gamma type that was lower than the median peak power for the other gamma type.

Phase-phase coupling shuffling procedures. The theta phase-gamma phase values associated with spike times were shuffled in two ways. The first method shuffled the pairings between theta and gamma phases for all spike times, thereby disrupting theta phase-gamma phase coupling (Belluscio et al., 2012) but maintaining theta and gamma phase distributions. The second method preserved the phase-phase coupling relationship

but reassigned a new time point to each spike based on each cell's theta phase distribution. This was achieved by randomly drawing a theta phase from the total collection that occurred for that cell on that day. The time point at which that theta phase occurred was identified and used to find the corresponding gamma phase.

Determination of gamma cycle number. For each theta sequence, gamma phases were determined across time, as described above. Individual gamma cycles were defined from peak to peak, using the time point closest to when the phase was 0°. The gamma cycle with the highest power was defined as cycle 0. Cycles occurring before cycle 0 were numbered with decreasing integer values, and cycles occurring after cycle 0 were numbered with increasing integer values. Incomplete cycles at the beginning or end of the sequence were excluded from analyses. The number of cycles analyzed within each theta sequence was limited to 3 (-1 to 1) for slow gamma and to 5 (-2 to 2) for fast gamma. These selection criteria correspond to the estimated average number of cycles encompassed within a gamma episode. Histograms of spike phases for each cycle number were plotted using 30° bins, and were smoothed across 5 bins.

Categorization of place cell locations. Within each theta cycle, active place cells were ordered according to the spatial location of their peak firing rate using all spikes recorded within a given session. Cells that were active during each sequence were grouped into three categories. The cell representing the earliest location (i.e. closest to the beginning of the track) and the second earliest location were placed in the "Early" and "Middle" categories, respectively. All subsequent cells were placed in the "Late" category. This method was chosen because 50% of sequences had only three active place cells.

Histograms of spike phases for each spatial category were plotted using 20° bins and smoothed across 7 bins.

Place cell activity during slow and fast gamma sequences. The number of spikes that each cell contributed to slow gamma sequences and fast gamma sequences was quantified for each recoding day. Cells were considered ‘high firing’ or ‘low firing’ for each gamma type if they contributed greater or fewer spikes, respectively, than the median spike count from all cells for that particular gamma type.

Chapter 4: Representation of novel and familiar object-place associations during slow and fast gamma rhythms

4.1 SUMMARY

Hippocampal gamma oscillations transiently increase during memory-dependent tasks (Johnson and Redish, 2007; Montgomery and Buzsaki, 2007; Sederberg et al., 2007; Jutras et al., 2009; Trimper et al., 2014) and are thought to play a role in memory encoding by coordinating the activity of neurons that code related information (Jensen and Lisman, 2005). Here we use a hippocampal-dependent novel object recognition (NOR) task (Clark et al., 2000; Broadbent et al., 2004; Eacott and Norman, 2004; Lee et al., 2005; Winters et al., 2008; Barker and Warburton, 2011) in rats to investigate the roles of slow and fast gamma rhythms during memory encoding of novel object-place associations, compared to memory retrieval for previously learned object-place associations. Because the level of hippocampal dependence varies depending on the type of novelty involved (Eichenbaum et al., 2007; Winters et al., 2008), we examined gamma activity during three conditions: a novel object placed in a familiar location, a familiar object placed in a novel location, and a novel object placed in a novel location. Considering both behavioral and physiological results together, the strongest and most consistent effects were observed for fast gamma during the novel object-novel place condition. We found that fast gamma power, CA3-CA1 phase synchrony, and phase-locking of place cell spike times significantly increased during exploration of novel objects in novel locations compared to familiar object-place associations. On the other hand, slow gamma CA3-CA1 phase synchrony was significantly higher during exploration of a familiar object-place association compared to exploration of a novel object in a novel location. These results support the hypothesis that fast gamma conveys

novel sensory information from MEC during encoding of new object-place associations, while slow gamma phase synchrony may allow previously learned object-place associations to be retrieved from CA3.

4.2 INTRODUCTION

Gamma oscillations (~25–100 Hz) are prominent in the entorhinal-hippocampal network and have been shown to appear during a variety of memory tasks in rats, monkeys, and humans (Fell et al., 2001; Johnson and Redish, 2007; Montgomery and Buzsaki, 2007; Sederberg et al., 2007; Jutras et al., 2009; Trimper et al., 2014). Gamma oscillations occur as two distinct variants that are thought to route different streams of information entering hippocampal subfield CA1 (Colgin et al, 2009; Schomburg et al., 2014). Slow gamma (~25–55 Hz) couples CA1 to inputs from CA3, a hippocampal subfield thought to be important for memory retrieval (Brun et al., 2002; Sutherland et al., 1983; Steffenach et al., 2002), while fast gamma (~60–100 Hz) supplies the hippocampal network with ongoing spatial information from the medial entorhinal cortex (MEC) (Brun et al., 2002; Fyhn et al., 2004; Hafting et al., 2005). Functional consequences of this selective coupling have been observed in single CA1 place cells, as well as ensembles of place cells, in the form of rapidly alternating spatial coding modes (Chapter 2; Bieri et al., 2014) and the coordination of spatial sequences (Chapter 3). The firing properties exhibited in each case were hypothesized to reflect cellular mechanisms of memory retrieval during slow gamma and memory encoding during fast gamma. However, if such coupling is critical for memory function, then slow and fast gamma should also be evident during behaviors in which these mnemonic processes are explicitly demonstrated. In this study, we identify periods of memory encoding and retrieval using

a novel object recognition (NOR) task and examine slow and fast gamma activity during each.

In the NOR task, rats are presented with a novel object and a familiar object in the same environment and are allowed to freely explore each item. Rats have been shown to spend more time exploring novel objects compared to familiar objects (Ennaceur and Delacour, 1988), providing behavioral evidence that memory formation of the familiar object has occurred, and presumably, that memory encoding takes place during exploration of the novel object. Importantly, the ability to discriminate between novel and familiar objects is impaired in rats with hippocampal lesions. Interestingly, however, this deficit is variable and appears to depend on the specific type of novelty involved (Eichenbaum et al., 2007; Winters et al., 2008). When novelty only involves the identity of the object, some studies report no deficits in rats with hippocampal lesions (Mumby et al., 2002; Winters et al., 2004), while others report variable deficits depending on the size of the lesion (Broadbent et al., 2004) or the length of delay between familiarization and novel exposure (Clark et al., 2000). In contrast, when novelty involves the location of an object, deficits are more reliably observed following hippocampal lesions (Eacott and Norman, 2004; Lee et al., 2005; Winters et al., 2008; Barker and Warburton, 2011). Due to the variable involvement of the hippocampus in the NOR task, we examined gamma activity during three types of object novelty: novel object identity, novel object location, and novel object identity in a novel location. Our results suggest involvement of fast gamma during novelty involving object and location changes, but not novelty that only

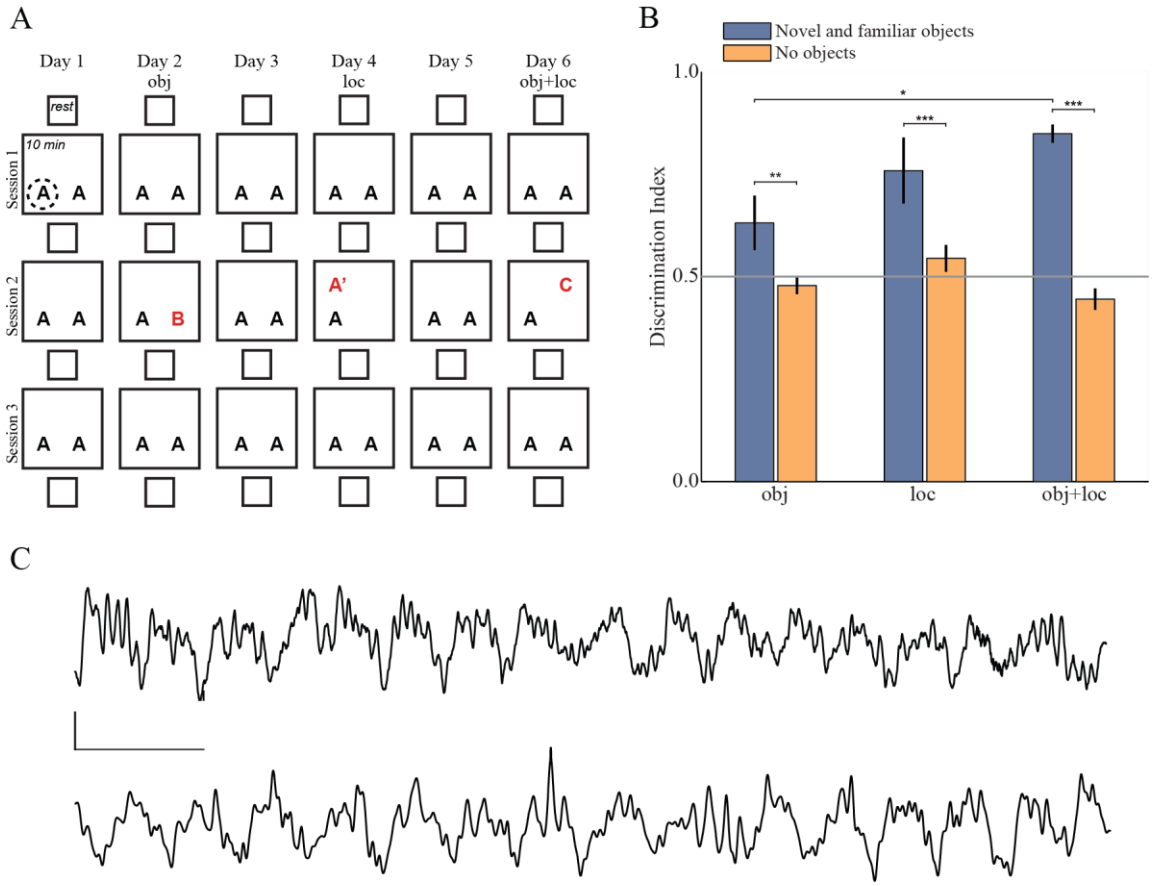

Figure 4.1: The NOR task and example traces.
A. The novel object recognition task showing the obj (day 2, object B), loc (day 4, object A'), and obj+loc (day 6, object C) conditions. Each day consisted of 3 ten-minute exploration sessions separated by ten-minute rest periods, and the order of the conditions was randomly assigned for each animal to avoid ordering effects. Two of the rats in this study did not undergo 're-familiarization' days (i.e., 'Day 3' and 'Day 5' in Figure 1A; see Methods). Data analysis was limited to the first three minutes of each session and to periods when the animal's head was within 10 cm of the center of the object (dotted line in top left session). **B.** The discrimination index (novel time /(novel time + familiar time)) (± SEM) for the obj, loc, and obj+loc novelty conditions. Animals explored the novel object significantly more than the familiar object for all novelty conditions. Also, animals explored the novel object significantly more during the obj+loc condition compared to the obj condition. **C.** Example recordings from CA1 stratum pyramidale during novel (obj+loc) exploration (top panel) and familiar exploration (bottom panel) (calibration; 250 ms, 0.5 mV). * $p < .05$; ** $p < .01$; *** $p < .001$.

involves object changes, in line with hippocampal lesion studies.

4.3 RESULTS

LFPs, and spiking activity from 84 place cells, were recorded in the cell body layers of hippocampal areas CA1 and CA3 of 6 rats performing a novel object recognition task (NOR) (Figure 4.1A). We examined three types of novelty: a change in object identity ("obj"), a change in object location ("loc") and a change in object identity and location ("obj+loc"). Evidence of memory formation for the familiar object (or familiar object-place association) was measured by an increase in exploration time of the novel condition compared to the familiar condition. The order of novelty condition was randomly assigned to avoid ordering affects. The behavioral effect was determined using the discrimination index (DI) between novel and familiar objects (novel time / (novel time + familiar time)), and the control DI was determined from the corresponding locations during sessions with no objects. The behavioral effect of novelty differed across conditions, as evidenced by a significant interaction between novelty condition and data type (i.e., experimental or control) on the DI (Figure 4.1B; Linear mixed model; $F(2,112) = 4.33$, $p = 0.02$). Also, post hoc univariate analysis of the experimental data revealed a significant effect of novelty condition on DI ($F(2,112) = 3.60$, $p = 0.03$). Pairwise comparisons revealed that the DI for obj+loc was significantly higher than the DI for obj (Bonferroni corrected $p = 0.03$) but not for loc (Bonferroni corrected $p = 0.9$), and the obj DI was not significantly different from the loc DI (Bonferroni corrected $p = 0.5$). The DI measures for all experimental conditions were significantly higher than controls (obj: $F(1,112) = 6.01$, $p = 0.02$; loc: $F(1,112) = 7.88$, $p = 0.01$; obj+loc: $F(1,112) = 42.04$, $p < 0.001$), and did not depend on the order of presentation ($F(1,14) = .14$, $p = 0.72$). These results indicate that the animals explored the novel objects significantly more than the

familiar objects for all novelty conditions and that the behavioral effect was larger for the obj+loc condition compared to the obj condition.

We next examined slow and fast gamma oscillations in CA1 during exploration of novel conditions compared to familiar conditions (Figure 4.1C). We first plotted slow and fast gamma power, averaged across all rats, across the different locations in the training enclosure for the three novelty conditions. The gamma power maps appeared to show a consistent increase in fast gamma power, but not slow gamma power, selectively at the location where the novel object was placed (Figure 4.2A). Thus, we hypothesized that slow and fast gamma power were differentially affected by novelty, with fast gamma power more likely to increase during novel conditions. In line with this hypothesis, we found a significant interaction between gamma type and novelty condition on the percent change in gamma power during novel exploration compared to familiar exploration (Figure 4.2B; linear mixed model; $F(2,64) = 4.39$, $p = 0.02$). Fast gamma power tended to increase with novelty, although only the novel obj+loc condition was significantly increased compared to the familiar condition ($t(12) = 6.70$, $p < 0.001$ for obj+loc; $t(13) = 1.94$, $p = 0.07$ for obj; $t(4) = 0.85$, $p = 0.4$ for loc). There was no significant effect of the type of novelty on the percent change in fast gamma power relative to the familiar condition ($F(2,64) = 1.60$, $p = 0.2$). On the other hand, there was a significant effect of novelty condition on percent change in slow gamma power ($F(2,64) = 8.18$, $p = 0.001$), reflecting the lack of consistent effects on slow gamma power in response to generalized novelty. Compared to the familiar condition, slow gamma power increased slightly but not significantly in the obj+loc condition ($t(12) = 1.60$, $p = 0.1$) and decreased slightly but not significantly in the loc condition ($t(4) = 1.90$, $p = 0.1$). During obj novelty, slow gamma power increased significantly relative to the familiar condition ($t(13) = 6.48$, $p < 0.001$). Pairwise comparisons revealed that the percent change in slow gamma power

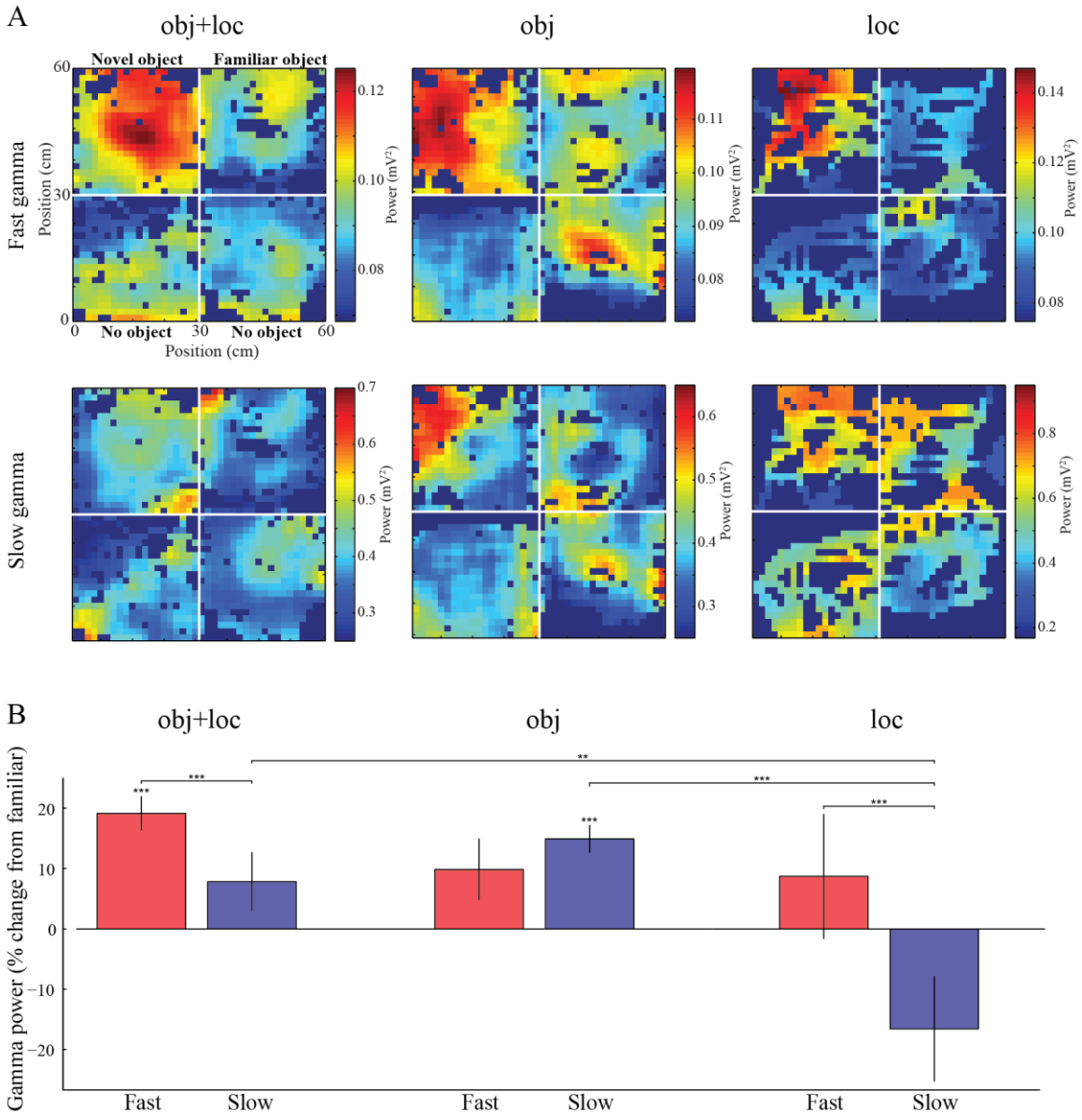

Figure 4.2: Slow and fast gamma power in response to novelty.
A. Color-coded fast (top row) and slow (bottom row) gamma power in CA1 across different positions in the recording enclosure during obj+loc (left column), obj (middle column), and loc (right column) novelty conditions. For all conditions, the configurations of the color maps were re-arranged such that the novel object is shown in the top left quadrant and the familiar object in the top right quadrant. Power estimates at each location were averaged across all animals. Note the strong fast gamma power that is apparent near the novel object across all novelty conditions. **B.** Percent change (± SEM) in gamma power during novel exploration compared to familiar exploration is shown. ** $p < .01$; *** $p < .001$.

relative to the familiar condition was significantly lower for the loc condition compared to the obj condition (Bonferroni corrected $p < 0.001$) and the obj+loc condition (Bonferroni corrected $p = 0.009$).

We next tested whether changes in fast gamma power differed from changes in slow gamma power within each novelty condition (Figure 4.2B). For the obj+loc and loc conditions, the percent change in gamma power relative to the familiar condition was significantly greater for fast gamma than for slow gamma ($F(1,9) = 345.38$, $p < 0.001$ for obj + loc and $F(1,3) = 335.18$, $p < 0.001$ for loc). However, for the obj condition, the percent change in gamma power did not significantly differ for slow and fast gamma ($F(1,10) = 0.06$, $p = 0.8$). There was, however, a significant main effect of novelty on gamma power ($t(27) = 4.46$, $p < 0.001$), reflecting the increases in both slow and fast gamma power that occurred in response to novelty in the obj condition. Together, these results indicate that the effects of novelty on slow and fast gamma power depend on whether the novelty involves object identity, location, or both. Fast gamma power was selectively enhanced compared to slow gamma for the two novelty conditions involving location changes. Slow gamma power changes were not significantly greater than fast gamma power changes in any novelty condition, but slow gamma power was significantly increased relative to familiar exploration for the novelty condition involving an object change.

Running speed has been shown to be positively correlated with fast gamma power and negatively correlated with slow gamma power (Kemere et al., 2013; Zheng et al., 2015). Thus, if animals exhibited different running speeds during novel and familiar conditions, it could potentially explain our effects. To assess whether running speed contributed to the above-reported differences in slow and fast gamma power, we averaged running speed during novel exploration and familiar exploration for each

novelty condition (Figure 4.3). We found no significant interaction between novelty condition and exploration type (i.e., novel vs familiar) on running speed (linear mixed model; $F(2,32) = 2.50$, $p = 0.1$), and pairwise comparisons of running speed during novel and familiar exploration revealed no significant differences for the obj (Bonferroni corrected $p = 0.2$), loc (Bonferroni corrected $p = 0.2$), or obj+loc (Bonferroni corrected $p = 0.08$) conditions. There was also no main effect of novel vs familiar exploration on running speed ($F(1,32) = 0.74$, $p = 0.40$). These results suggest that it is unlikely that changes in fast gamma power and slow gamma power during the NOR task were due to systematic changes in running speed.

CA3 is thought to be critical for forming associations between different aspects of a spatial memory, such as associations between objects and locations (Treves and Rolls, 1994). Thus, we hypothesized that oscillatory coupling between CA3 and CA1 would be enhanced during encoding of novel object-place associations. To test this hypothesis, we examined slow and fast gamma coupling between CA1 and CA3 by estimating phase synchrony, which measures the consistency of phase differences between two signals (Figure 4.4). We found a significant interaction between gamma type and novelty condition on the percent change in gamma phase synchrony during novel exploration compared to familiar exploration (linear mixed model; $F(2,194) = 5.50$, $p = 0.005$), indicating that novelty conditions differentially affected slow and

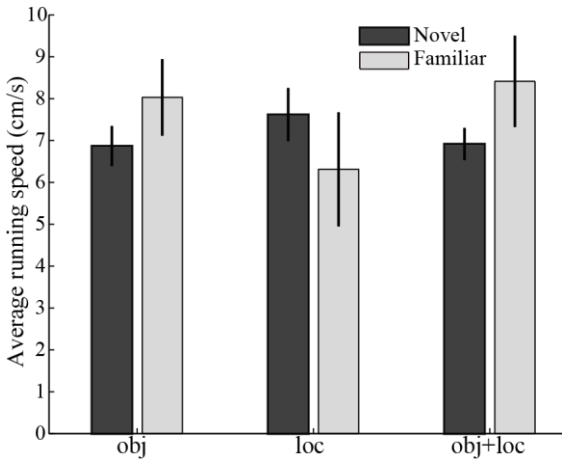

Figure 4.3: Running speed.
Average running speed (± SEM) during novel and familiar exploration for all novelty conditions. There were no significant differences in running speed between novel and familiar exploration periods for any of the novelty conditions.

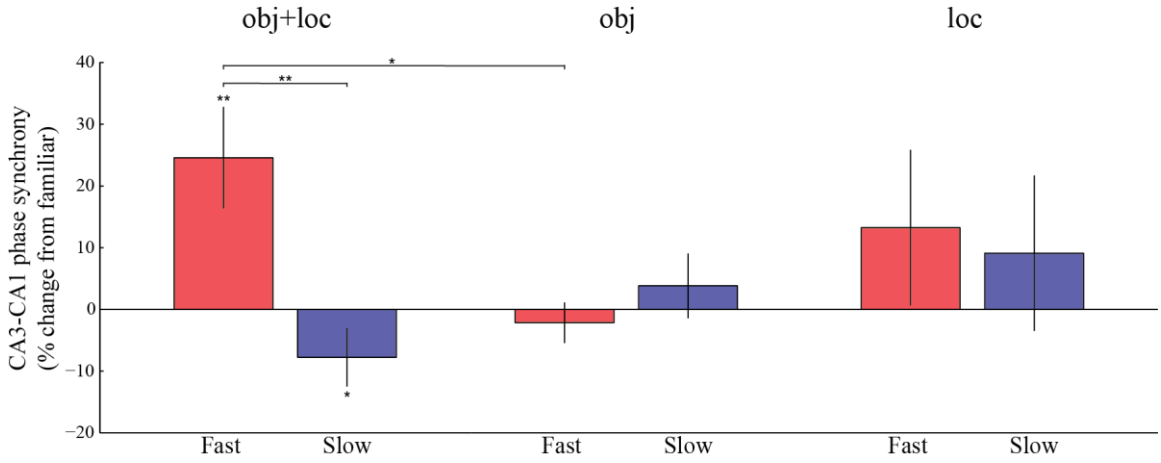

Figure 4.4: CA3-CA1 phase synchrony in response to novelty.
Percent change (± SEM) in CA3-CA1 phase synchrony during novel exploration compared to familiar exploration for slow and fast gamma. * $p < .05$; ** $p < .01$.

fast gamma synchrony. Post hoc analysis revealed a significant effect of novelty condition on the percent change in fast gamma synchrony ($F(2,194) = 3.34$, $p = 0.04$), indicating that different novelty conditions produced different effects on fast gamma synchrony between CA3 and CA1. Pairwise comparisons between novelty conditions showed that the percent change in fast gamma synchrony was increased for obj+loc compared to obj (Bonferroni corrected $p = 0.03$), but did not significantly differ between loc and obj conditions (Bonferroni corrected $p = 0.4$) or between loc and obj+loc conditions (Bonferroni corrected $p = 1.0$). The percent change in slow gamma synchrony relative to familiar exploration was also differentially affected by different novelty conditions (significant effect of novelty condition: $F(2,194) = 3.13$, $p = 0.05$), although none of the pairwise comparisons were statistically significant (obj+loc compared to obj: Bonferroni corrected $p = 0.1$; loc compared to obj: Bonferroni corrected $p = 1.0$; and loc compared to obj+loc: Bonferroni corrected $p = 0.08$). Moreover, planned comparisons of the percent change in fast vs slow gamma synchrony during novel exploration relative to familiar exploration for the obj+loc condition revealed an increase in fast gamma

synchrony compared to slow gamma synchrony ($F(1,30) = 8.99$, $p = 0.005$). Also, fast gamma synchrony in the obj+loc condition was significantly greater during novel exploration than during familiar exploration ($t(35) = 3.37$, $p = 0.002$), whereas slow gamma synchrony was significantly greater during familiar exploration ($t(36) = 2.74$, $p = 0.01$). Changes in CA3-CA1 gamma synchrony did not differ significantly for slow and fast gamma during the obj ($F(1,31) = 2.36$, $p = 0.1$), or loc conditions ($F(1,20) = 0.033$, $p = 0.9$). And, CA3-CA1 slow and fast gamma synchrony during novel exploration did not change significantly compared to synchrony during familiar exploration for obj (fast: $t(36) = 0.65$, $p = 0.5$; slow: $t(36) = 0.73$, $p = 0.5$) and loc (fast: $t(23) = 1.05$, $p = 0.3$; slow: $t(23) = .72$, $p = 0.5$) conditions. These results raise the possibility that selectively enhanced fast gamma coupling between CA3 and CA1 during the obj+loc condition serves to facilitate encoding of novel object-place associations.

One possibility is that enhanced fast gamma coupling in the hippocampal network during novel object-place encoding coordinates ensembles of place cells that code information about the location and the objects. If so, then place cell activity should be more strongly modulated by fast gamma oscillations during encoding of novel object-place associations. To investigate this possibility, we quantified phase-locking to CA1 slow and fast gamma in place cells that coded locations that overlapped with novel and familiar objects. We then tested whether place cells were differentially phase-locked to slow and fast gamma during the three novelty conditions compared to exploration of familiar object-place associations (Figure 4.5). We found a significant interaction between exploration type (i.e., novel or familiar), gamma type, and novelty condition on place cell phase-locking ($F(2,168) = 3.00$, $p = 0.05$). Phase-locking to fast gamma was greater during novel obj+loc exploration compared to familiar exploration (Bonferroni corrected $p = 0.001$), and compared to novel exploration in the obj (Bonferroni corrected

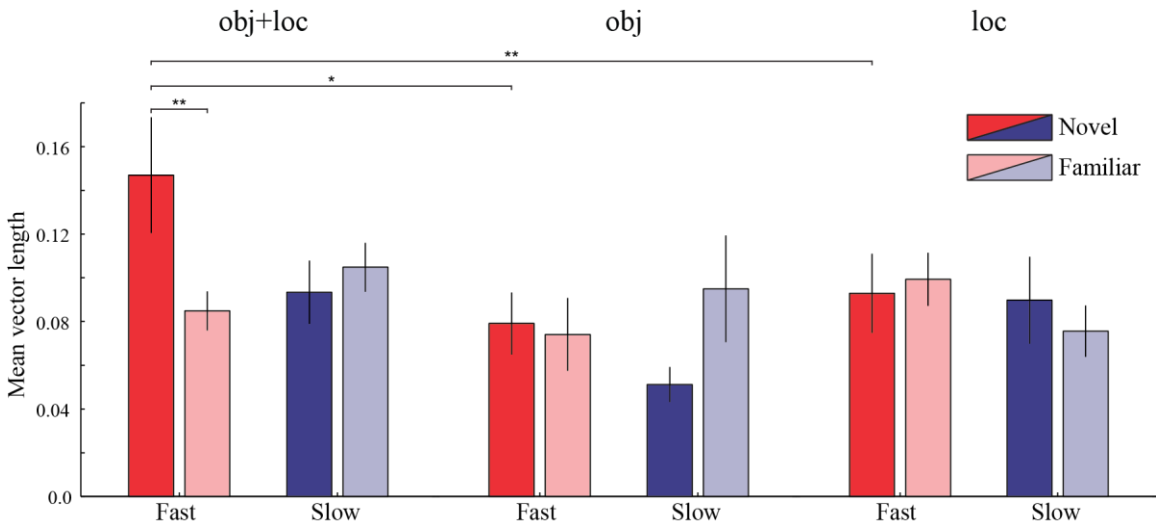

Figure 4.5: Place cell phase locking to CA1 gamma in response to novelty.
Mean vector length (± SEM) of CA1 slow and fast gamma phases for place cell spike times. Place cells were significantly more phase-locked to fast gamma during novel exploration than during familiar exploration for the obj+loc condition. Fast gamma phase-locking during novel exploration was significantly higher for the obj+loc condition than for the obj and loc conditions. * $p < .05$; ** $p < .01$.

$p = 0.04$) and loc (Bonferroni corrected $p = 0.008$) conditions. Analogous effects were not observed for slow gamma phase-locking. These findings suggest that place cells are selectively coordinated by fast gamma during encoding of novel object-place associations, when novelty involves changes in both object identity and object location.

4.4 Discussion

Our results suggest that fast gamma may coordinate neuronal activity in the hippocampal network during encoding of novel object-place associations. When novelty was defined by a new object in a location where an object had not been presented previously (obj+loc), there was a significant increase in fast gamma power and CA3-CA1 phase synchrony relative to familiar object exploration, and place cells that fired near the location of the new object became strongly modulated by fast gamma. In contrast, slow

gamma power did not increase, and CA3-CA1 slow gamma phase synchrony decreased relative to familiar object exploration during encoding of entirely novel object-place associations.

However, analogous results were not observed when novelty only involved a change in object identity (obj condition). Instead, an overall increase in power for both gamma types was observed during novel exploration compared to familiar exploration. When novelty only involved location (loc), there was a larger increase in fast gamma power compared to slow gamma power during novel exploration, but neither slow nor fast gamma power was significantly different during novel exploration compared to familiar exploration.

The fast gamma findings during the obj+loc and loc conditions are consistent with previous studies suggesting that fast gamma is important for transmitting information about spatial location from the MEC to the hippocampus. Place cells in area CA1 code 'place-based' representations of space during fast gamma (Cabral et al., 2014), and ensembles of CA1 place cells are coordinated by fast gamma when representing an animal's location in real-time (Chapter 3; Bieri et al., 2014). Such communication about current spatial experience may reflect a broader role of fast gamma in encoding memories of novel experiences. Increases in fast gamma power have been observed in area CA1 in rats during exploration of a novel maze, compared to a familiar maze (Kemere et al., 2013). A previous study in monkeys demonstrated an increase in spike-field coherence between cells and fast gamma oscillations in the hippocampal formation during successful encoding of novel images (Jutras et al., 2009). In humans, an increase in fast gamma power, but not slow gamma power, was observed in the hippocampus during successful encoding of words in a free recall task (Sederberg et al., 2007). Our results may therefore indicate formation of an associative memory for a novel object in a novel

location during enhanced fast gamma activity, when transmission of novel sensory information to the hippocampus is likely to be strongest.

Slow gamma, on the other hand, is thought to be generated by CA3 inputs to CA1 (Colgin et al., 2009; Schomburg et al., 2014), and CA3 is thought to play a key role in memory retrieval (Brun et al., 2002; Sutherland et al., 1983; Steffenach et al., 2002). The increase in slow gamma CA3-CA1 phase synchrony during the familiar condition compared to the novel object-novel location condition may therefore reflect memory retrieval of the previously learned object-place association.

Our results also indicate selective involvement of slow and fast gamma during novel exploration depending on whether the identity of the object, the location of the object, or both, were changed. Fast gamma measures consistently increased during novel exploration when novelty involved changes in object and location. One possible explanation is that fast gamma in the hippocampus is involved in integrating distinct 'what' and 'where' streams of information from the MEC and LEC, respectively (Hargreaves et al., 2005; Knierim et al., 2006; Eichenbaum et al., 2007; Knierim et al., 2014), as novel object-place associations are encoded.

Slow gamma activity only increased during object novelty (obj) but not when novelty involved location changes (obj+loc and loc). Interestingly, a recent study by Igarashi and colleagues (Igarashi et al., 2014) demonstrated strong oscillatory coupling between LEC and CA1 in the beta frequency range (~25 Hz) during sampling of a familiar odor cue. Because beta oscillations overlap in frequency with slow gamma, it is possible that beta oscillatory input from LEC might be misinterpreted as slow gamma. Alternatively, the findings may support the hypothesis that slow gamma carries 'what' information from LEC in contrast to fast gamma transmission of 'where' information from MEC. Interestingly, however, neither slow gamma power nor place cell phase-

locking to slow gamma was significantly increased during novel exploration compared to familiar exploration in the obj+loc condition. Moreover, there was a decrease in CA3-CA1 slow gamma phase synchrony during novel exploration relative to familiar exploration for the obj+loc condition. If slow gamma carried object-related information and fast gamma carried location information, one would expect both slow and fast gamma to be increased during novelty exploration in the obj+loc condition.

In contrast to the present study, other studies have reported increased slow gamma power and/or coherence during novel stimulus encoding (Kemere et al., 2013; Trimper et al., 2014). However, there are multiple differences between the current experimental paradigm and the experimental paradigms used in these earlier studies that may explain the seemingly contradictory findings. The study by Trimper and colleagues used a different novel object paradigm, which did not examine changes in location but instead only changed the objects that were presented in an unchanging set of locations. And, rats were tested across multiple novelty trials in the Trimper et al. study (2014), as opposed to the single novelty trials in the current study. It is thus possible that trial-to-trial learning produced an 'over-training' effect that reduced the saliency of each 'novel' experience. The animals may have then retrieved a memory of the general experience of encountering objects in these locations as they gained familiarity with the task, instead of primarily responding to the novel aspects of the experience. The latter point may also explain the results of another study that reported increased slow gamma in response to novelty (Kemere et al., 2013). In this study, increased slow gamma was observed as animals explored a novel W-maze containing no objects (Kemere et al., 2013). However, the animals had been trained on a similar W-maze previously and thus may have been retrieving their memory of the general task, rather than simply responding to novel stimuli in the novel maze.

Another potential explanation for the contrasting results in our study and the earlier study by Trimper and colleagues (2014) relates to running speed. In rats, gamma is modulated by running speed. At higher running speeds, fast gamma power increases, while slow gamma power decreases (Ahmed and Mehta, 2012; Kemere et al., 2013; Zheng et al., 2015). The study by Trimper and colleagues required animals to be stationary during novel object exploration but not during the control period. Thus, lower running speed may explain why they observed increases in slow gamma during novel object exploration. Another possibility is involvement of sharp wave ripples (SWRs), which occur during stationary periods and increase in frequency during novel object exploration (Larkin et al., 2014). Importantly, SWRs coincide with large, transient increases in slow gamma power and coherence between CA3 and CA1 (Carr et al., 2012). Although only a small number of SWRs were observed during novel exploration in Trimper et al., explicit removal of these events was not performed, making undetected SWRs a possible source of slow gamma activity. In the current study, however, no differences in running speed were observed between novel and familiar exploration (Figure 4.3), and animals were not required to remain stationary during novel object exploration. Thus, running speed and SWRs were less likely to be confounding factors.

In any event, the question of whether slow gamma plays a role during memory encoding and/or retrieval remains unresolved. In the present study, slow gamma coupling between CA3 and CA1 increased during familiar exploration in the obj+loc condition, supporting the hypothesis that slow gamma plays a role in memory retrieval. However, slow gamma power increased during novel exploration in the obj condition, which does not support this hypothesis. Determining the exact role of slow gamma power, and slow gamma coupling between CA3-CA1 during the NOR task may be explained by considering the differences across novelty conditions. Specifically, rather than a purely

spatial memory encoding condition, the obj condition may instead represent a 'mismatch' condition, during which the animal recognizes that the object is different than the one that was previously placed in that location. If so, then novel exploration in this condition would be expected to involve a combination of memory retrieval, as animals remember the previously presented object in this location, and memory encoding, as animals form a new memory for the novel object in the same location. Similar arguments could be made for the loc condition. In any case, the role of slow gamma in spatial memory processes remains an interesting question for future study and one that may be addressed more directly using different behavioral paradigms.

4.5 METHODS

Subjects. Six male Long-Evans rats weighing approximately 350–500 g were used in the study.

Novel object recognition task. Simultaneous local field potential (LFP) and single unit recordings were recorded in areas CA1 and CA3 using surgically implanted 14-tetrode 'hyperdrives' (Gothard et al., 1996). On each day of the experiment, animals were allowed to freely explore an open field environment (60 cm x 60 cm box) for 3 ten-minute sessions, alternated with ten-minute rest sessions in a towel-lined pot. The open field environment contained a single index card on the upper edge of one wall to provide a visual orientation cue. Prior to testing, the animal was habituated to the open field for at least 3 days with no objects present. On day 1 of the experiment, two identical objects were placed into the environment during all three exploration sessions. On day 2, the same two objects were placed in the environment during sessions 1 and 3, but during session 2, one of the objects was replaced with a novel object. Days 1 and 2 were

repeated two additional times to include all three novelty conditions (i.e., obj, loc, and obj+loc). The order of novelty type, specific location of the objects, and identity of objects were randomly assigned to avoid ordering effects. Objects were built with plastic toy blocks and were cleaned after each ten minute exploration session to remove scent cues. Two rats were only tested with the obj and obj+loc conditions, and did not have a 're-familiarization' day (i.e., a day with only familiar object-place associations in all three sessions) between the two experimental days with novel object-place associations.

Behavioral analysis. The total time during which the animal's head was within 10 cm of the center of the object during the first 3 minutes of the 10 minute novelty session was determined and used to calculate the discrimination index (DI) between the novel and familiar object (i.e., (novel time) / (novel time + familiar time). DI values of ~0.5 would indicate no preference for the novel object. DI values from the novelty conditions were compared to DI values from corresponding locations during sessions when no objects were present, in order to control for innate location preferences.

Slow and fast gamma power. The time varying oscillatory power was calculated using a Morlet wavelet convolution technique (see Appendix A for full description) for slow gamma (25–55 Hz), fast gamma (60–100 Hz), theta (6–10 Hz), and delta (2–4 Hz). The average power measures in the slow and fast gamma ranges were determined for each recording tetrode at each position using 1.5 x 1.5 cm sized bins. For plotting the heat maps (Figure 4.2A), the resulting powers were smoothed with a Gaussian distribution (σ = 6 cm), and averaged across all tetrodes and all animals. To avoid periods when the animal was not actively exploring, recordings were excluded if they did not have a theta to delta power ratio above 3 in every session (Csicsvari et al., 1999). To quantify the

results, the power for each tetrode was averaged across all bins within 10 cm of the center of the novel or familiar object, yielding a single slow gamma and fast gamma measure during novel exploration and familiar exploration for each tetrode. Statistical analyses considered each tetrode as a repeated measure within each animal subject.

Running speed. The running speed associated with each novelty condition was found by averaging the velocity across all time points when the animal's head was within 10 cm of the center of the object during the first 3 minutes of the 10 minute session.

Phase synchrony. Time varying phase synchrony between areas CA1 and CA3 was calculated using a previously described method (Lachaux et al., 1999). This method assesses covariance between the instantaneous phases of each oscillation frequency for a pair of recordings across a given span of time. Phase synchrony for slow gamma (25–55 Hz) and fast gamma (60–100 Hz) were determined during periods of exploration when the animal's head was within 10 cm of the center of the object. For each CA1 and CA3 tetrode pair, a single slow gamma and fast gamma phase synchrony measure was found by averaging across time for each frequency, and then averaging across frequencies within each respective frequency range. Statistical analyses considered each tetrode pair as a repeated measure within each animal subject.

Place cell phase-locking. CA1 and CA3 place cells that had spikes within 15 cm of the center of either object were included in the analysis. The larger radius compared to previous analyses was required to include a large enough number of spikes for reliable analysis. A total of 21 CA1 and 9 CA3 cells were included for the obj condition, 7 CA1 cells and 11 CA3 cells for the loc condition, and 19 CA1 and 17 CA3 cells for the

obj+loc condition. Cells that fired near the familiar object were included in analyses across all novelty conditions. The time-varying phases for slow gamma (25–55 Hz) and fast gamma (60–100 Hz) in area CA1 were determined using the Hilbert transform of the bandpass filtered signal for each respective frequency range. The slow and fast gamma spike phase distributions for each cell were then determined by identifying the slow and fast gamma phase, respectively, at the EEG time point closest to each spike time. Phase-locking was quantified using the mean vector length of the resulting collection of phases. For CA1, spike phases were determined using the LFP recorded from the same tetrode on which the cell was recorded. For CA3 place cells, phases for each spike time were estimated from all CA1 LFP recordings.

Chapter 5: Conclusion

5.1 SUMMARY

The experiments in this dissertation provide evidence that slow and fast gamma support distinct functional processing states in the hippocampus. In Chapter 2, it was shown that the hippocampal network alternates rapidly between a prospective and retrospective firing mode. During the prospective mode, place cells fired in advance of an animal's location, representing retrieval of maps of upcoming locations, and this mode was associated with slow gamma activity. During the retrospective mode, place cells coded recently passed locations, and this mode was associated with fast gamma, which may be important for maintaining active representations of recent experiences during memory encoding.

In Chapter 3, this concept was expanded to the coordination of place cell sequences. During slow gamma, spatial sequences were represented in a temporally compressed manner, providing a predictive 'sweep ahead' of the upcoming trajectory. Place cells for specific locations within the sequence were associated with different phases of the slow gamma cycle. This might be a mechanism for retrieving sequences of information, in which the relatively longer slow gamma cycle allows activity to spread from extrinsically driven cells to other cells that were linked sequentially during earlier learning. In contrast, place cell sequences were more likely to depict an animal's real-time physical location during fast gamma. Moreover, different phases of the fast gamma cycle did not code specific locations. Instead, place cells were phase-locked to the same gamma phase, regardless of the location they represented. In this way, the fast gamma cycle might segregate chunks of spatial information, such that each cycle is associated with a single location coded by a separate place cell assembly.

In Chapter 4, slow and fast gamma were examined during the encoding and retrieval of object-place associations. During exploration of novel object-place associations, there was a strong increase in fast gamma power and coupling between CA3-CA1. Moreover, place cells that coded the location of the novel object fired phase-locked to fast gamma. This suggests that fast gamma is involved with transmission of novel information from the EC to the hippocampus during the encoding of object-place associations. Slow gamma CA3-CA1 coupling was strong during retrieval of familiar object-place associations, although other slow gamma measures were inconsistent. This slow gamma coupling might reflect a retrieval process from CA3 to CA1, but more work is needed to determine if this is the case.

5.2 DISCUSSION

Chapters 2 and 3 demonstrated spatial coding modes during slow and fast gamma in area CA1, which receives dual input from EC and CA3. The spatial firing properties in CA1 were hypothesized to result from selective input of these regions during each respective coding mode. An important question is how this is reflected in the activity of neurons in each of these input regions. One possibility is that CA3 and EC selectively increase their activity during prospective and retrospective coding. Alternatively, CA3 and EC neurons might also exhibit coding modes, and their input might be enhanced through oscillatory coupling between regions. In support of the latter, De Almeida et al. showed that the spatial coding cells of the MEC ('grid cells') exhibit spatial coding modes similar to those observed in place cells (De Almeida et al., 2012). However, it is not known if CA3 place cells exhibit spatial coding modes. Future experiments involving dual recordings from CA1 and its inputs would help to reveal how neuronal activity in these regions is coordinated during the different coding modes.

It also remains to be seen whether spatial coding modes in the hippocampus are explicitly linked to memory function. Encoding and retrieval were inferred from the spatial coding properties of place cells; however, the behavioral task in Chapters 2 and 3 did not directly measure memory performance, per se. However, place cell sequences were linked to memory retrieval in a recent study by Wikenheiser and Redish, in which sequences were predictive of the animal's future path (Wikenheiser and Redish, 2015). An interesting question for future study is how slow gamma activity might relate to the memory aspects of this finding. The role of fast gamma in representing incoming sensory information has been suggested by recent studies (Cabral et al., 2014; Zheng et al., 2015), and its temporal dynamics appear to be optimal for plasticity (as in spike timing dependent plasticity, Bi and Poo, 1988; and plasticity induced by theta-burst stimulation, Larson et al., 1986; Larson and Lynch, 1986), but this has also not been directly shown. Advances in intracellular recording techniques in behaving animals may provide a way to observe synaptic changes concurrent with fast gamma activity during a memory-dependent task.

Behavioral studies attempting to link slow and fast gamma to specific encoding and retrieval processes have produced a variety of conflicting results (Trimper et al., 2012, Kemere et al., 2012, Jutras et al., 2009). One explanation is the inherent ambiguity in using animal behavior to define exclusive periods of memory encoding and retrieval, and the differences in the behavioral tasks themselves. Another explanation is provided by the results in Chapters 2 and 3. It is likely that encoding new information, as well as retrieval of stored information, involves communication about both types of information within the hippocampus, which are compared in CA1. For example, encoding a novel object-place association might rely on retrieval of stored information in order to recognize the situation as new. Similarly, correct memory retrieval requires cues about

current experience. It appears that communication about these different types of information alternate rapidly in the hippocampus, switching every 2-3 theta cycles (Colgin et al., 2009), which translates to a fraction of a second. Thus, measuring gamma activity over relatively longer behavioral periods may partially obscure this precise coordination. Nonetheless, dominant periods of memory encoding or memory retrieval might bias the hippocampus towards one type of gamma over a given span of time, explaining results such as those presented in Chapter 4.

It has been suggested that encoding and retrieval are optimal at specific phases of the theta cycle (Hasselmo et al., 2002; Kunec et al., 2005; Manns et al., 2007; Lever et al., 2010; Douchamps et al., 2013; Siegle and Wilson, 2014). Similarly, multiple studies have shown that slow and fast gamma occur at distinct theta phases (Colgin et al., 2009; Belluscio et al., 2012; Lasztoczi and Klausberger, 2014; Yamamoto et al., 2014; Schomburg et al., 2014). It is possible that these two correspond to one another; however, inconsistent results about the theta phase with which each gamma type is associated makes this conclusion difficult. A variety of factors may be responsible for the varying phase results, such as different recording techniques, behavioral tasks, or frequency ranges used to define gamma. The reasons for these discrepancies, as well as the relationship between gamma and the encoding/retrieval phases of theta, remain to be determined.

A related question is what coordinates the switching between each gamma type. It might occur spontaneously within the hippocampal formation, or it might be controlled by a separate region. Moreover, the alternation between modes might happen continuously at some rate, or it might be skewed towards one type depending on the different demands made on the network. Also, it is not known if switching between gamma modes occurs within a single collection of interneurons that change their firing

dynamics, or if it involves the recruitment of distinct sub-populations that separately support each gamma type. The latter is supported by recent results from Lastoczi and Klausberger (2014), which showed that CA1 interneurons selectively couple to oscillations in either the slow or fast gamma range. Furthermore, a study by Leao et al. (2012) showed that CA3-driven interneurons in CA1 inhibit input from EC, while disinhibiting input from CA3. Such a class of interneurons might be involved in generating slow gamma, while inhibiting fast gamma.

It has also been suggested that place cells tend to be driven by a single gamma type. In Colgin et al. (2009), it was found that 38% of CA1 place cells fired rhythmically with fast gamma, and 25% fired rhythmically with slow gamma, but only 6% of place cells fired rhythmically with both. Senior et al. (2008) reported distinct classes of place cells that had unique coding properties and fired at different phases of gamma and theta. These distinct classes of place cells may correspond to slow and fast gamma-modulated cells, considering that slow and fast gamma-modulated place cells preferentially fire at distinct gamma and theta phases (Colgin et al., 2009; Belluscio et al., 2012; Lasztoczi and Klausberger, 2014; Yamamoto et al., 2014; Schomburg et al., 2014). If this is the case, then functions supported by slow and fast gamma would be performed by different sets of hippocampal neurons. However, it was shown in Chapters 2 and 3 that neurons participate in both prospective and retrospective coding modes, and that individual place cells were equally active during both gamma types (Figure 3.6). Moreover, the properties associated with the place cell classes described in Senior et al. (2008) do not correspond to the properties associated with the different gamma subtypes without producing contradictions (see Chapters 2 and 3 for a more in depth discussion). A different conclusion, based on the current results, is that slow and fast gamma equally engage

place cells, allowing the same populations of cells to participate in both memory encoding and retrieval.

5.3 FINAL THOUGHTS

As our understanding of the brain grows, its remarkable complexity as a computational system becomes increasingly apparent. Evidence that oscillations support distinct processing states adds a fascinating layer to this complexity. The function of a neural network might not be solely determined by the physical layout of its connectivity, but also by its electrical state. The influence of this state may provide multiple levels of functionality to identical groups of neurons without requiring any physical changes to take place. In the case of gamma, the hippocampus might possess the ability to perform two opposing functions – memory reading and writing – without relying on distinct subsets of functionally specialized neurons. This versatility might be crucial for maximizing the efficiency of the brain, providing flexibility that is rapid and energetically inexpensive. As research on oscillations continues, it will be fascinating to see if these properties apply to other brain regions and the multitude of complex functions that they perform.

Appendix A: Methods

Subjects. A total of 10 rats were used. 2 of the rats were used in all chapters, 2 of the rats were used in Chapters 2 and 3, 1 of the rats was used in Chapters 3 and 4, and the remaining 5 were specific to a single chapter. Animals were housed on a reverse light dark cycle (lights off from 8 a.m.-8 p.m.) and tested during the dark phase. After surgery, animals were housed individually in cages (~40 cm x 40 cm x 40 cm) built from clear acrylic and containing enrichment materials (e.g., plastic balls, cardboard tubes, wooden blocks). Rats were allowed to recover from surgery for at least one week prior to the start of training. All experiments were conducted according to the guidelines of the United States National Institutes of Health Guide for the Care and Use of Laboratory Animals under a protocol approved by the University of Texas at Austin Institutional Animal Care and Use Committee.

Tetrode and recording drive preparation. Recording drives contained 13-14 independently movable tetrodes (13 in one rat, 14 in all others). Tetrodes were constructed from 17 μm polyimide-coated platinum-iridium (90%-10%) wire (California Fine Wire). Electrode tips in tetrodes targeted toward cell body layers were plated with platinum to reduce single channel impedances to ~150-300 kΩ at 1 kHz.

Surgical implantation and tetrode placement. Recording drives were implanted above the right hippocampus (in mm: AP 5.0, ML 5.0, DV 1 in one rat in Chapter 3 and one rat in Chapter 4; AP 3.8, ML 3.0, DV 1 all other rats) on the day of surgery. Bone screws were placed in the skull, and the screws and the base of the drive were covered with dental cement to affix the drive to the skull. Two screws in the skull were connected to the recording drive ground.

Tetrode placement. Over the course of a few weeks after drive implantation, tetrodes were slowly lowered toward their target locations. In Chapter 2, 11-12 of the tetrodes (11 in one rat, 12 in the other four rats) were targeted toward CA3 and CA1 cell body layers. In Chapter 3, 6 of the 14 tetrodes were targeted toward the CA1 cell body layer and 6 toward the CA3 cell body layer in 4 rats, and 12 of the tetrodes were targeted toward the CA1 cell body layer in 1 rat (CA3 data was not used for this study). In Chapter 4, 6 of the 14 tetrodes were targeted toward the CA1 cell body layer and 6 toward the CA3 cell body layer in 5 rats, and all tetrodes were targeted to the ventral portion of the hippocampus in 1 rat. In the latter case, dorsal CA1 and CA3 recordings were taken as the tetrode passed through these regions. In all animals, 1 tetrode was targeted toward the apical dendritic layers of CA1 and was used for hippocampal depth estimation as the rest of the tetrodes were turned down. Another tetrode was used as a reference for differential recording. This reference tetrode was placed at the level of the corpus callosum or higher and was recorded against ground to make sure that it was placed in a quiet location. All recording locations were verified histologically after experiments were finished. Representative examples of final recording locations are shown in Figure A.1. Final hippocampal recording sites used in all Chapters were located in or near CA1 and CA3 strata pyramidale. In one rat used for Chapter 2 and 3, two tetrodes targeted toward CA1 appeared in histological sections to be on the border of CA2-CA1. However, place cells and LFPs recorded from these tetrodes were indistinguishable from other CA1 recordings collected simultaneously. Therefore, place cells, interneurons, and LFPs from these tetrodes were included. In Chapter 2, the majority of CA3 tetrodes were located in CA3c (i.e., in the hilus). Because gamma oscillations exhibit large amplitudes in the hilus (Buzsaki et al., 1983; Bragin et al., 1995), volume-conducted gamma oscillations from the hilus contaminated LFP recordings from these tetrodes. Thus, LFP recordings from

CA3 tetrodes were not included in Chapter 2. Single unit recordings from CA3 tetrodes were included in Bayesian decoding analyses of activity during periods of slow and fast gamma in CA1 for Chapter 2. However, Bayesian decoding in Chapter 3 did not used CA3 data. In 2 rats in Chapter 2, some of the tetrodes targeted toward CA3 ended up in the dentate gyrus (1 tetrode in 1 of the rats and 2 tetrodes in the other). Recordings from dentate gyrus tetrodes were not used.

Estimating oscillatory power. Time varying power for slow gamma, fast gamma, theta, and delta were computed across the 25–55 Hz, 60–100 Hz, 6–10 Hz and 2–4 Hz frequency ranges, respectively, using a wavelet transform method described previously (Tallon-Baudry et al., 1997). Although fast gamma has previously been defined as extending up to 140 Hz (Colgin et al., 2009), we chose to cut it off at 100 Hz to avoid overlap with the recently defined epsilon band (90-150 Hz; Belluscio et al., 2012) and to avoid contamination by spike waveforms, which can generate power across a broad range of high frequencies, sometimes extending down to ~150 Hz (Colgin et al., 2009). Signals were convolved by a family of complex Morlet's wavelets w(t, f), one for each frequency, as a function of time:

$$w(t,f) = Ae^{-t^2/2\sigma_t^2} e^{2i\pi ft}$$

With $\sigma_f = \frac{1}{2}\pi\sigma_t$. The coefficient A was set at:

$$\left(\sigma_t\sqrt{\pi}\right)^{-1/2}$$

in order to normalize the wavelets such that their total energy was equal to 1. The family of wavelets was characterized by a constant ratio f/σ_f, which was set to 5.

Data acquisition. Experiments began when spikes emerged approximately at the proper depth for the region of interest (~2 mm for CA1 and ~3 mm for CA3) with amplitudes exceeding ~5 times the noise levels. Robust theta rhythms and sharp wave ripple activity helped to verify that tetrodes were in the CA1 cell body layer. The recording drive was connected to a multichannel, unity gain headstage (HS-54, Neuralynx, Bozeman, MT, USA). The output of the headstage was conducted via two lightweight tether cables through a multichannel slip-ring commutator to a data acquisition system that processed the signals through individual 24 bit AD converters (Digital Lynx, Neuralynx, Bozeman, MT, USA). Unit activity was bandpass filtered from 600 to 6000 Hz. Spike waveforms above a threshold set by the experimenter (~55-75 μV) were time-stamped and recorded at 32 kHz for 1 ms. Light-emitting diodes (LEDs) on the headstage were used to track the animal's movements at a 30 Hz sampling rate. Additionally, video files were collected during every recording session. LFPs (1 per tetrode) were recorded continuously in the 0.1-500 Hz band at a sampling rate of 2000 Hz. Notch filters were not used. Continuously sampled LFPs were recorded differentially against a common reference electrode placed in an electrically silent region. The common reference signal was duplicated using a breakout board (MDR-50 breakout board, Neuralynx, Bozeman,MT, USA) and recorded continuously against ground.

Results, statistics, and data analyses. Results are reported as means ± SD and depicted in figures as means ± SEM, unless indicated otherwise. Reported t-tests are 2-tailed. Data were analyzed using custom software written in MATLAB (MathWorks, Natick, MA), unless indicated otherwise. Statistics were computed with MATLAB, SPSS 22 (IBM),

and Oriana 4.02 (Kovach Computing Services). Specific analysis methods are described in detail in the Methods section of each chapter.

Spike sorting and cell classification. Spike sorting was performed offline using graphical cluster-cutting software (MClust v3.5; A.D. Redish, University of Minnesota, Minneapolis). Spikes were clustered manually in two-dimensional projections of the multidimensional parameter space (consisting of waveform amplitudes, energies, and peak-to-valley ratios). Autocorrelation and cross-correlation functions were additionally used to identify single units. Putative place cells were distinguished from putative interneurons on the basis of spike width, average firing rate, and bursting properties (Fox and Ranck, 1981; Henze et al., 2000; Harris et al., 2000; Frank et al., 2001). Firing rate maps across behavioral sessions were also used to identify place cells.

Estimation of running speed. The running speed (v_t) at time point (t) was estimated by calculating the distance between the preceding position (x_{t-1}, y_{t-1}) and the following position (x_{n+1}, y_{n+1}), and dividing by the elapsed time (2*1/position sampling frequency). For Chapters 2 and 3, only the x dimension was used since the animal was confined to a linear path. The sampling frequency of the position data was 30 Hz, yielding a temporal resolution of 1/15 second.

Histology. For verification of tetrode locations, brains were cut coronally at 30 μm and stained with cresyl violet (Figure A.1). Each section through the relevant part of the hippocampus was collected. All tetrode locations were identified, and the tip of each tetrode was localized by comparison across adjacent sections.

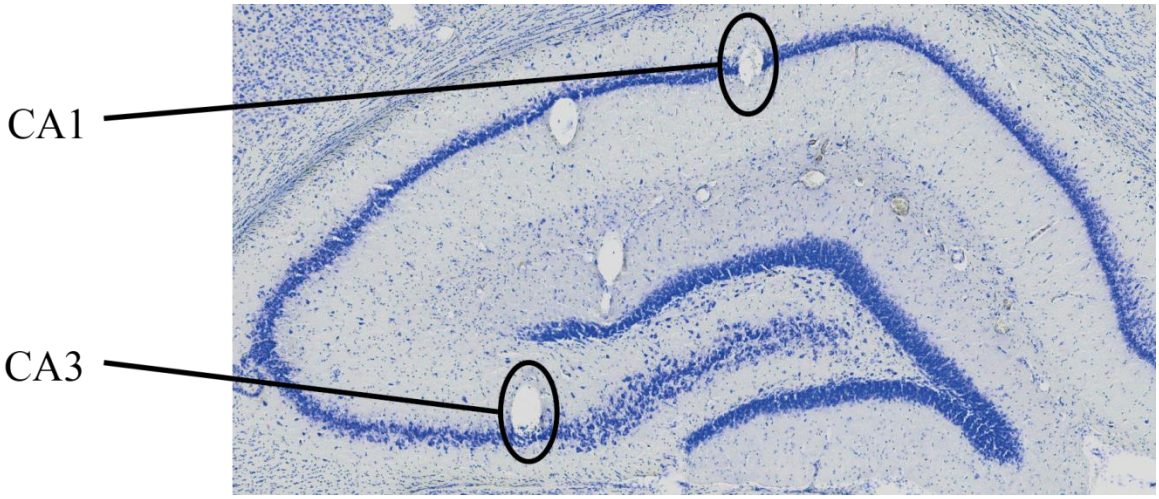

Figure A.1: Representative histology identifying tetrode tracks in CA1 and CA3. Coronal sections stained with cresyl violet show typical tetrode tracks terminating in CA3 and CA1 cell body layers.

References

Adey WR, Dunlop CW, Hendrix CE (1960) Hippocampal slow waves. Distribution and phase relationships in the course of approach learning. Archives of neurology 3:74-90.

Ahmed OJ, Mehta MR (2012) Running speed alters the frequency of hippocampal gamma oscillations. The Journal of neuroscience : the official journal of the Society for Neuroscience 32:7373-7383.

Amaral DG, Ishizuka N, Claiborne B (1990) Neurons, numbers and the hippocampal network. Progress in brain research 83:1-11.

Andersen P (2007) The hippocampus book. Oxford ; New York: Oxford University Press.

Barbieri R, Wilson MA, Frank LM, Brown EN (2005) An analysis of hippocampal spatio-temporal representations using a Bayesian algorithm for neural spike train decoding. IEEE transactions on neural systems and rehabilitation engineering : a publication of the IEEE Engineering in Medicine and Biology Society 13:131-136.

Barker GR, Warburton EC (2011) When is the hippocampus involved in recognition memory? The Journal of neuroscience : the official journal of the Society for Neuroscience 31:10721-10731.

Battaglia FP, Sutherland GR, McNaughton BL (2004) Local sensory cues and place cell directionality: additional evidence of prospective coding in the hippocampus. The Journal of neuroscience : the official journal of the Society for Neuroscience 24:4541-4550.

Belluscio MA, Mizuseki K, Schmidt R, Kempter R, Buzsaki G (2012) Cross-frequency phase-phase coupling between theta and gamma oscillations in the hippocampus. The Journal of neuroscience : the official journal of the Society for Neuroscience 32:423-435.

Berry SD, Thompson RF (1978) Prediction of learning rate from the hippocampal electroencephalogram. Science 200:1298-1300.

Bi GQ, Poo MM (1998) Synaptic modifications in cultured hippocampal neurons: dependence on spike timing, synaptic strength, and postsynaptic cell type. The Journal of neuroscience : the official journal of the Society for Neuroscience 18:10464-10472.

Bieri KW, Bobbitt KN, Colgin LL (2014) Slow and fast gamma rhythms coordinate different spatial coding modes in hippocampal place cells. Neuron 82:670-681.

Bragin A, Jando G, Nadasdy Z, Hetke J, Wise K, Buzsaki G (1995) Gamma (40-100 Hz) oscillation in the hippocampus of the behaving rat. The Journal of neuroscience : the official journal of the Society for Neuroscience 15:47-60.

Bremer, F (1938) L'activité électrique de l'écorce cérébrale. Actualités Scientifiques et Industrielles. 658:3–46.

Bremer F (1949) [Not Available]. Electroencephalography and clinical neurophysiology 1:177-193.

Broadbent NJ, Squire LR, Clark RE (2004) Spatial memory, recognition memory, and the hippocampus. Proceedings of the National Academy of Sciences of the United States of America 101:14515-14520.

Brown EN, Frank LM, Tang D, Quirk MC, Wilson MA (1998) A statistical paradigm for neural spike train decoding applied to position prediction from ensemble firing patterns of rat hippocampal place cells. The Journal of neuroscience : the official journal of the Society for Neuroscience 18:7411-7425.

Brun VH, Leutgeb S, Wu HQ, Schwarcz R, Witter MP, Moser EI, Moser MB (2008) Impaired spatial representation in CA1 after lesion of direct input from entorhinal cortex. Neuron 57:290-302.

Brun VH, Otnass MK, Molden S, Steffenach HA, Witter MP, Moser MB, Moser EI (2002) Place cells and place recognition maintained by direct entorhinal-hippocampal circuitry. Science 296:2243-2246.

Buzsaki G, Leung LW, Vanderwolf CH (1983) Cellular bases of hippocampal EEG in the behaving rat. Brain research 287:139-171.

Buzsaki G, Wang XJ (2012) Mechanisms of gamma oscillations. Annual review of neuroscience 35:203-225.

Cabral HO, Vinck M, Fouquet C, Pennartz CM, Rondi-Reig L, Battaglia FP (2014) Oscillatory dynamics and place field maps reflect hippocampal ensemble processing of sequence and place memory under NMDA receptor control. Neuron 81:402-415.

Carr MF, Karlsson MP, Frank LM (2012) Transient slow gamma synchrony underlies hippocampal memory replay. Neuron 75:700-713.

Chen J, Olsen RK, Preston AR, Glover GH, Wagner AD (2011) Associative retrieval processes in the human medial temporal lobe: hippocampal retrieval success and CA1 mismatch detection. Learn Mem 18:523-528.

Clark RE, Zola SM, Squire LR (2000) Impaired recognition memory in rats after damage to the hippocampus. The Journal of neuroscience : the official journal of the Society for Neuroscience 20:8853-8860.

Colgin LL, Denninger T, Fyhn M, Hafting T, Bonnevie T, Jensen O, Moser MB, Moser EI (2009) Frequency of gamma oscillations routes flow of information in the hippocampus. Nature 462:353-357.

Colgin LL, Moser EI (2010) Gamma oscillations in the hippocampus. Physiology 25:319-329.

Csicsvari J, Hirase H, Czurko A, Mamiya A, Buzsaki G (1999) Oscillatory coupling of hippocampal pyramidal cells and interneurons in the behaving Rat. The Journal of neuroscience : the official journal of the Society for Neuroscience 19:274-287.

de Almeida L, Idiart M, Lisman JE (2009) A second function of gamma frequency oscillations: an E%-max winner-take-all mechanism selects which cells fire. The Journal of neuroscience : the official journal of the Society for Neuroscience 29:7497-7503.

De Almeida L, Idiart M, Villavicencio A, Lisman J (2012) Alternating predictive and short-term memory modes of entorhinal grid cells. Hippocampus 22:1647-1651.

Douchamps V, Jeewajee A, Blundell P, Burgess N, Lever C (2013) Evidence for encoding versus retrieval scheduling in the hippocampus by theta phase and acetylcholine. The Journal of neuroscience : the official journal of the Society for Neuroscience 33:8689-8704.

Dragoi G, Buzsaki G (2006) Temporal encoding of place sequences by hippocampal cell assemblies. Neuron 50:145-157.

Duncan K, Ketz N, Inati SJ, Davachi L (2012) Evidence for area CA1 as a match/mismatch detector: a high-resolution fMRI study of the human hippocampus. Hippocampus 22:389-398.

Eacott MJ, Norman G (2004) Integrated memory for object, place, and context in rats: a possible model of episodic-like memory? The Journal of neuroscience : the official journal of the Society for Neuroscience 24:1948-1953.

Eccles JC (1951) Interpretation of action potentials evoked in the cerebral cortex. Electroencephalography and clinical neurophysiology 3:449-464.

Eichenbaum H, Yonelinas AP, Ranganath C (2007) The medial temporal lobe and recognition memory. Annual review of neuroscience 30:123-152.

Einevoll GT, Kayser C, Logothetis NK, Panzeri S (2013) Modelling and analysis of local field potentials for studying the function of cortical circuits. Nature reviews Neuroscience 14:770-785.

Ekstrom AD, Caplan JB, Ho E, Shattuck K, Fried I, Kahana MJ (2005) Human hippocampal theta activity during virtual navigation. Hippocampus 15:881-889.

Ekstrom AD, Kahana MJ, Caplan JB, Fields TA, Isham EA, Newman EL, Fried I (2003) Cellular networks underlying human spatial navigation. Nature 425:184-188.

Ekstrom AD, Meltzer J, McNaughton BL, Barnes CA (2001) NMDA receptor antagonism blocks experience-dependent expansion of hippocampal "place fields". Neuron 31:631-638.

Ennaceur A, Delacour J (1988) A new one-trial test for neurobiological studies of memory in rats. 1: Behavioral data. Behavioural brain research 31:47-59.

Fell J, Klaver P, Lehnertz K, Grunwald T, Schaller C, Elger CE, Fernandez G (2001) Human memory formation is accompanied by rhinal-hippocampal coupling and decoupling. Nat Neurosci 4:1259-1264.

Ferbinteanu J, Shapiro ML (2003) Prospective and retrospective memory coding in the hippocampus. Neuron 40:1227-1239.

Foster DJ, Wilson MA (2007) Hippocampal theta sequences. Hippocampus 17:1093-1099.

Fox SE, Ranck JB, Jr. (1981) Electrophysiological characteristics of hippocampal complex-spike cells and theta cells. Experimental brain research 41:399-410.

Frank LM, Brown EN, Wilson MA (2001) A comparison of the firing properties of putative excitatory and inhibitory neurons from CA1 and the entorhinal cortex. Journal of neurophysiology 86:2029-2040.

Fries P (2005) A mechanism for cognitive dynamics: neuronal communication through neuronal coherence. Trends in cognitive sciences 9:474-480.

Fries P (2009) Neuronal gamma-band synchronization as a fundamental process in cortical computation. Annual review of neuroscience 32:209-224.

Fyhn M, Molden S, Witter MP, Moser EI, Moser MB (2004) Spatial representation in the entorhinal cortex. Science 305:1258-1264.

Gardner-Medwin AR (1976) The recall of events through the learning of associations between their parts. Proceedings of the Royal Society of London Series B, Biological sciences 194:375-402.

Gloveli T, Dugladze T, Schmitz D, Heinemann U (2001) Properties of entorhinal cortex deep layer neurons projecting to the rat dentate gyrus. The European journal of neuroscience 13:413-420.

Gothard KM, Skaggs WE, Moore KM, McNaughton BL (1996) Binding of hippocampal CA1 neural activity to multiple reference frames in a landmark-based navigation task. The Journal of neuroscience : the official journal of the Society for Neuroscience 16:823-835.

Goutagny R, Jackson J, Williams S (2009) Self-generated theta oscillations in the hippocampus. Nat Neurosci 12:1491-1493.

Grastyan E, Lissak K, Madarasz I, Donhoffer H (1959) Hippocampal electrical activity during the development of conditioned reflexes. Electroencephalography and clinical neurophysiology 11:409-430.

Gray CM, Konig P, Engel AK, Singer W (1989) Oscillatory responses in cat visual cortex exhibit inter-columnar synchronization which reflects global stimulus properties. Nature 338:334-337.

Gray JA (1982) The neuropsychology of anxiety : an enquiry into the functions of the septo-hippocampal system. Clarendon Press; Oxford University Press, Oxford; New York.

Green JD, Arduini AA (1954) Hippocampal electrical activity in arousal. Journal of neurophysiology 17:533-557.

Greenstein YJ, Pavlides C, Winson J (1988) Long-term potentiation in the dentate gyrus is preferentially induced at theta rhythm periodicity. Brain research 438:331-334.

Gruber T, Tsivilis D, Montaldi D, Muller MM (2004) Induced gamma band responses: an early marker of memory encoding and retrieval. Neuroreport 15:1837-1841.

Gupta AS, van der Meer MA, Touretzky DS, Redish AD (2012) Segmentation of spatial experience by hippocampal theta sequences. Nat Neurosci 15:1032-1039.

Hafting T, Fyhn M, Molden S, Moser MB, Moser EI (2005) Microstructure of a spatial map in the entorhinal cortex. Nature 436:801-806.

Hahn TT, McFarland JM, Berberich S, Sakmann B, Mehta MR (2012) Spontaneous persistent activity in entorhinal cortex modulates cortico-hippocampal interaction in vivo. Nat Neurosci 15:1531-1538.

Hangya B, Borhegyi Z, Szilagyi N, Freund TF, Varga V (2009) GABAergic neurons of the medial septum lead the hippocampal network during theta activity. The Journal of neuroscience : the official journal of the Society for Neuroscience 29:8094-8102.

Hargreaves EL, Rao G, Lee I, Knierim JJ (2005) Major dissociation between medial and lateral entorhinal input to dorsal hippocampus. Science 308:1792-1794.

Harris KD, Csicsvari J, Hirase H, Dragoi G, Buzsaki G (2003) Organization of cell assemblies in the hippocampus. Nature 424:552-556.

Harris KD, Henze DA, Csicsvari J, Hirase H, Buzsaki G (2000) Accuracy of tetrode spike separation as determined by simultaneous intracellular and extracellular measurements. Journal of neurophysiology 84:401-414.

Hasselmo ME, Bodelon C, Wyble BP (2002) A proposed function for hippocampal theta rhythm: separate phases of encoding and retrieval enhance reversal of prior learning. Neural computation 14:793-817.

Hasselmo ME, Eichenbaum H (2005) Hippocampal mechanisms for the context-dependent retrieval of episodes. Neural networks : the official journal of the International Neural Network Society 18:1172-1190.

Hasselmo ME, Schnell E (1994) Laminar selectivity of the cholinergic suppression of synaptic transmission in rat hippocampal region CA1: computational modeling and brain slice physiology. The Journal of neuroscience : the official journal of the Society for Neuroscience 14:3898-3914.

Hasselmo ME, Stern CE (2006) Mechanisms underlying working memory for novel information. Trends in cognitive sciences 10:487-493.

Hasselmo ME, Wyble BP (1997) Free recall and recognition in a network model of the hippocampus: simulating effects of scopolamine on human memory function. Behavioural brain research 89:1-34.

Henze DA, Borhegyi Z, Csicsvari J, Mamiya A, Harris KD, Buzsaki G (2000) Intracellular features predicted by extracellular recordings in the hippocampus in vivo. Journal of neurophysiology 84:390-400.

Hopfield JJ (1982) Neural networks and physical systems with emergent collective computational abilities. Proceedings of the National Academy of Sciences of the United States of America 79:2554-2558.

Hyman JM, Wyble BP, Goyal V, Rossi CA, Hasselmo ME (2003) Stimulation in hippocampal region CA1 in behaving rats yields long-term potentiation when delivered to the peak of theta and long-term depression when delivered to the trough. The Journal of neuroscience : the official journal of the Society for Neuroscience 23:11725-11731.

Igarashi J, Isomura Y, Arai K, Harukuni R, Fukai T (2013) A theta-gamma oscillation code for neuronal coordination during motor behavior. The Journal of neuroscience : the official journal of the Society for Neuroscience 33:18515-18530.

Igarashi KM, Lu L, Colgin LL, Moser MB, Moser EI (2014) Coordination of entorhinal-hippocampal ensemble activity during associative learning. Nature 510:143-147.

Jensen O, Lisman JE (1996) Hippocampal CA3 region predicts memory sequences: Accounting for the phase precession of place cells. Learn Memory 3:279-287.

Jensen O, Lisman JE (2000) Position reconstruction from an ensemble of hippocampal place cells: contribution of theta phase coding. Journal of neurophysiology 83:2602-2609.

Jensen O, Lisman JE (2005) Hippocampal sequence-encoding driven by a cortical multi-item working memory buffer. Trends in neurosciences 28:67-72.

Jezek K, Henriksen EJ, Treves A, Moser EI, Moser MB (2011) Theta-paced flickering between place-cell maps in the hippocampus. Nature 478:246-249.

Johnson A, Redish AD (2007) Neural ensembles in CA3 transiently encode paths forward of the animal at a decision point. The Journal of neuroscience : the official journal of the Society for Neuroscience 27:12176-12189.

Jutras MJ, Fries P, Buffalo EA (2009) Gamma-band synchronization in the macaque hippocampus and memory formation. The Journal of neuroscience : the official journal of the Society for Neuroscience 29:12521-12531.

Kamondi A, Acsady L, Wang XJ, Buzsaki G (1998) Theta oscillations in somata and dendrites of hippocampal pyramidal cells in vivo: activity-dependent phase-precession of action potentials. Hippocampus 8:244-261.

Karlsson MP, Frank LM (2009) Awake replay of remote experiences in the hippocampus. Nat Neurosci 12:913-918.

Kay LM (2003) Two species of gamma oscillations in the olfactory bulb: dependence on behavioral state and synaptic interactions. Journal of integrative neuroscience 2:31-44.

Kemere C, Carr MF, Karlsson MP, Frank LM (2013) Rapid and continuous modulation of hippocampal network state during exploration of new places. PloS one 8:e73114.

Klimesch W, Doppelmayr M, Russegger H, Pachinger T (1996) Theta band power in the human scalp EEG and the encoding of new information. Neuroreport 7:1235-1240.

Klink R, Alonso A (1997) Muscarinic modulation of the oscillatory and repetitive firing properties of entorhinal cortex layer II neurons. Journal of neurophysiology 77:1813-1828.

Knierim JJ, Lee I, Hargreaves EL (2006) Hippocampal place cells: parallel input streams, subregional processing, and implications for episodic memory. Hippocampus 16:755-764.

Knierim JJ, Neunuebel JP, Deshmukh SS (2014) Functional correlates of the lateral and medial entorhinal cortex: objects, path integration and local-global reference frames. Philosophical transactions of the Royal Society of London Series B, Biological sciences 369:20130369.

Kohonen T (1984) Self-organization and associative memory. Berlin ; New York: Springer-Verlag.

Kramis R, Vanderwolf CH, Bland BH (1975) Two types of hippocampal rhythmical slow activity in both the rabbit and the rat: relations to behavior and effects of atropine, diethyl ether, urethane, and pentobarbital. Experimental neurology 49:58-85.

Kunec S, Hasselmo ME, Kopell N (2005) Encoding and retrieval in the CA3 region of the hippocampus: a model of theta-phase separation. Journal of neurophysiology 94:70-82.

Lachaux JP, Rodriguez E, Martinerie J, Varela FJ (1999) Measuring phase synchrony in brain signals. Human brain mapping 8:194-208.

Landfield PW, McGaugh JL, Tusa RJ (1972) Theta rhythm: a temporal correlate of memory storage processes in the rat. Science 175:87-89.

Larkin MC, Lykken C, Tye LD, Wickelgren JG, Frank LM (2014) Hippocampal output area CA1 broadcasts a generalized novelty signal during an object-place recognition task. Hippocampus 24:773-783.

Larson J, Lynch G (1986) Induction of synaptic potentiation in hippocampus by patterned stimulation involves two events. Science 232:985-988.

Larson J, Wong D, Lynch G (1986) Patterned stimulation at the theta frequency is optimal for the induction of hippocampal long-term potentiation. Brain research 368:347-350.

Lasztoczi B, Klausberger T (2014) Layer-specific GABAergic control of distinct gamma oscillations in the CA1 hippocampus. Neuron 81:1126-1139.

Leao RN, Mikulovic S, Leao KE, Munguba H, Gezelius H, Enjin A, Patra K, Eriksson A, Loew LM, Tort AB, Kullander K (2012) OLM interneurons differentially modulate CA3 and entorhinal inputs to hippocampal CA1 neurons. Nat Neurosci 15:1524-1530.

Lee I, Hunsaker MR, Kesner RP (2005) The role of hippocampal subregions in detecting spatial novelty. Behavioral neuroscience 119:145-153.

Lee I, Rao G, Knierim JJ (2004) A double dissociation between hippocampal subfields: differential time course of CA3 and CA1 place cells for processing changed environments. Neuron 42:803-815.

Leutgeb S, Leutgeb JK, Treves A, Moser MB, Moser EI (2004) Distinct ensemble codes in hippocampal areas CA3 and CA1. Science 305:1295-1298.

Lever C, Burton S, Jeewajee A, Wills TJ, Cacucci F, Burgess N, O'Keefe J (2010) Environmental novelty elicits a later theta phase of firing in CA1 but not subiculum. Hippocampus 20:229-234.

Liebe S, Hoerzer GM, Logothetis NK, Rainer G (2012) Theta coupling between V4 and prefrontal cortex predicts visual short-term memory performance. Nat Neurosci 15:456-462, S451-452.

Lisman J (2005) The theta/gamma discrete phase code occuring during the hippocampal phase precession may be a more general brain coding scheme. Hippocampus 15:913-922.

Lisman J, Redish AD (2009) Prediction, sequences and the hippocampus. Philosophical transactions of the Royal Society of London Series B, Biological sciences 364:1193-1201.

Lisman JE, Grace AA (2005) The hippocampal-VTA loop: controlling the entry of information into long-term memory. Neuron 46:703-713.

Lisman JE, Idiart MA (1995) Storage of 7 +/- 2 short-term memories in oscillatory subcycles. Science 267:1512-1515.

Lisman JE, Jensen O (2013) The theta-gamma neural code. Neuron 77:1002-1016.

Lisman JE, Otmakhova NA (2001) Storage, recall, and novelty detection of sequences by the hippocampus: elaborating on the SOCRATIC model to account for normal and aberrant effects of dopamine. Hippocampus 11:551-568.

Lubenov EV, Siapas AG (2009) Hippocampal theta oscillations are travelling waves. Nature 459:534-539.

MacDonald CJ, Lepage KQ, Eden UT, Eichenbaum H (2011) Hippocampal "time cells" bridge the gap in memory for discontiguous events. Neuron 71:737-749.

Macrides F, Eichenbaum HB, Forbes WB (1982) Temporal relationship between sniffing and the limbic theta rhythm during odor discrimination reversal learning. The Journal of neuroscience : the official journal of the Society for Neuroscience 2:1705-1717.

Manabe H, Mori K (2013) Sniff rhythm-paced fast and slow gamma-oscillations in the olfactory bulb: relation to tufted and mitral cells and behavioral states. Journal of neurophysiology 110:1593-1599.

Manns JR, Zilli EA, Ong KC, Hasselmo ME, Eichenbaum H (2007) Hippocampal CA1 spiking during encoding and retrieval: relation to theta phase. Neurobiology of learning and memory 87:9-20.

Marr D (1971) Simple memory: a theory for archicortex. Philosophical transactions of the Royal Society of London Series B, Biological sciences 262:23-81.

McNaughton N, Morris RG (1987) Chlordiazepoxide, an anxiolytic benzodiazepine, impairs place navigation in rats. Behavioural brain research 24:39-46.

Mehta MR, Barnes CA, McNaughton BL (1997) Experience-dependent, asymmetric expansion of hippocampal place fields. Proceedings of the National Academy of Sciences of the United States of America 94:8918-8921.

Mehta MR, Lee AK, Wilson MA (2002) Role of experience and oscillations in transforming a rate code into a temporal code. Nature 417:741-746.

Mehta MR, Quirk MC, Wilson MA (2000) Experience-dependent asymmetric shape of hippocampal receptive fields. Neuron 25:707-715.

M'Harzi M, Jarrard LE (1992) Effects of medial and lateral septal lesions on acquisition of a place and cue radial maze task. Behavioural brain research 49:159-165.

Milner B, Corkin S, Teuber HL (1968) Further analysis of the hippocampal amnesic syndrome: 14-year follow-up study of H.M.. Neuropsychologia 6:215–234.

Mitchell SJ, Rawlins JN, Steward O, Olton DS (1982) Medial septal area lesions disrupt theta rhythm and cholinergic staining in medial entorhinal cortex and produce impaired radial arm maze behavior in rats. The Journal of neuroscience : the official journal of the Society for Neuroscience 2:292-302.

Mizumori SJ, Perez GM, Alvarado MC, Barnes CA, McNaughton BL (1990) Reversible inactivation of the medial septum differentially affects two forms of learning in rats. Brain research 528:12-20.

Montgomery SM, Buzsaki G (2007) Gamma oscillations dynamically couple hippocampal CA3 and CA1 regions during memory task performance. Proceedings of the National Academy of Sciences of the United States of America 104:14495-14500.

Morris RG, Anderson E, Lynch GS, Baudry M (1986) Selective impairment of learning and blockade of long-term potentiation by an N-methyl-D-aspartate receptor antagonist, AP5. Nature 319:774-776.

Moser EI, Kropff E, Moser MB (2008) Place cells, grid cells, and the brain's spatial representation system. Annual review of neuroscience 31:69-89.

Muller RU, Kubie JL (1989) The firing of hippocampal place cells predicts the future position of freely moving rats. The Journal of neuroscience : the official journal of the Society for Neuroscience 9:4101-4110.

Mumby DG, Gaskin S, Glenn MJ, Schramek TE, Lehmann H (2002) Hippocampal damage and exploratory preferences in rats: memory for objects, places, and contexts. Learn Mem 9:49-57.

Newman EL, Gillet SN, Climer JR, Hasselmo ME (2013) Cholinergic blockade reduces theta-gamma phase amplitude coupling and speed modulation of theta frequency consistent with behavioral effects on encoding. The Journal of neuroscience : the official journal of the Society for Neuroscience 33:19635-19646.

Nyhus E, Curran T (2010) Functional role of gamma and theta oscillations in episodic memory. Neuroscience and biobehavioral reviews 34:1023-1035.

O'Keefe J (1976) Place units in the hippocampus of the freely moving rat. Experimental neurology 51:78-109.

O'Keefe J, Dostrovsky J (1971) The hippocampus as a spatial map. Preliminary evidence from unit activity in the freely-moving rat. Brain research 34:171-175.

O'Keefe J, Recce ML (1993) Phase relationship between hippocampal place units and the EEG theta rhythm. Hippocampus 3:317-330.

O'Keefe JM, Nadel L (1978) The hippocampus as a cognitive map. Clarendon Press; Oxford University Press, Oxford; New York.

O'Reilly RC, McClelland JL (1994) Hippocampal conjunctive encoding, storage, and recall: avoiding a trade-off. Hippocampus 4:661-682.

Orr G, Rao G, Houston FP, McNaughton BL, Barnes CA (2001) Hippocampal synaptic plasticity is modulated by theta rhythm in the fascia dentata of adult and aged freely behaving rats. Hippocampus 11:647-654.

Osipova D, Takashima A, Oostenveld R, Fernandez G, Maris E, Jensen O (2006) Theta and gamma oscillations predict encoding and retrieval of declarative memory. The Journal of neuroscience : the official journal of the Society for Neuroscience 26:7523-7531.

Patel J, Fujisawa S, Berenyi A, Royer S, Buzsaki G (2012) Traveling theta waves along the entire septotemporal axis of the hippocampus. Neuron 75:410-417.

Pavlides C, Greenstein YJ, Grudman M, Winson J (1988) Long-term potentiation in the dentate gyrus is induced preferentially on the positive phase of theta-rhythm. Brain research 439:383-387.

Penttonen M, Kamondi A, Acsady L, Buzsaki G (1998) Gamma frequency oscillation in the hippocampus of the rat: intracellular analysis in vivo. The European journal of neuroscience 10:718-728.

Pettersen KH, Einevoll GT (2008) Amplitude variability and extracellular low-pass filtering of neuronal spikes. Biophysical journal 94:784-802.

Pfeiffer BE, Foster DJ (2013) Hippocampal place-cell sequences depict future paths to remembered goals. Nature 497:74-79.

Robbe D, Buzsaki G (2009) Alteration of theta timescale dynamics of hippocampal place cells by a cannabinoid is associated with memory impairment. The Journal of neuroscience : the official journal of the Society for Neuroscience 29:12597-12605.

Rosenblatt F (1962) Principles of neurodynamics; perceptrons and the theory of brain mechanisms. Washington,: Spartan Books.

Roth ED, Yu X, Rao G, Knierim JJ (2012) Functional differences in the backward shifts of CA1 and CA3 place fields in novel and familiar environments. PloS one 7:e36035.

Rutishauser U, Ross IB, Mamelak AN, Schuman EM (2010) Human memory strength is predicted by theta-frequency phase-locking of single neurons. Nature 464:903-907.

Schomburg EW, Anastassiou CA, Buzsaki G, Koch C (2012) The spiking component of oscillatory extracellular potentials in the rat hippocampus. The Journal of neuroscience : the official journal of the Society for Neuroscience 32:11798-11811.

Schomburg EW, Fernandez-Ruiz A, Mizuseki K, Berenyi A, Anastassiou CA, Koch C, Buzsaki G (2014) Theta phase segregation of input-specific gamma patterns in entorhinal-hippocampal networks. Neuron 84:470-485.

Scoville WB, Milner B (1957) Loss of recent memory after bilateral hippocampal lesions. Journal of neurology, neurosurgery, and psychiatry 20:11-21.

Sederberg PB, Schulze-Bonhage A, Madsen JR, Bromfield EB, Litt B, Brandt A, Kahana MJ (2007) Gamma oscillations distinguish true from false memories. Psychological science 18:927-932.

Sederberg PB, Schulze-Bonhage A, Madsen JR, Bromfield EB, McCarthy DC, Brandt A, Tully MS, Kahana MJ (2007) Hippocampal and neocortical gamma oscillations predict memory formation in humans. Cerebral cortex 17:1190-1196.

Senior TJ, Huxter JR, Allen K, O'Neill J, Csicsvari J (2008) Gamma oscillatory firing reveals distinct populations of pyramidal cells in the CA1 region of the hippocampus. The Journal of neuroscience : the official journal of the Society for Neuroscience 28:2274-2286.

Shirvalkar PR, Rapp PR, Shapiro ML (2010) Bidirectional changes to hippocampal theta-gamma comodulation predict memory for recent spatial episodes. Proceedings of the National Academy of Sciences of the United States of America 107:7054-7059.

Siegel M, Warden MR, Miller EK (2009) Phase-dependent neuronal coding of objects in short-term memory. Proceedings of the National Academy of Sciences of the United States of America 106:21341-21346.

Siegle JH, Wilson MA (2014) Enhancement of encoding and retrieval functions through theta phase-specific manipulation of hippocampus. eLife 3:e03061.

Sirota A, Montgomery S, Fujisawa S, Isomura Y, Zugaro M, Buzsaki G (2008) Entrainment of neocortical neurons and gamma oscillations by the hippocampal theta rhythm. Neuron 60:683-697.

Skaggs WE, McNaughton BL (1996) Replay of neuronal firing sequences in rat hippocampus during sleep following spatial experience. Science 271:1870-1873.

Skaggs WE, McNaughton BL, Wilson MA, Barnes CA (1996) Theta phase precession in hippocampal neuronal populations and the compression of temporal sequences. Hippocampus 6:149-172.

Soltesz I, Deschenes M (1993) Low- and high-frequency membrane potential oscillations during theta activity in CA1 and CA3 pyramidal neurons of the rat hippocampus under ketamine-xylazine anesthesia. Journal of neurophysiology 70:97-116.

Staubli U, Lynch G (1987) Stable hippocampal long-term potentiation elicited by 'theta' pattern stimulation. Brain research 435:227-234.

Steffenach HA, Sloviter RS, Moser EI, Moser MB (2002) Impaired retention of spatial memory after transection of longitudinally oriented axons of hippocampal CA3 pyramidal cells. Proceedings of the National Academy of Sciences of the United States of America 99:3194-3198.

Stewart M, Fox SE (1990) Do septal neurons pace the hippocampal theta rhythm? Trends in neurosciences 13:163-168.

Sutherland RJ, Whishaw IQ, Kolb B (1983) A behavioural analysis of spatial localization following electrolytic, kainate- or colchicine-induced damage to the hippocampal formation in the rat. Behavioural brain research 7:133-153.

Suzuki WA, Miller EK, Desimone R (1997) Object and place memory in the macaque entorhinal cortex. Journal of neurophysiology 78:1062-1081.

Swanson LW, Cowan WM (1977) An autoradiographic study of the organization of the efferent connections of the hippocampal formation in the rat. The Journal of comparative neurology 172:49-84.

Takahashi M, Nishida H, Redish AD, Lauwereyns J (2014) Theta phase shift in spike timing and modulation of gamma oscillation: a dynamic code for spatial alternation during fixation in rat hippocampal area CA1. Journal of neurophysiology 111:1601-1614.

Tallon-Baudry C, Bertrand O, Delpuech C, Permier J (1997) Oscillatory gamma-band (30-70 Hz) activity induced by a visual search task in humans. The Journal of neuroscience : the official journal of the Society for Neuroscience 17:722-734.

Tort AB, Komorowski RW, Manns JR, Kopell NJ, Eichenbaum H (2009) Theta-gamma coupling increases during the learning of item-context associations. Proceedings of the National Academy of Sciences of the United States of America 106:20942-20947.

Toth K, Freund TF, Miles R (1997) Disinhibition of rat hippocampal pyramidal cells by GABAergic afferents from the septum. The Journal of physiology 500 (Pt 2):463-474.

Treves A, Rolls ET (1994) Computational analysis of the role of the hippocampus in memory. Hippocampus 4:374-391.

Trimper JB, Stefanescu RA, Manns JR (2014) Recognition memory and theta-gamma interactions in the hippocampus. Hippocampus 24:341-353.

Tsodyks MV, Skaggs WE, Sejnowski TJ, McNaughton BL (1996) Population dynamics and theta rhythm phase precession of hippocampal place cell firing: a spiking neuron model. Hippocampus 6:271-280.

van der Meer MA, Redish AD (2009) Low and High Gamma Oscillations in Rat Ventral Striatum have Distinct Relationships to Behavior, Reward, and Spiking Activity on a Learned Spatial Decision Task. Frontiers in integrative neuroscience 3:9.

van Haeften T, Baks-te-Bulte L, Goede PH, Wouterlood FG, Witter MP (2003) Morphological and numerical analysis of synaptic interactions between neurons in deep and superficial layers of the entorhinal cortex of the rat. Hippocampus 13:943-952.

Vanderwolf CH (1969) Hippocampal electrical activity and voluntary movement in the rat. Electroencephalography and clinical neurophysiology 26:407-418.

Vanderwolf CH, Zibrowski EM (2001) Pyriform cortex beta-waves: odor-specific sensitization following repeated olfactory stimulation. Brain research 892:301-308.

von der Malsburg C (1981) The correlation theory of brain function. Internal Report 81-2, Dept. of Neurobiology, Max-Planck-Institute for Biophysical Chemistry, Göttingen, Germany.

Whittington MA, Traub RD, Jefferys JG (1995) Synchronized oscillations in interneuron networks driven by metabotropic glutamate receptor activation. Nature 373:612-615.

Wikenheiser AM, Redish AD (2015) Hippocampal theta sequences reflect current goals. Nat Neurosci 18:289-294.

Willshaw DJ, Buneman OP, Longuet-Higgins HC (1969) Non-holographic associative memory. Nature 222:960-962.

Wilson MA, McNaughton BL (1993) Dynamics of the hippocampal ensemble code for space. Science 261:1055-1058.

Winson J (1978) Loss of hippocampal theta rhythm results in spatial memory deficit in the rat. Science 201:160-163.

Winters BD, Forwood SE, Cowell RA, Saksida LM, Bussey TJ (2004) Double dissociation between the effects of peri-postrhinal cortex and hippocampal lesions on tests of object recognition and spatial memory: heterogeneity of function within the temporal lobe. The Journal of neuroscience : the official journal of the Society for Neuroscience 24:5901-5908.

Winters BD, Saksida LM, Bussey TJ (2008) Object recognition memory: neurobiological mechanisms of encoding, consolidation and retrieval. Neuroscience and biobehavioral reviews 32:1055-1070.

Womelsdorf T, Schoffelen JM, Oostenveld R, Singer W, Desimone R, Engel AK, Fries P (2007) Modulation of neuronal interactions through neuronal synchronization. Science 316:1609-1612.

Wood ER, Dudchenko PA, Eichenbaum H (1999) The global record of memory in hippocampal neuronal activity. Nature 397:613-616.

Yamamoto J, Suh J, Takeuchi D, Tonegawa S (2014) Successful execution of working memory linked to synchronized high-frequency gamma oscillations. Cell 157:845-857.

Yoshida M, Fransen E, Hasselmo ME (2008) mGluR-dependent persistent firing in entorhinal cortex layer III neurons. The European journal of neuroscience 28:1116-1126.

Zhang K, Ginzburg I, McNaughton BL, Sejnowski TJ (1998) Interpreting neuronal population activity by reconstruction: unified framework with application to hippocampal place cells. Journal of neurophysiology 79:1017-1044.

Zhang SJ, Ye J, Miao C, Tsao A, Cerniauskas I, Ledergerber D, Moser MB, Moser EI (2013) Optogenetic dissection of entorhinal-hippocampal functional connectivity. Science 340:1232627.

Zheng C, Bieri KW, Trettel SG, Colgin LL (2015) The relationship between gamma frequency and running speed differs for slow and fast gamma rhythms in freely behaving rats. Hippocampus.

Vita

Kevin Bieri graduated *summa cum laude* with a B.S. in biochemistry from University of Texas at Austin in 2007. For his undergraduate thesis he developed a novel assay to screen genetic mutations involved with alcohol tolerance in *Drosophila melanogaster*. He went on to work in the lab of Dr. Xin Lin as a research assistant at M.D. Anderson Cancer Center studying cell signaling involved with breast cancer. In Fall 2009 he began the M.D./Ph.D. program at UTMB/UT Austin and decided to pursue his interest in neurophysiology. In 2011 he joined the lab of Dr. Laura Colgin and began work on this dissertation.

Permanent email address: kevbieri@gmail.com

This dissertation was typed by the author.